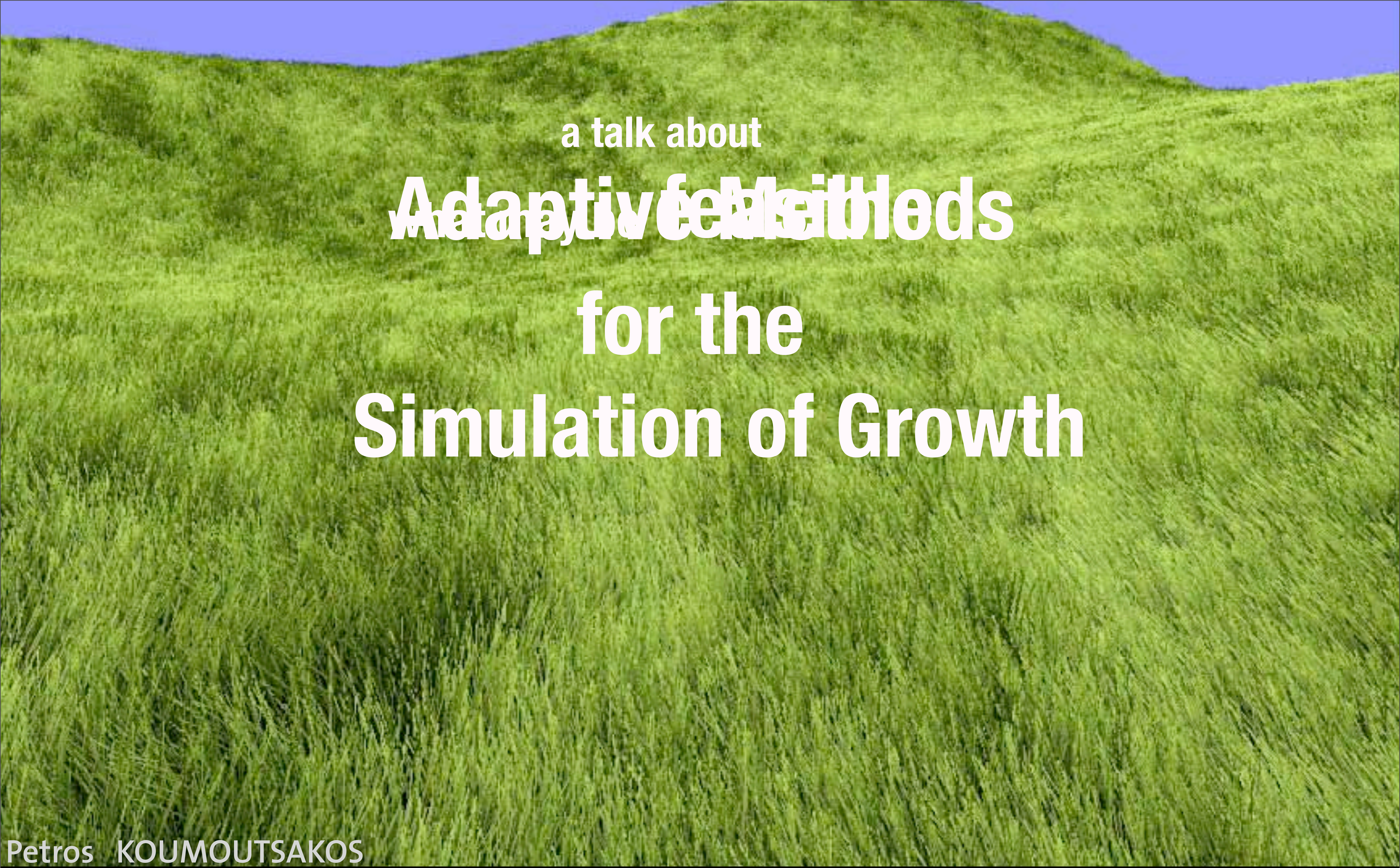

a talk about

Adaptive Methods

for the

Simulation of Growth

Petros KOUMOUTSAKOS

with : Basil BAYATI, Michael BERGDORF, Philippe CHATELAIN, Florian MILDE, Diego ROSSINELI, Gerardo TAURIELLO

CSE LAB
COMPUTATIONAL SCIENCE & ENGINEERING LABORATORY

WWW.CSE-LAB.ETHZ.CH

ETH
Eidgenössische Technische Hochschule Zürich
Swiss Federal Institute of Technology Zurich

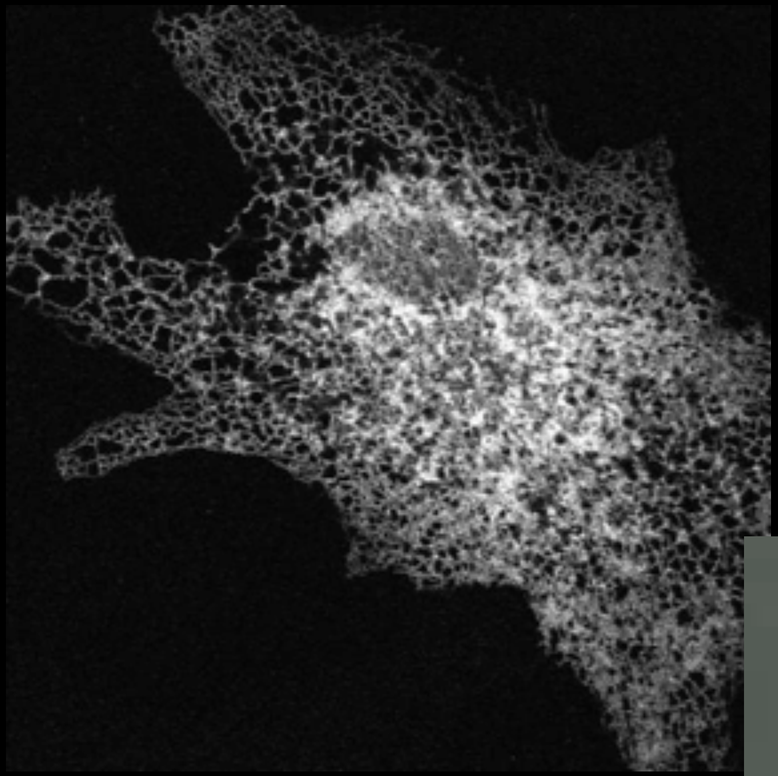

GEOMETRIES

- Complex
- Deforming
- Multiscale

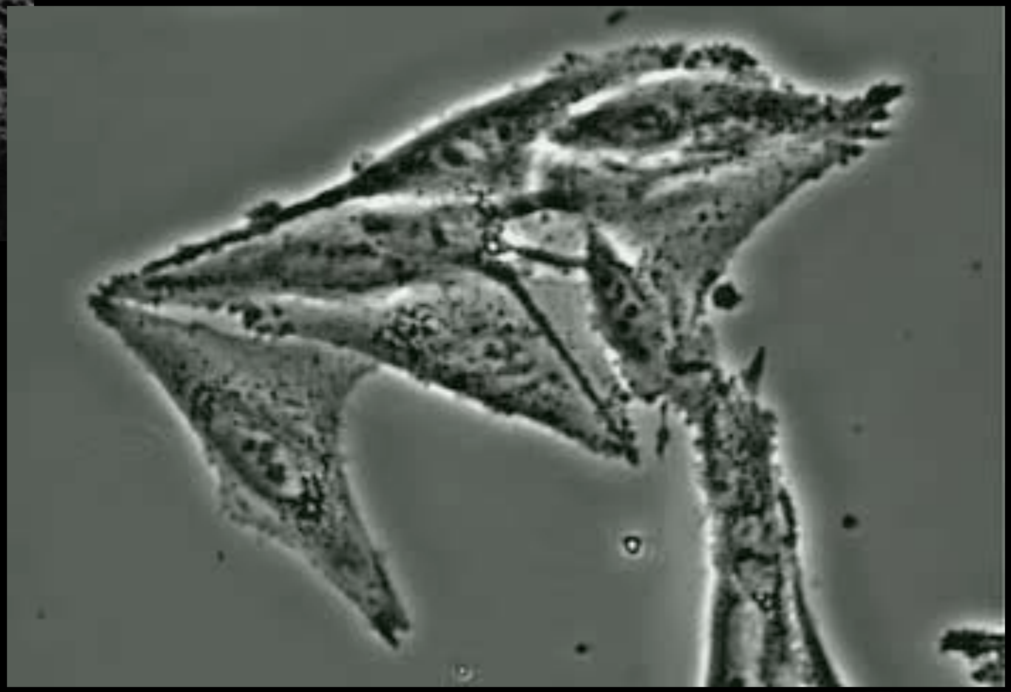

PHYSICS

- Heterogeneous
- Unsteady
- Multiscale

What methods do we need ?

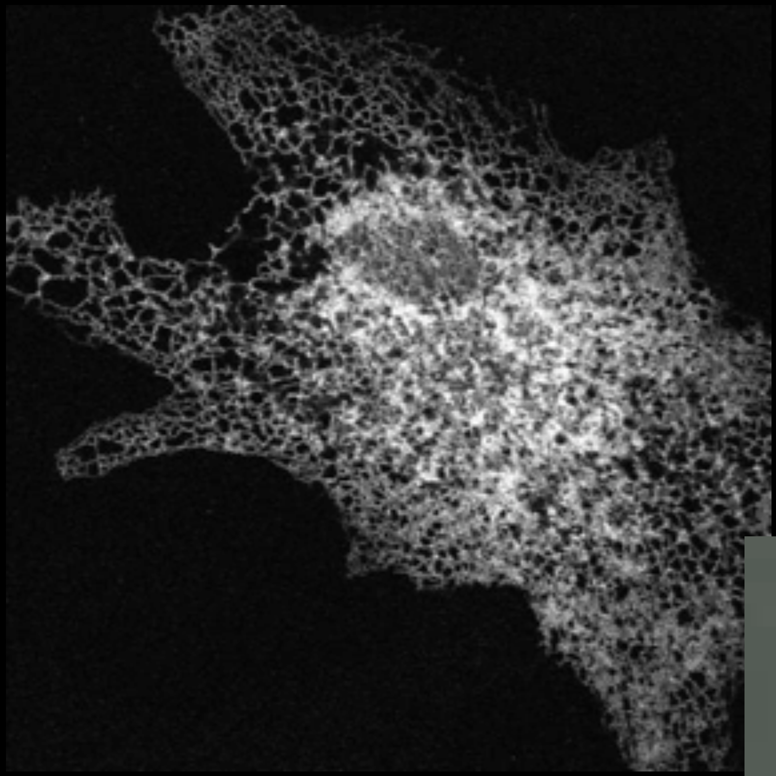

Adaptivity

Multiscaling (multi-resolution/physics)

Large Deformations

Heterogeneity

Efficient

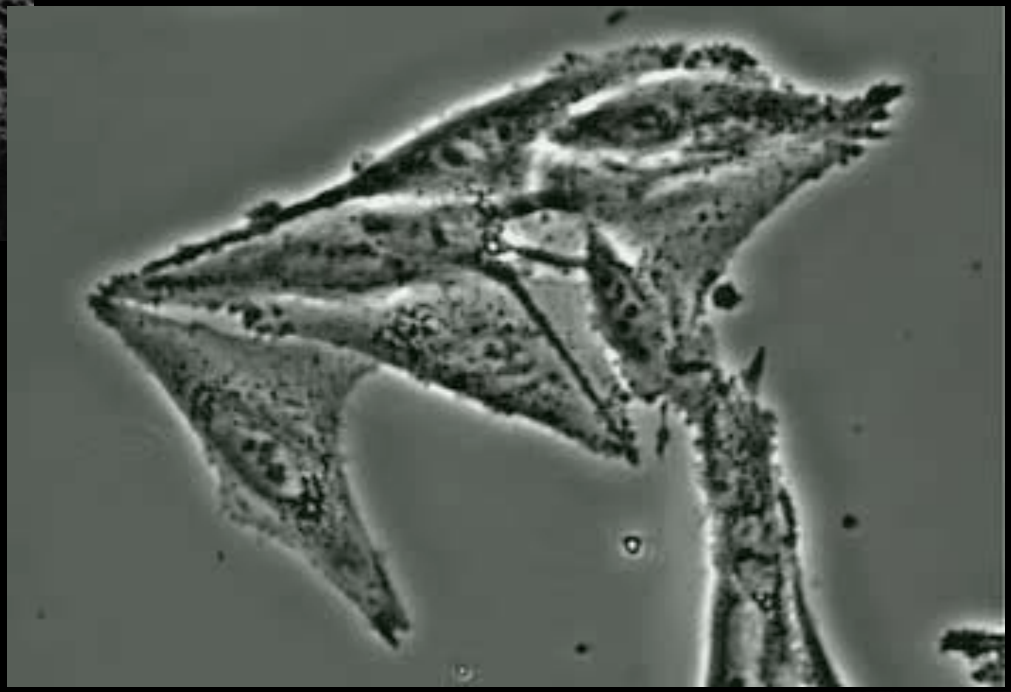

- LAGRANGIAN
- HETEROGENEOUS
- SCALABLE

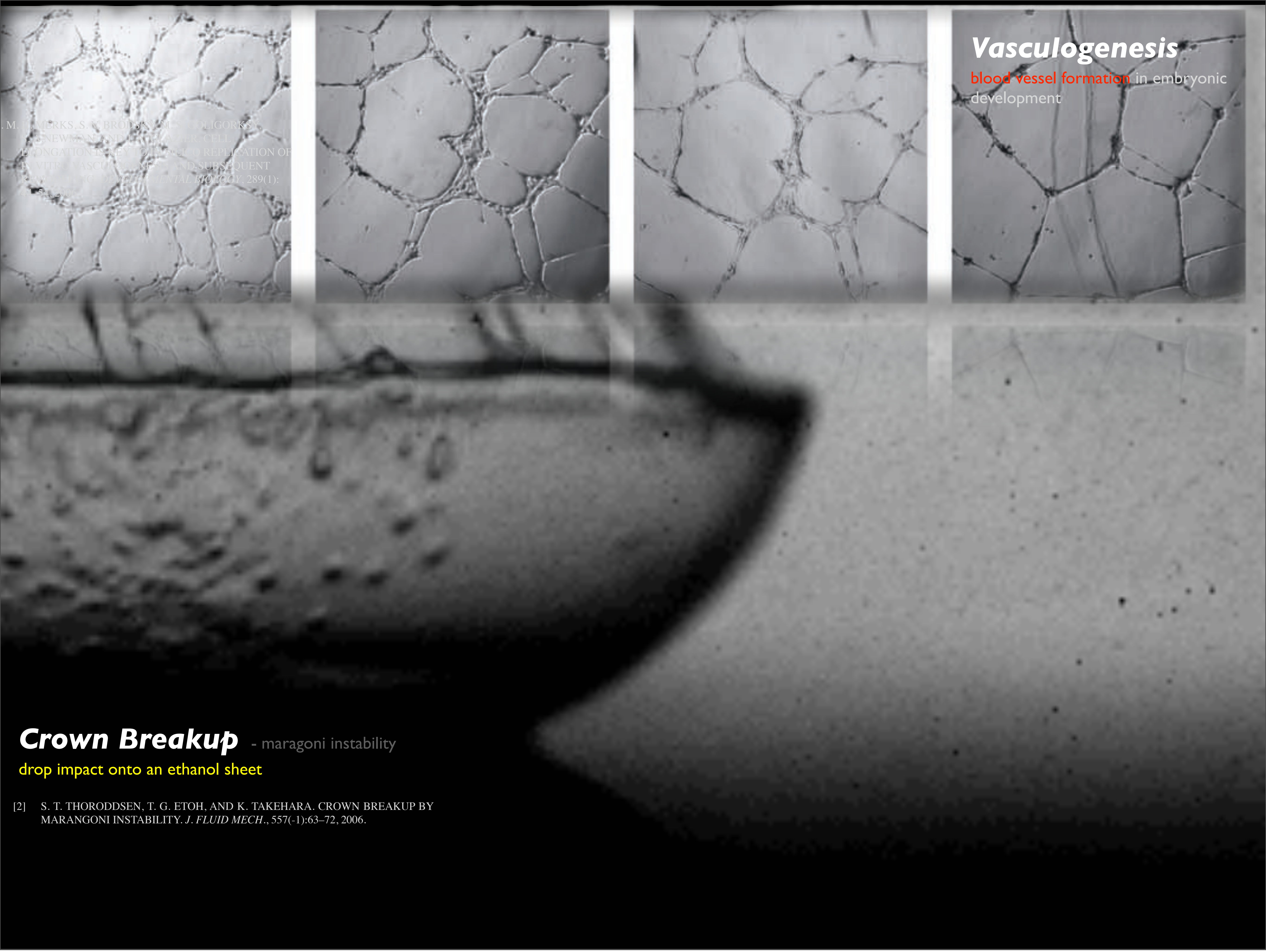
Vasculogenesis
blood vessel formation in embryonic development
Crown Breakup - maragoni instability
drop impact onto an ethanol sheet
[2] S. T. THORODDSEN, T. G. ETOH, AND K. TAKEHARA. CROWN BREAKUP BY MARANGONI INSTABILITY. J. FLUID MECH., 557(-1):63–72, 2006.

16384 Cores - 10 Billion Particles - 60% efficiency

Runs at IBM Watson Center - BLue Gene/L

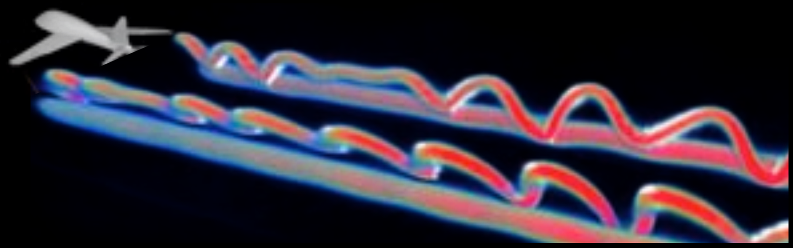

Chatelain P., Curioni A., Bergdorf M., Rossinelli D., Andreoni W., Koumoutsakos P., Billion Vortex Particle Direct Numerical Simulations of Aircraft Wakes, Computer Methods in Applied Mech. and Eng. 197/13-16, 1296-1304, 2008

512 Cores - 10 Million Particles

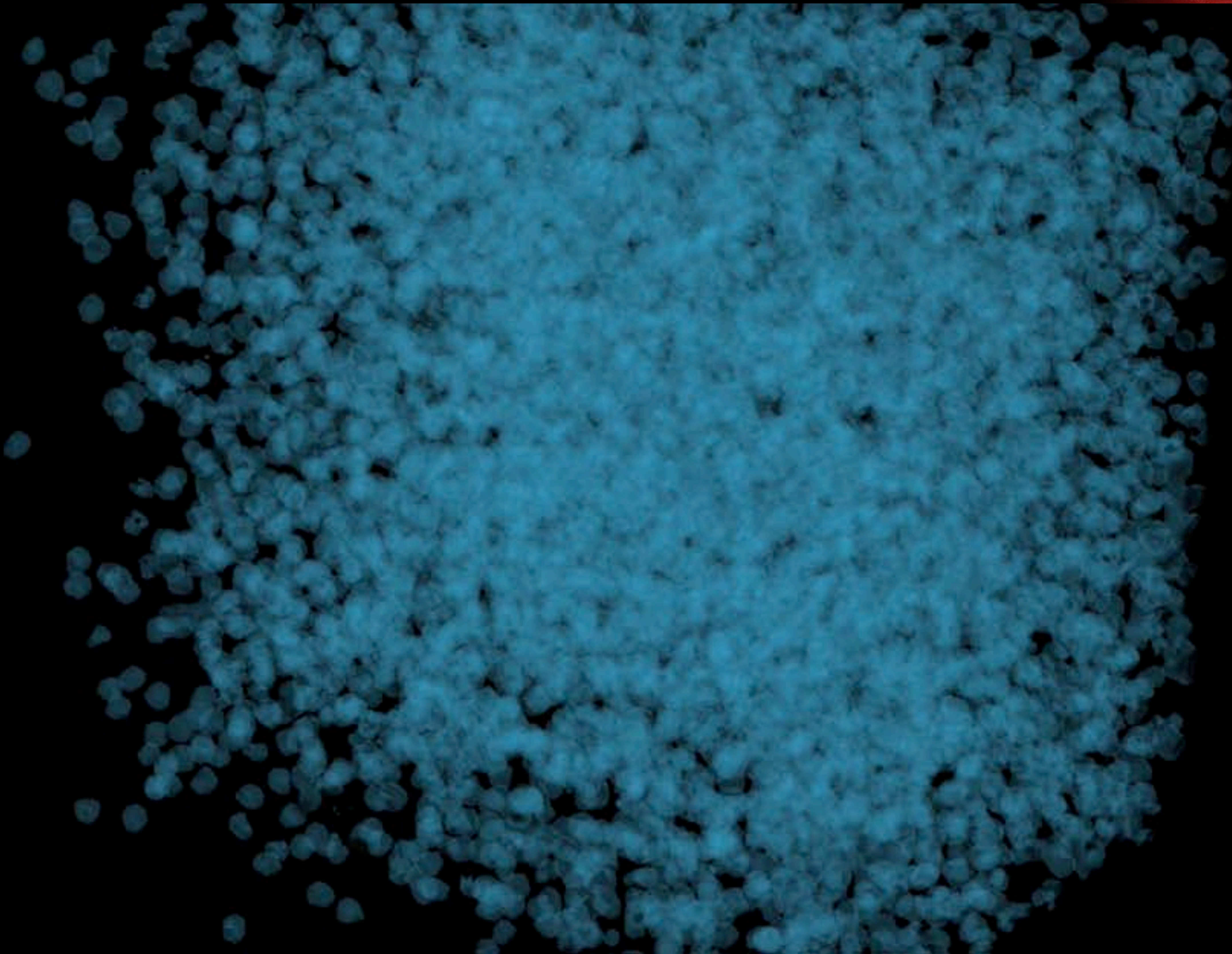

Milde F., Bergdorf M., Koumoutsakos P., A hybrid model of sprouting angiogenesis, Biophysical J.. 2008

Particle Simulation of Elastic Solid

Plane Strain Compression Test

- Pistons move with constant velocity
- Elastic solid fixed to the pistons
- Highly dynamic deformation of large extent

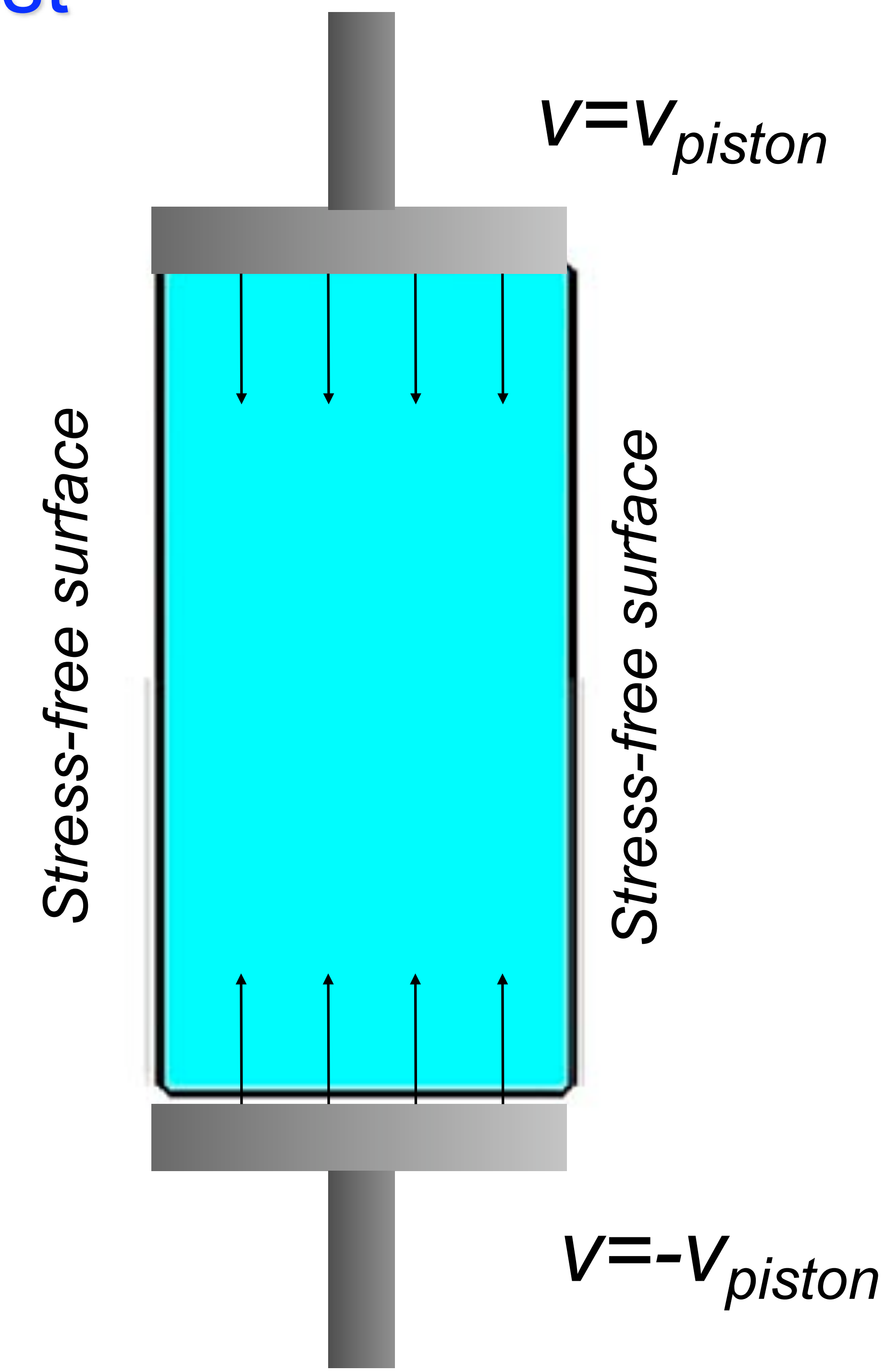

Particle Simulation of Elastic Solid

Plane Strain Compression Test

- Pistons move with constant velocity
- Elastic solid fixed to the pistons
- Highly dynamic deformation of large extent

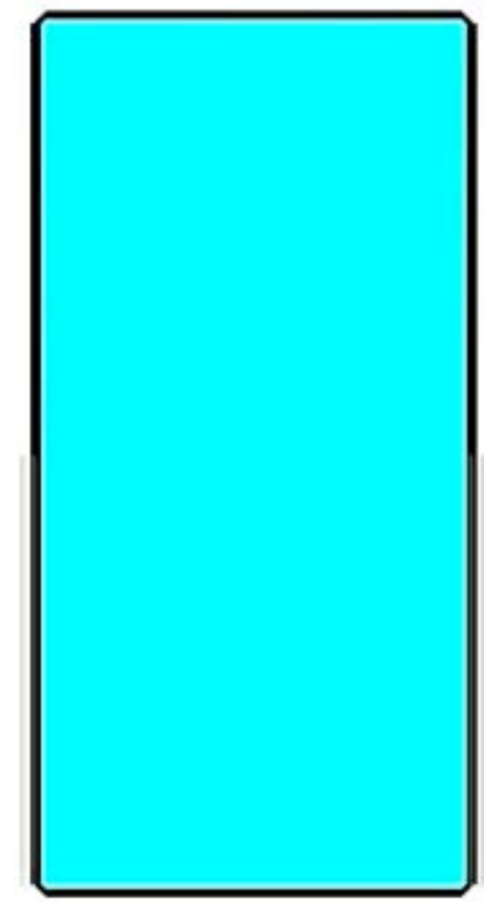

Plane Strain Compression Test

Redistributed Particle solution

FEM solution (ABAQUS 6.4/Explicit)

Linear Elasticity

Young's Modulus =100
Poisson ratio=0.49 ~2000 particles/nodes

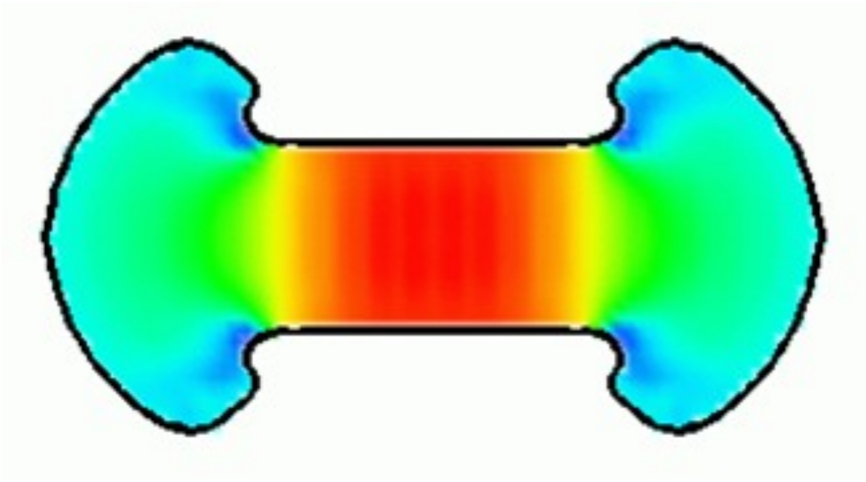

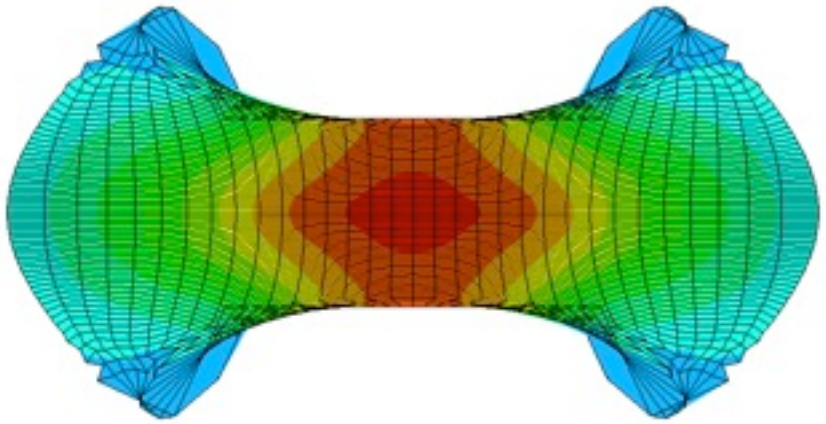

Nonlinear Elasticity

Hyperelastic Material

C_{10}=2.2, D=0.001

~2000 particles/nodes

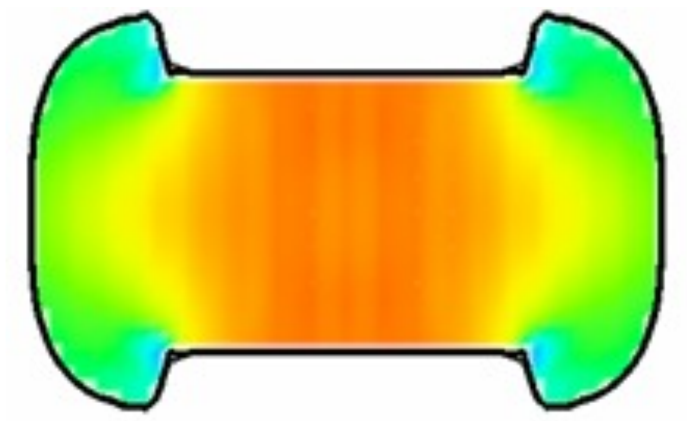

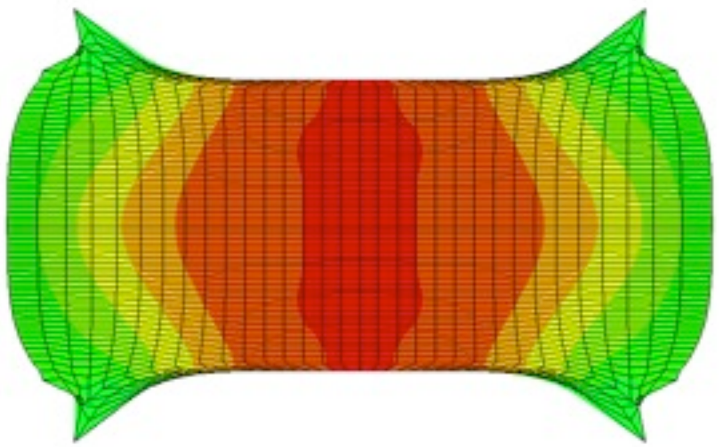

S.E. Hieber and P. Koumoutsakos A Lagrangian particle method for the simulation of linear and nonlinear elastic models of soft tissue. *al., J. Comp. Physics, 2008*

Why Adaptive Methods ?

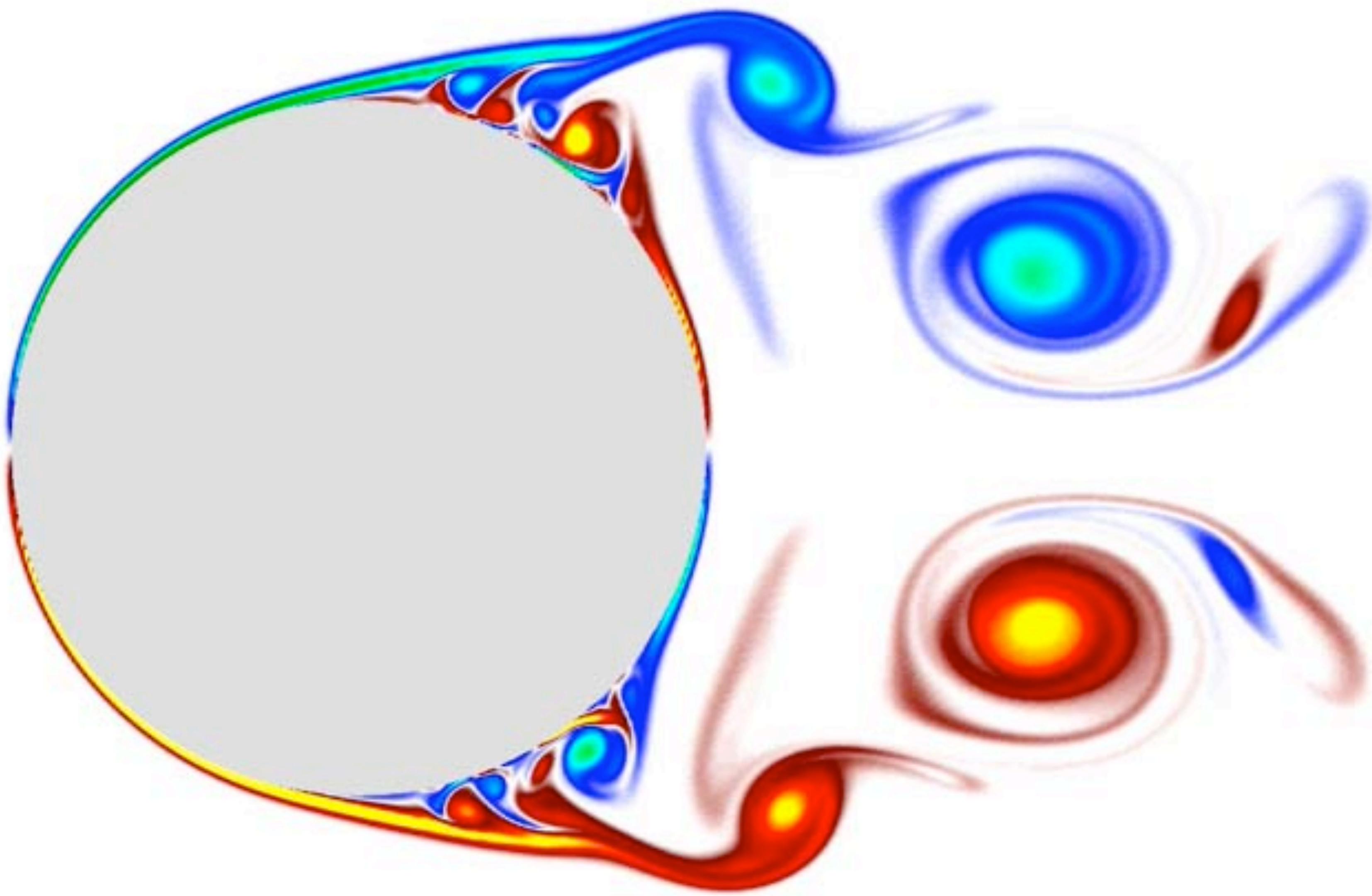

Koumoutsakos & Leonard, JFM,1995

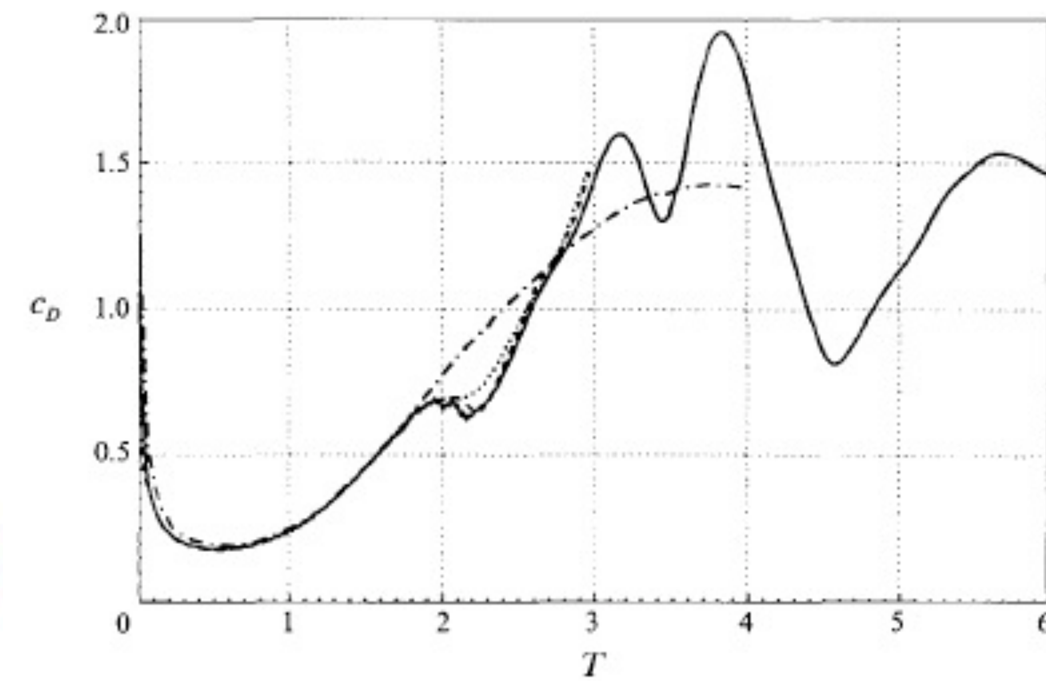

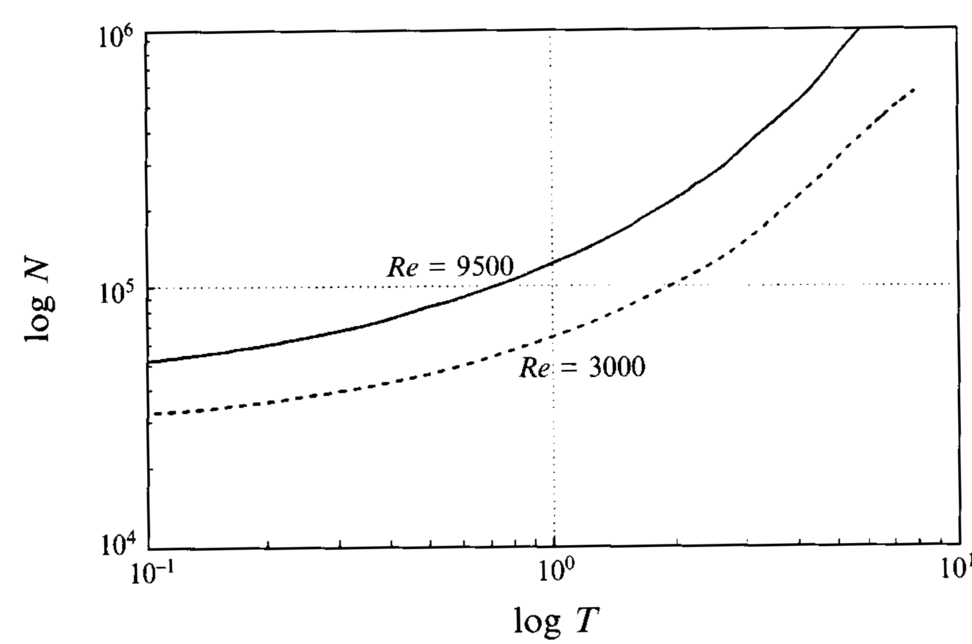

Anatomy of a Simulation & 3 Gaps in Computing

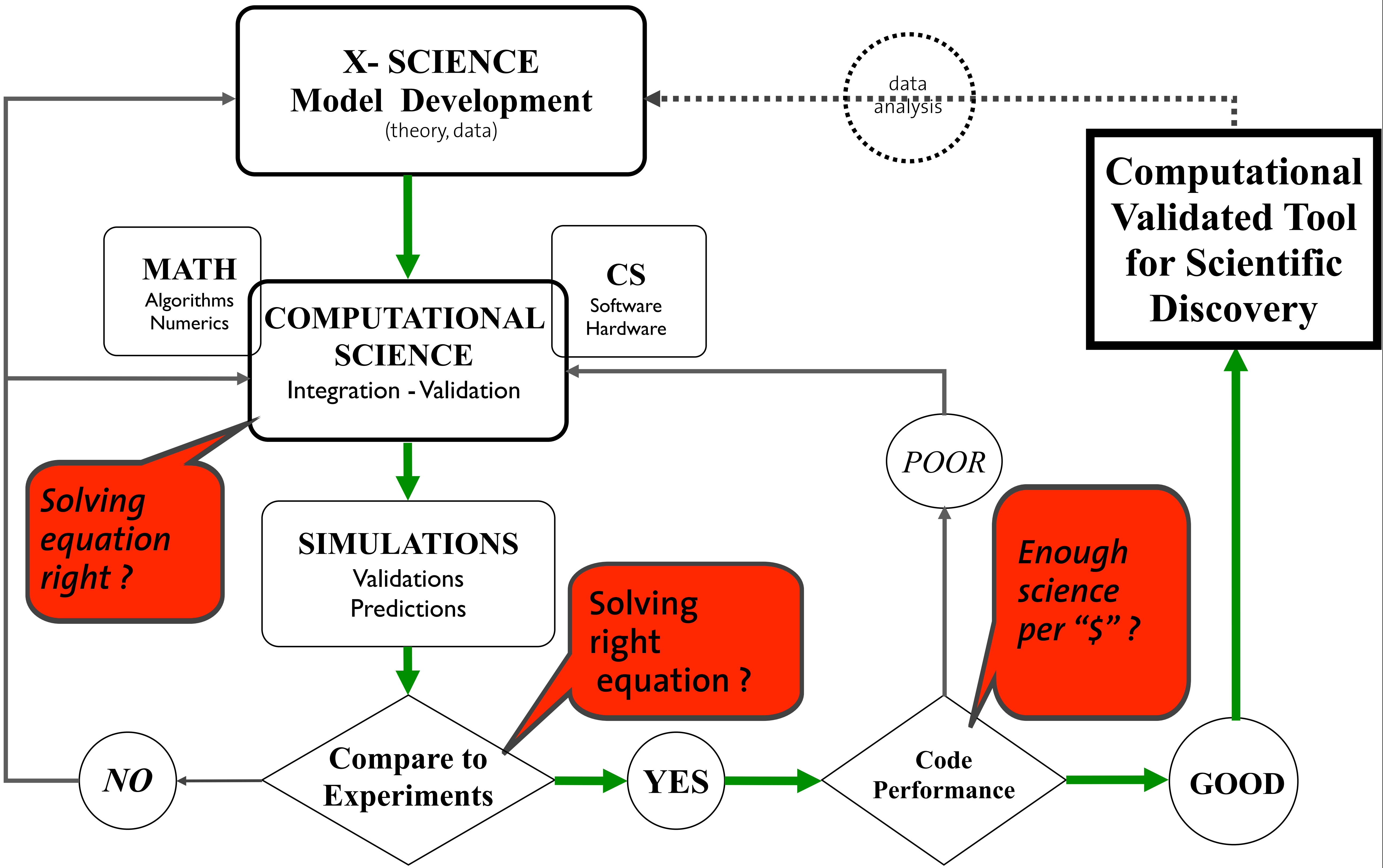

Adapted from : US-DOE

Particles : "Smooth" - Discrete

Smooth = APPROXIMATE

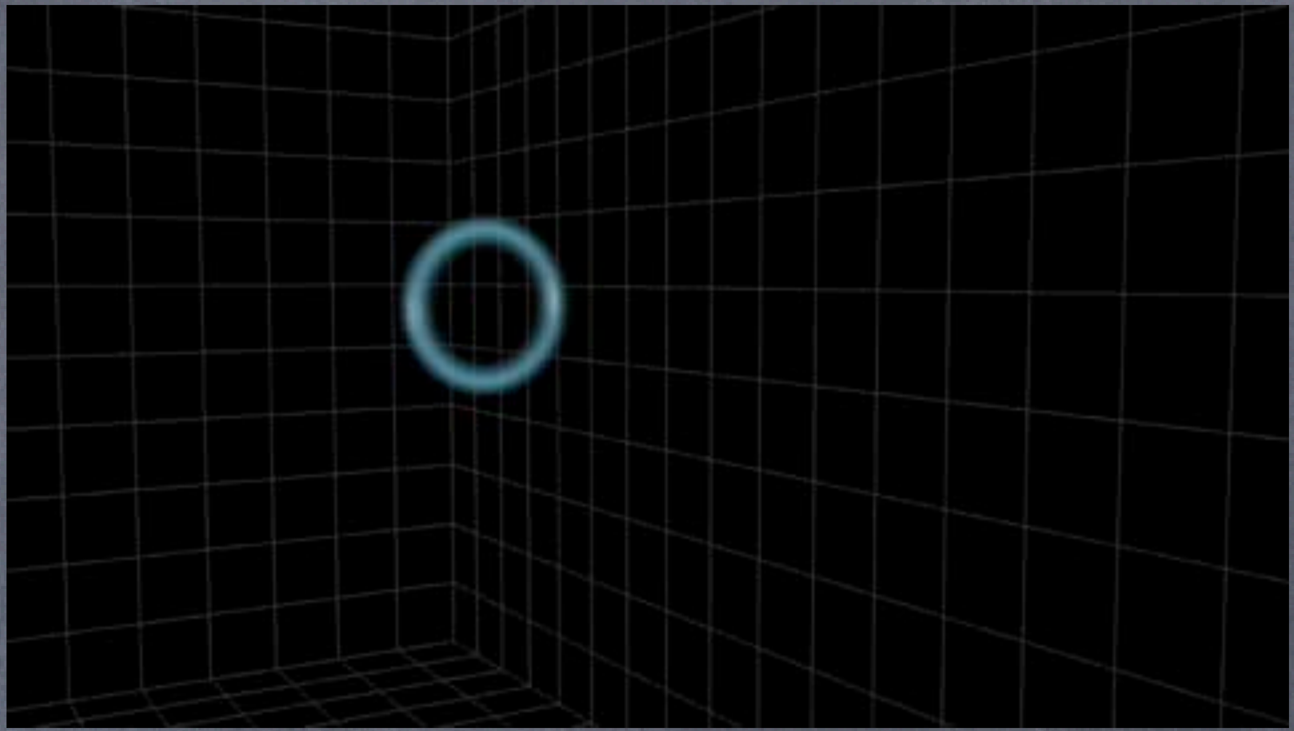

- Smoothed Particle Hydrodynamics
- Vortex Methods
- Lagrangian level sets

Discrete = MODEL

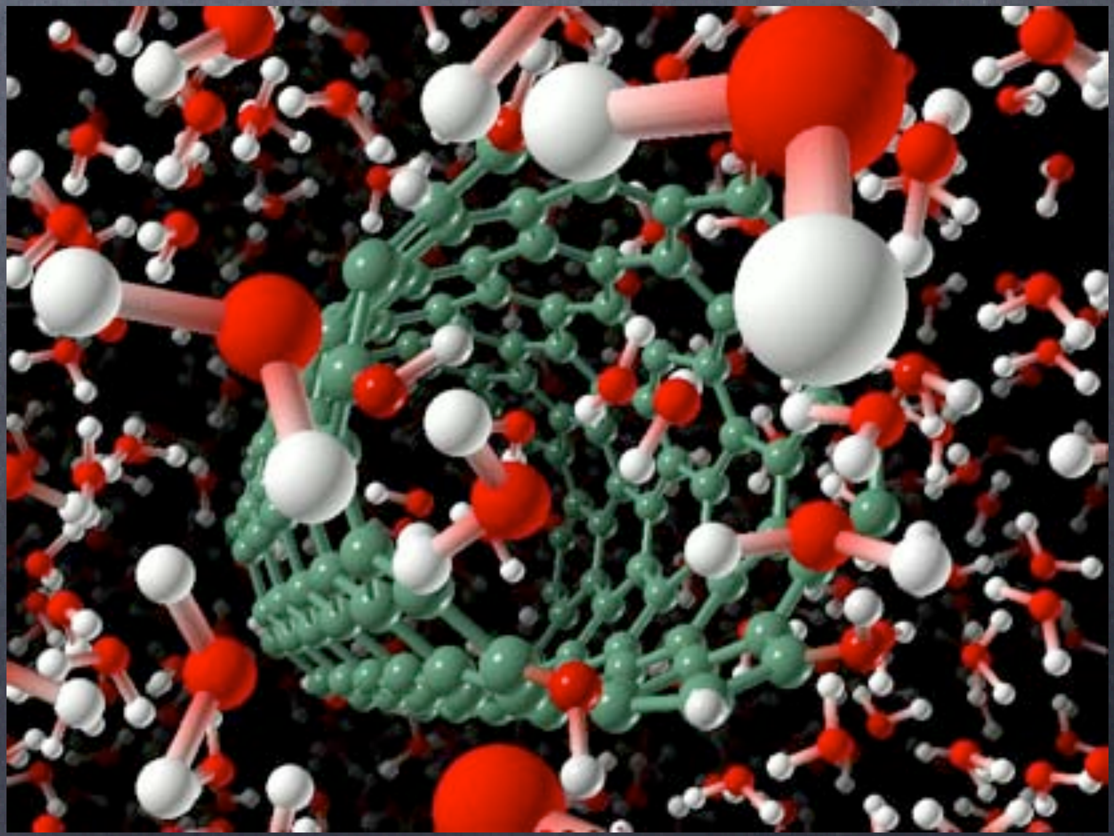

- Molecular Dynamics (MD)
- Dissipative Particle Dynamics
- Stochastic Simulation

Particle Methods: an N-BODY problem

Particle (position, value)

$i, j = 1, \cdots, N$

$$\frac{dx_i}{dt} = U(q_j, q_i, x_i, x_j, \cdots)$$

$$\frac{dq_i}{dt} = F(q_j, q_i, x_i, x_j, \cdots)$$

SMOOTH

Particles are quadrature points for continuum properties

RHS of ODEs: quadratures of integral equations

DISCRETE:

Particles as carriers of physical properties - Models

RHS of ODEs : Physical models - Particle interactions

+ • Multipole Algorithms, Fast Poisson solvers , Adaptivity, multiresolution, multiphysics

PARTICLES Smooth & Discrete

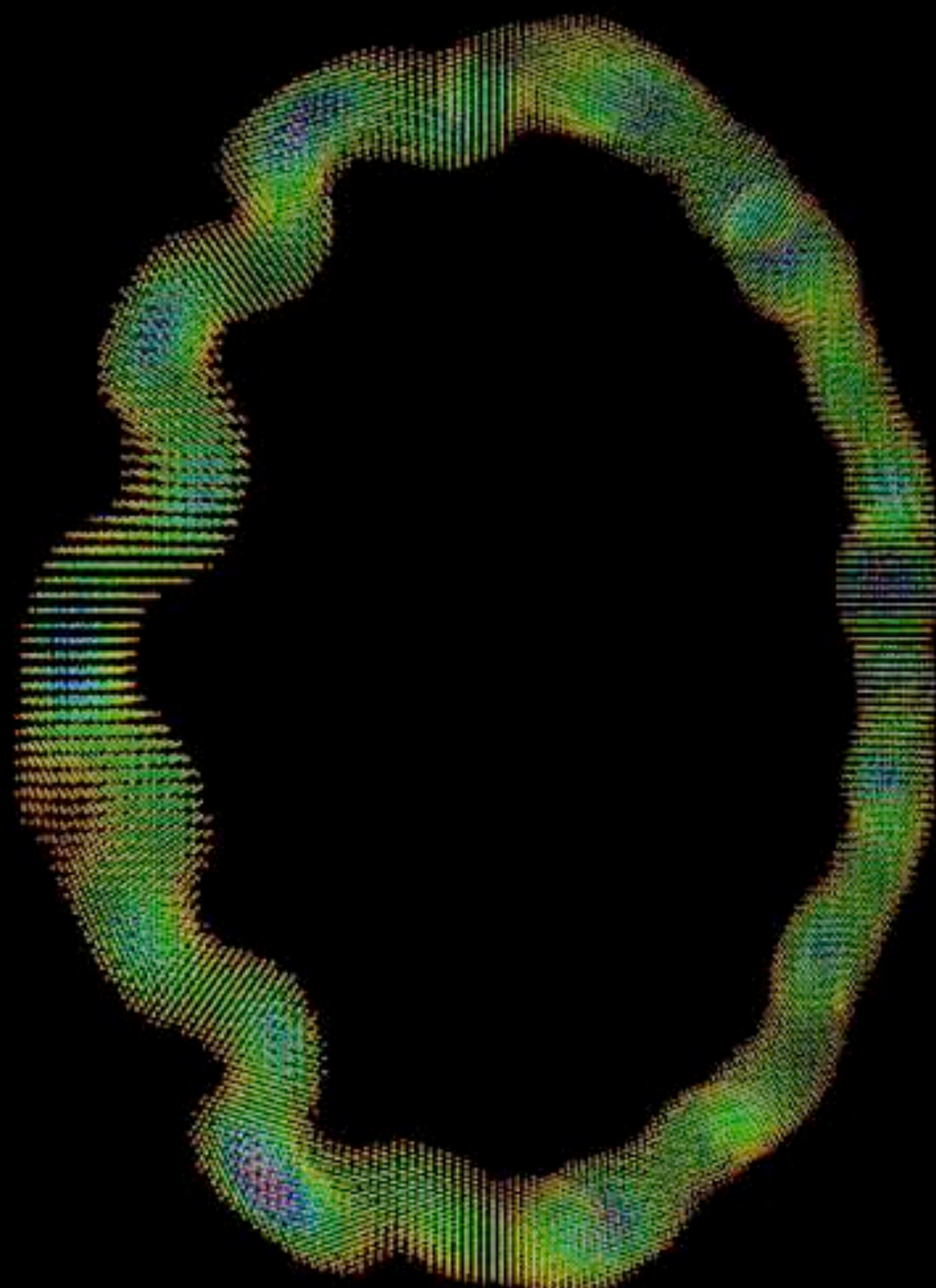

Smooth/Discrete Particles

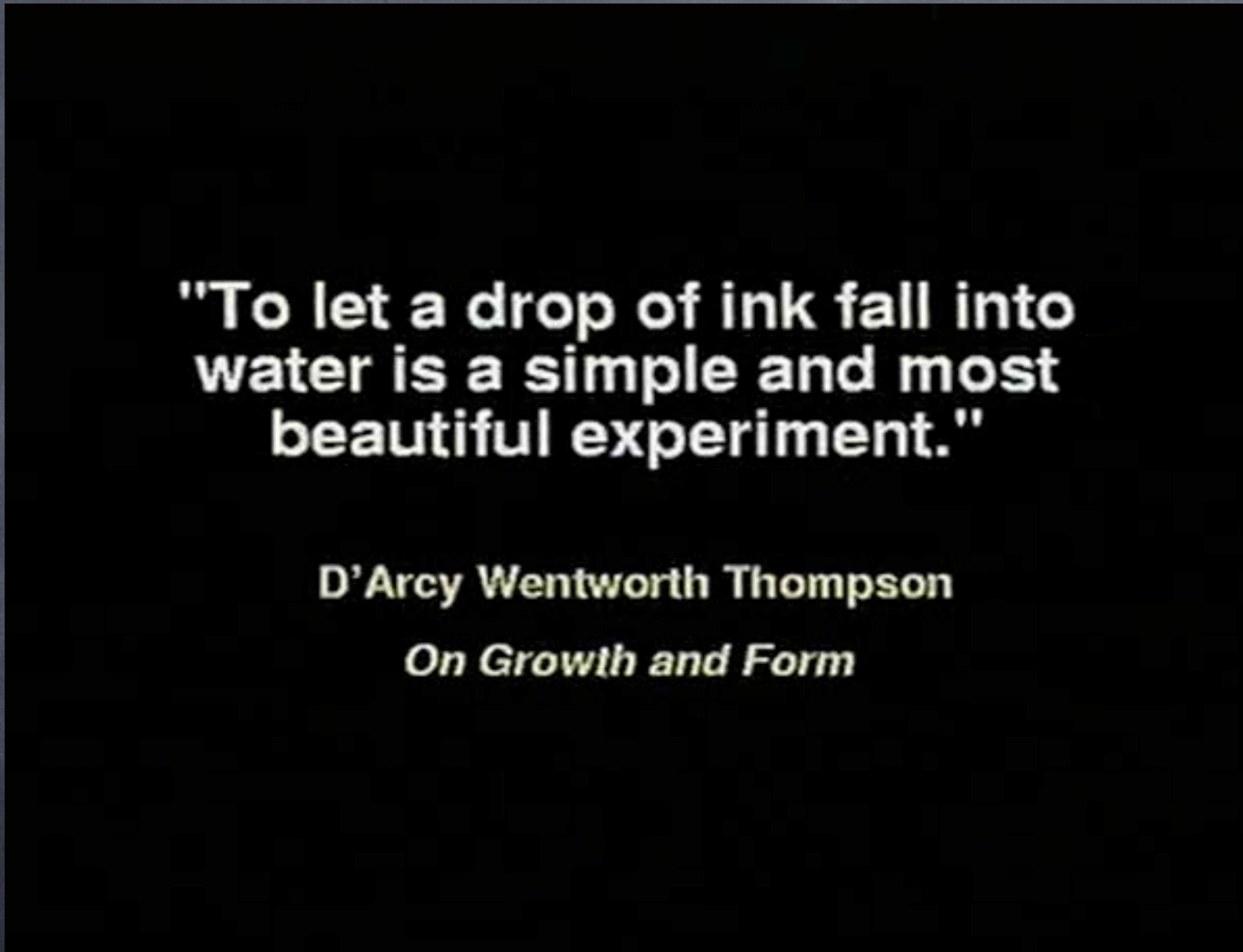

J. H. Walther, P. Koumoutsakos, Three-dimensional vortex methods for particle-laden flows with two-way coupling, J. Comput. Phys., 167, 39-71, 2001

A BRIEF HISTORY of PARTICLE METHODS

The 1920's

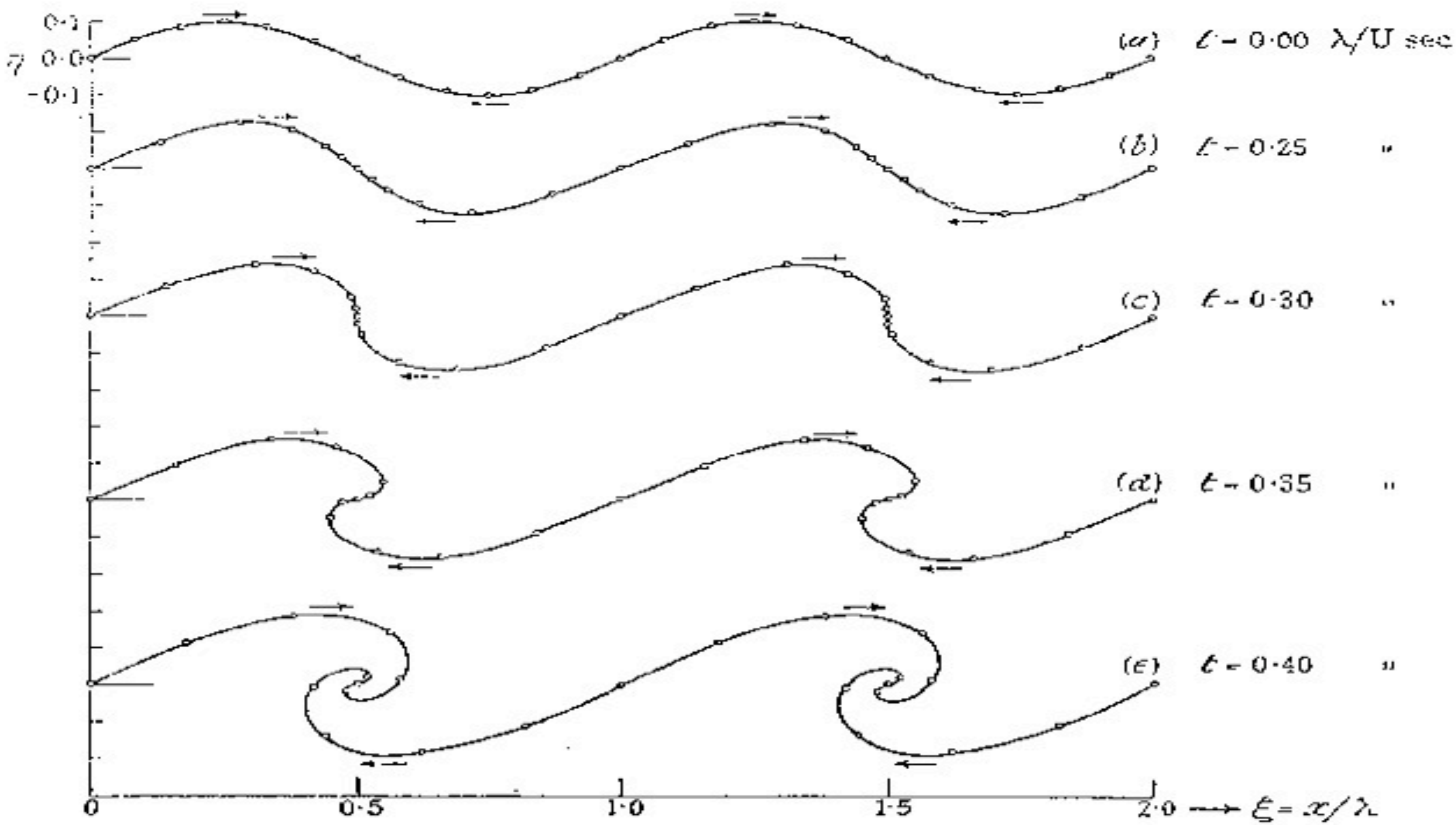

FIG. 4.

Rosenhead - Hand Calculations of a Vortex Sheet

The 50's

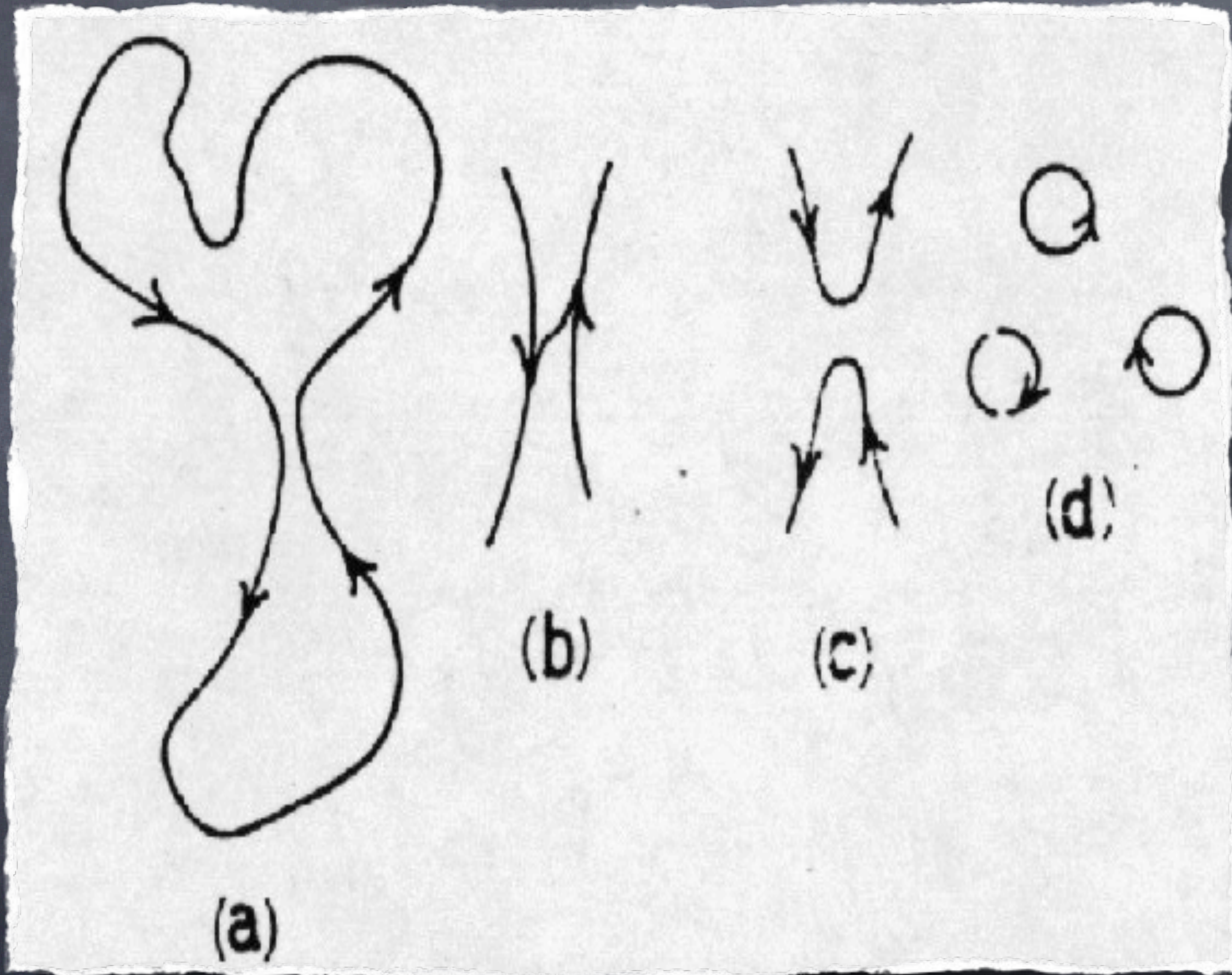

Feynman – Vortex Filaments: How do they break and reconnect ?

The 60's : Marker And Cell (MAC) - (velocity - pressure)

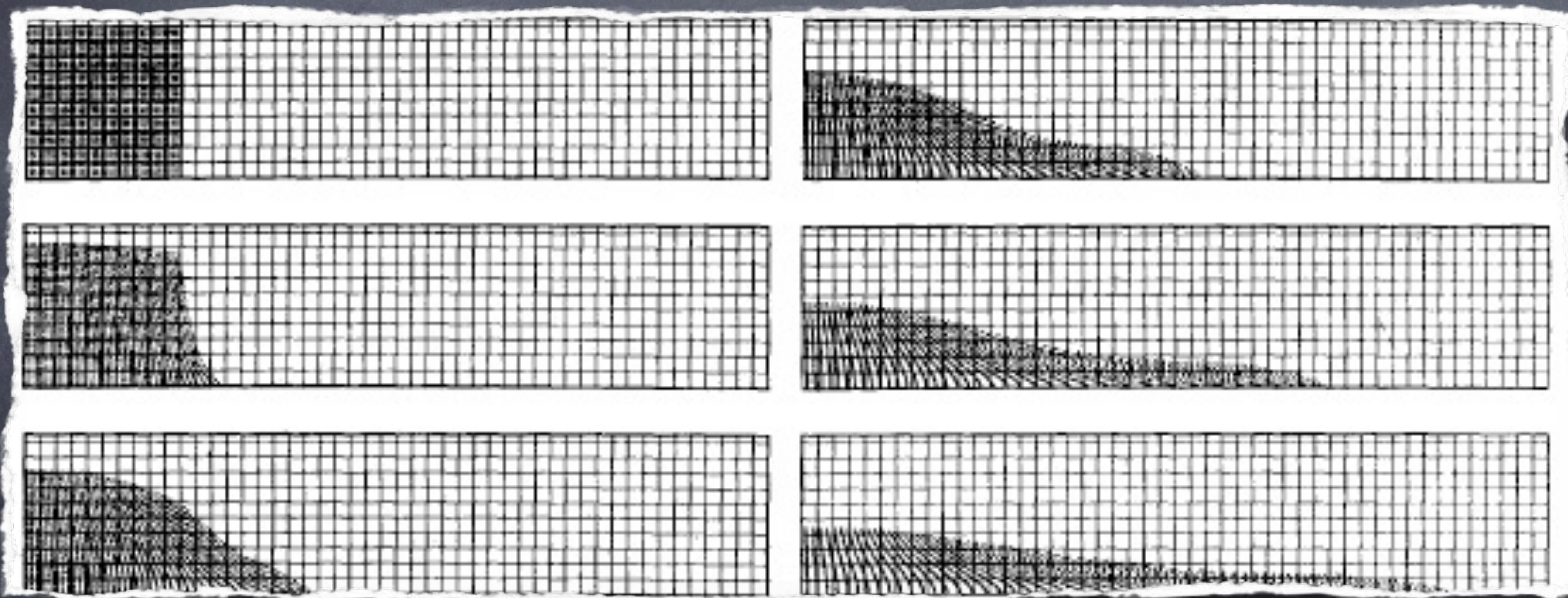

F.H. Harlow and E.J. Welch

Numerical Calculation of Time-Dependent Viscous Incompressible Flow of Fluid with Free Surface,, Harlow, Francis H. and Welch, J. Eddie, Physics of Fluids, 1965

vortex Particle Methods : From the 60's to the 80's

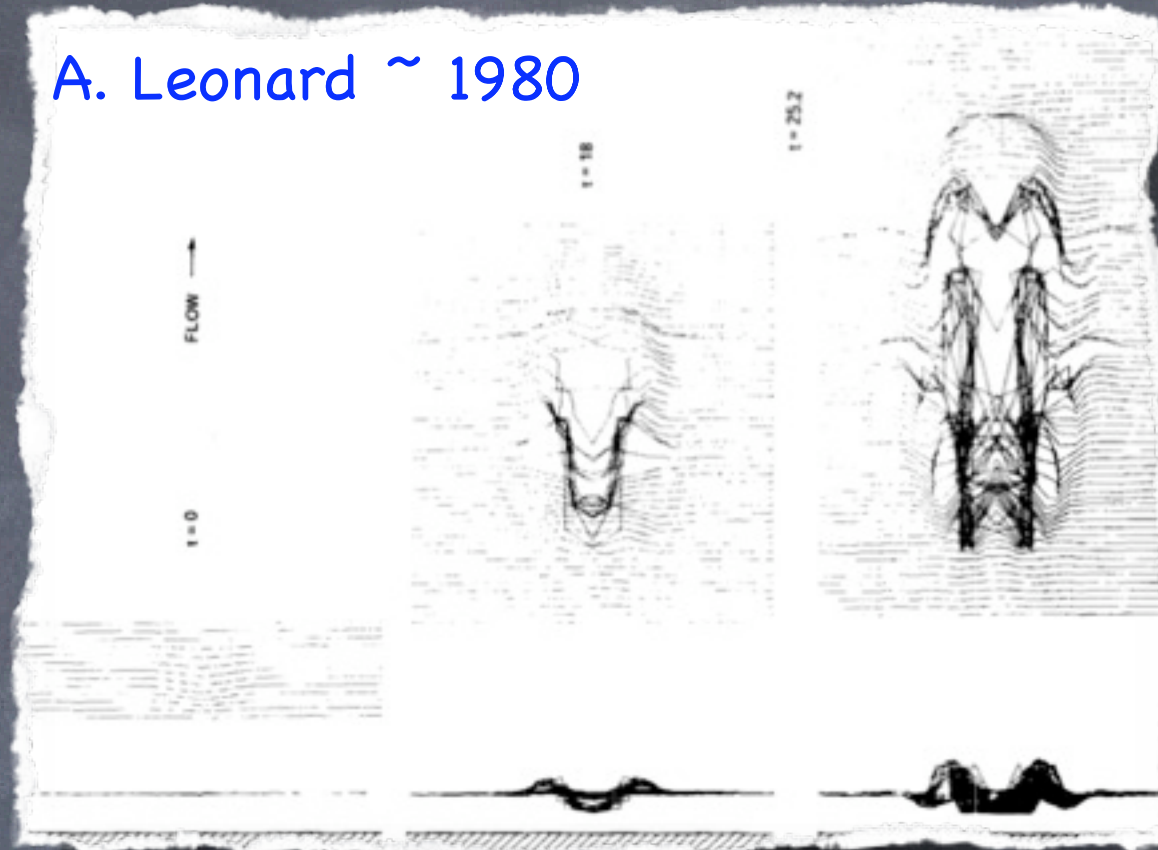

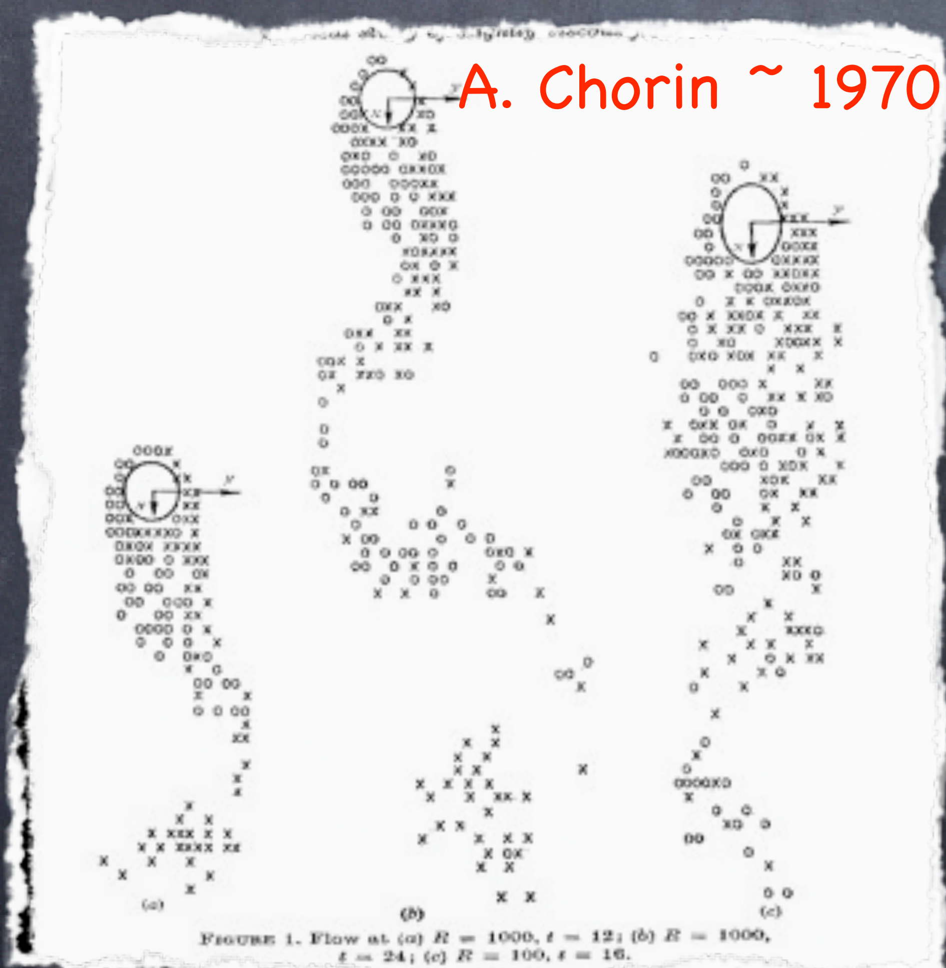

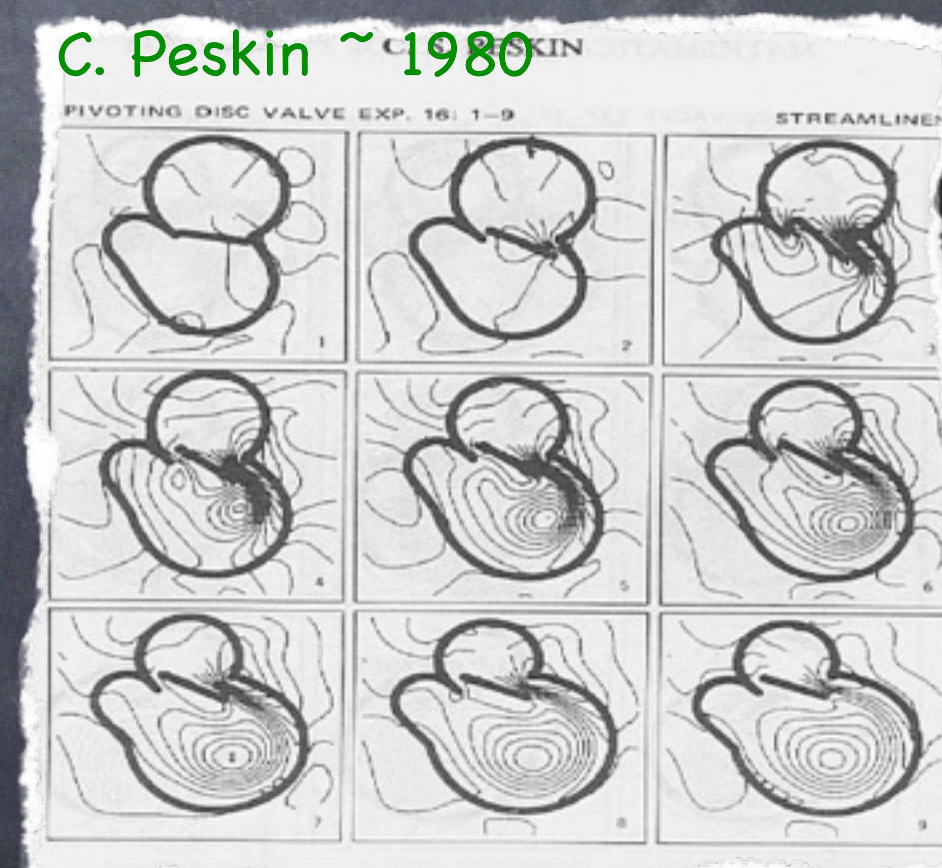

t = 00.01

What stopped Vortex Methods ?

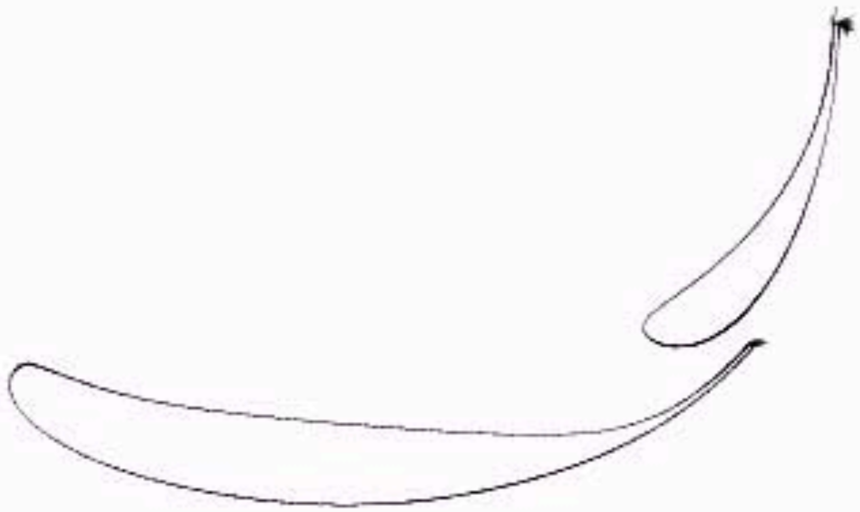

3D - Boundaries

Cost

No theory of convergence

....

Particles strike back : SPH (Monaghan, Lucy, 1970's)

GRID FREE + LAGRANGIAN/ADAPTIVE + NO POISSON EQUATION

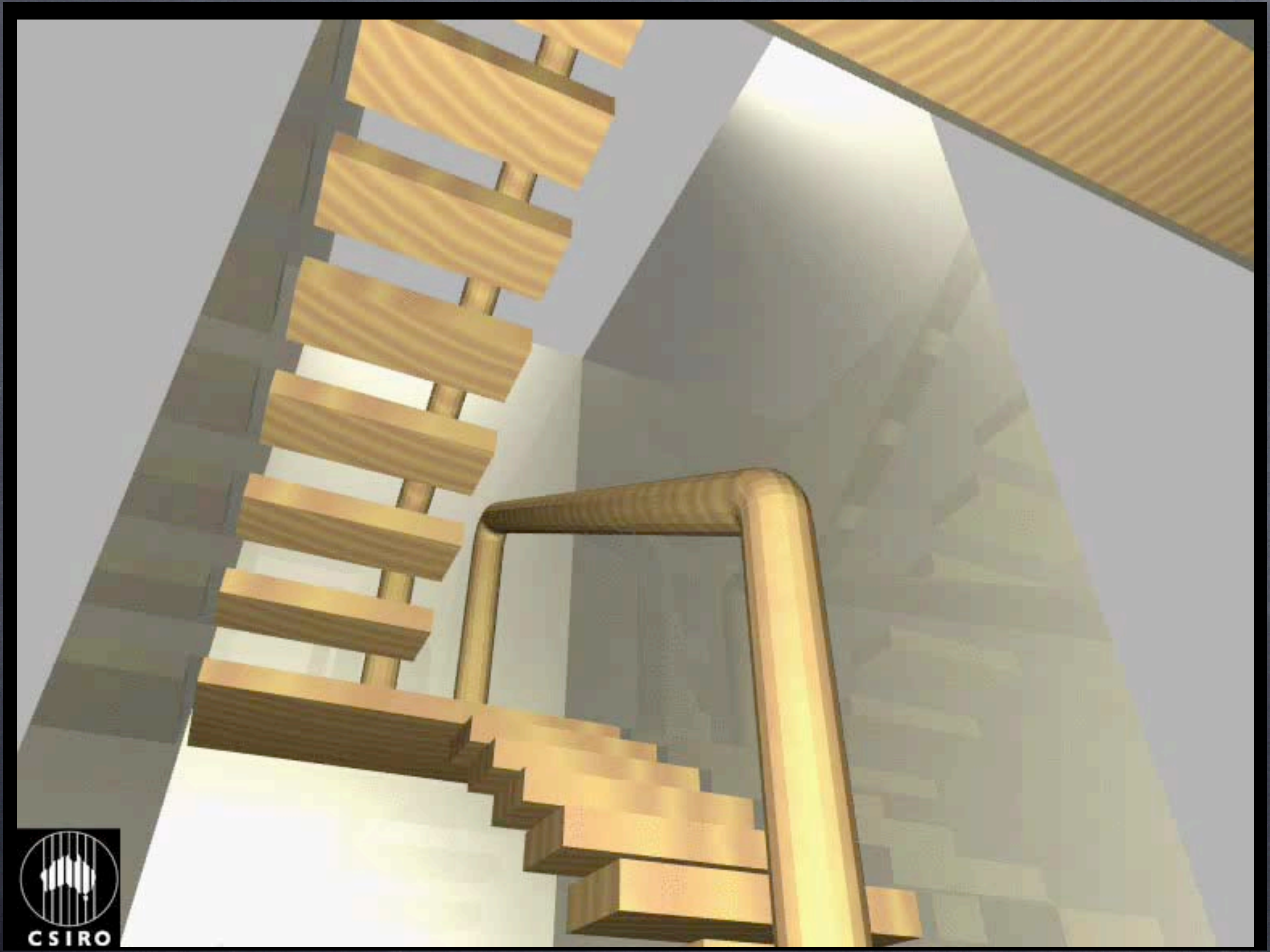

Growth of Black Holes
Springel, MPI – Hernquist, Harvard

Lucy, 1974 : A numerical scheme for the testing of the fission hypothesis, Astron. J.

FLUIDS and PARTICLES : CFD and GRAPHICS

Star Trek

How does it work ?

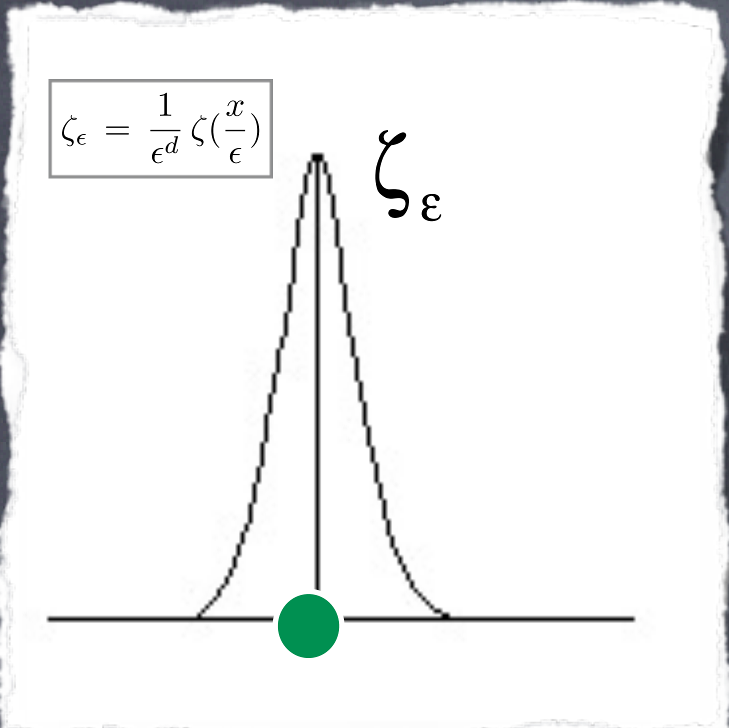

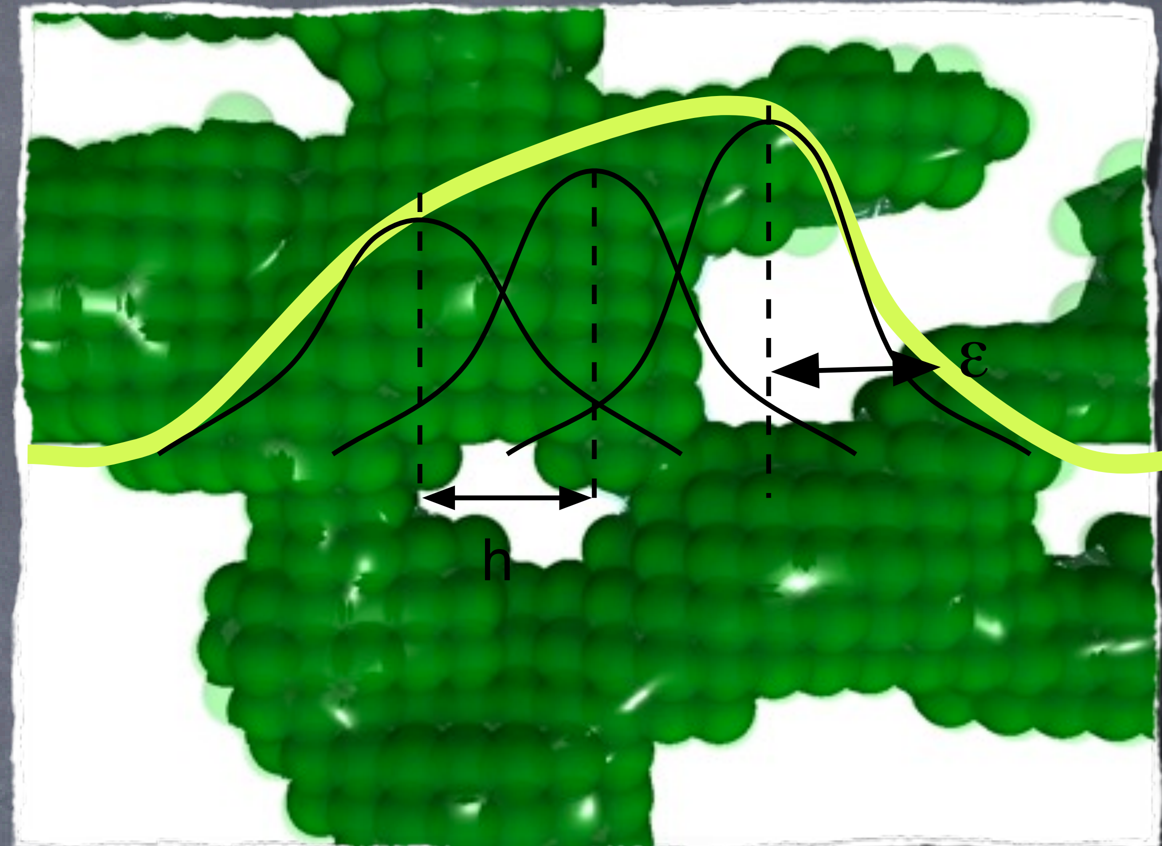

Particles $p = 1, \cdots, N$

locations x_p **volumes** $v_p = h_p^d$

properties

$\mathbf{Q}_p(t) = q(x_p, t)$

Function approximation $$q_\epsilon^h(x,t) = \sum_{p=1}^{N_p} h_p^d \, Q_p(t) \, \zeta_\epsilon(x - x_p(t))$$

Interface Tracking versus Capturing

Tracking

- Explicit description
- Lagrangian framework
- Interface distortion requires reseeding

Capturing

- Implicit description
- Eulerian framework

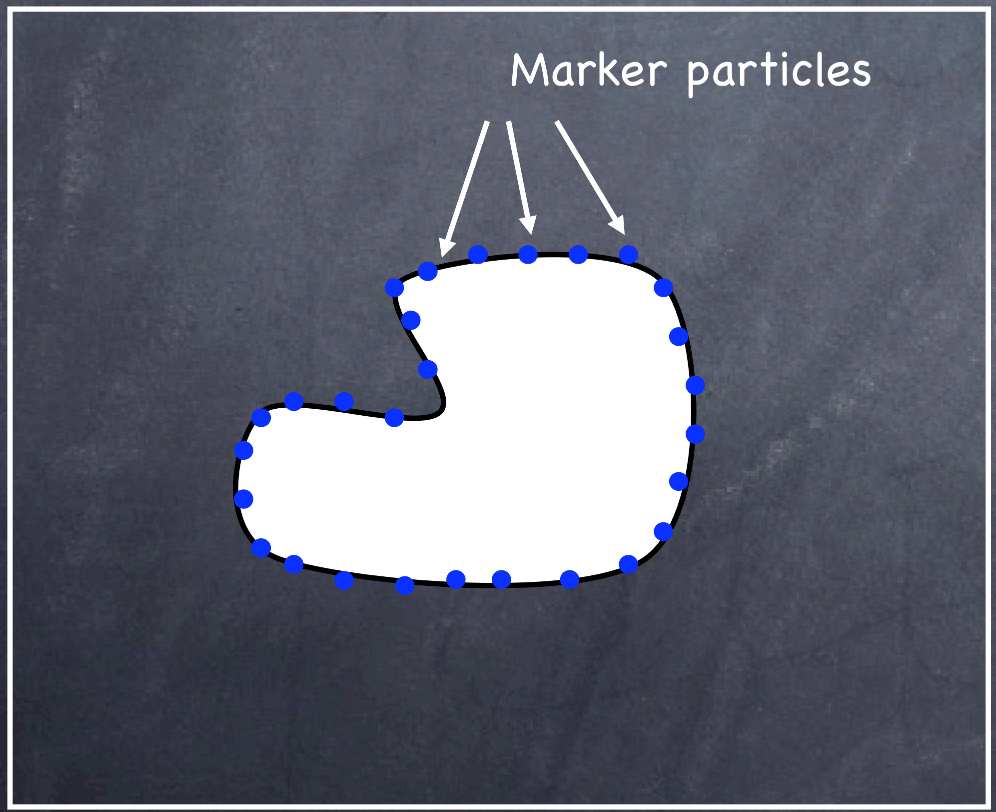

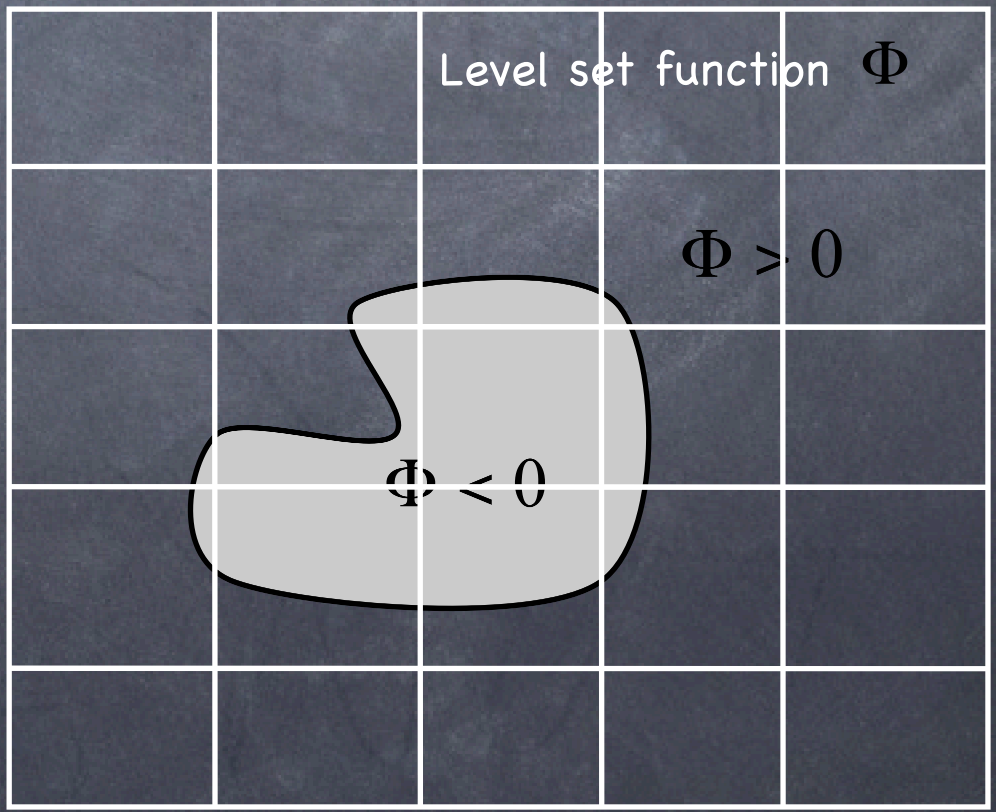

PARTICLE METHODS : Geometry

Volume particles

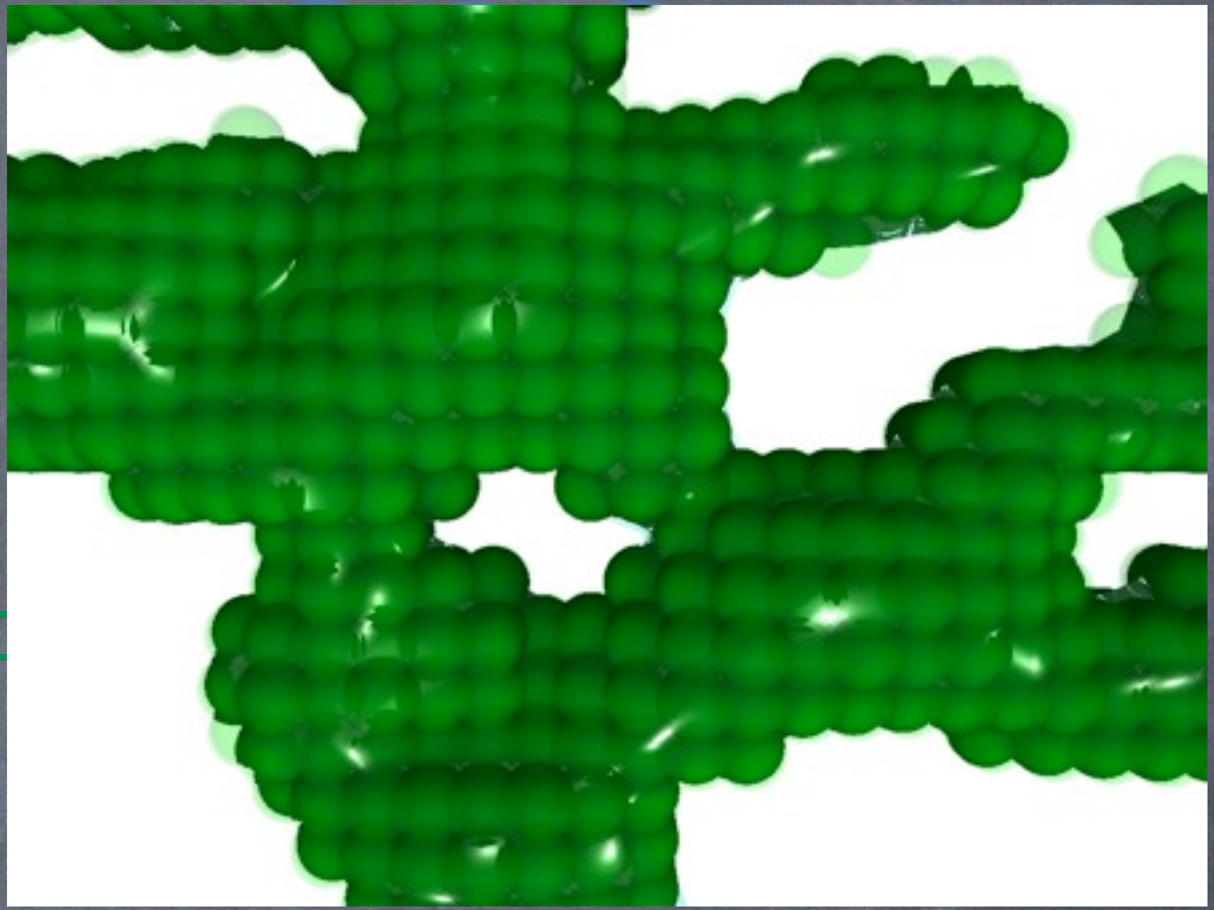

- Particles are quadrature points
- Easy to discretize COMPLEX GEOMETRI

Surface particles

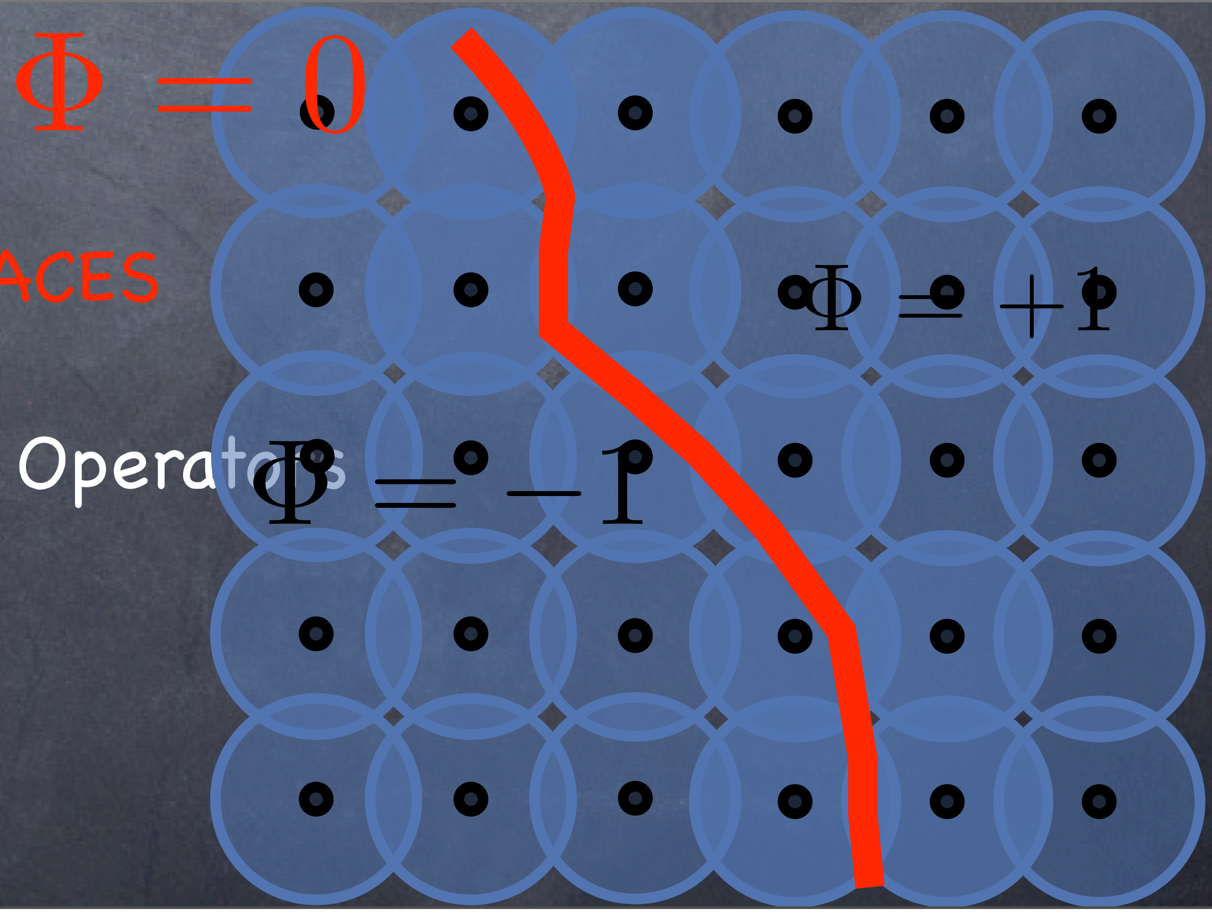

- Particle - Level Sets - COMPLEX SURFACES
- Surface Operators - Anisotropic Volume Operators

PARTICLES + LAGRANGIAN ADAPTIVITY

$$\frac{\partial q}{\partial t} + \nabla \cdot (\boldsymbol{u} q) = \mathcal{L}(q, x; t)$$

Lagrangian form: $$\frac{Dq}{Dt} = \mathcal{L}(q, x; t)$$

PARTICLES

→ no linear stability constraints
= no CFL (dt<dx/u) condition

		initial values
$\frac{d\mathbf{x}_p}{dt} = \mathbf{u}(\mathbf{x}_p, t)\,,$	positions	on lattice
$\frac{dv_p}{dt} = v_p\ (\nabla \cdot \mathbf{u})\,(\mathbf{x}_p, t)\,,$	volumes	$v_p = h^d$
$\frac{dQ_p}{dt} = v_p\, \mathcal{L}^{\varepsilon,h}(q, \mathbf{x}_p, t)\,.$	weights	$Q_p = q(\boldsymbol{x}_p, 0)\, v_p$

CONTINUUM : Lagrangian Form of Governing Equations

Positions

$$\frac{Dx_p}{Dt} = u_p$$

Volumes

$$\frac{Dv_p}{Dt} = v_p(\nabla \cdot \mathbf{u})_p$$

Mass Conservation

Properties

$$\rho_p \frac{D\mathbf{u_p}}{Dt} = (\nabla \cdot \sigma)_p$$

Momentum Conservation

$$\sigma_p = -p_p I + \bar{\sigma}_p$$

evaluation depends on
the constitutive model

Interfaces

$$\frac{D\Phi_p}{Dt} = 0$$

Particle Level sets : 3D curvature-driven flow: Collapsing Dumbbell

$$\frac{\partial \Phi}{\partial t} + u \cdot \nabla \Phi = 0$$

$$\Gamma(t) = \{\mathbf{x} \in \Omega \mid \phi(\mathbf{x}, t) = 0\}$$

$$|\nabla \phi| = 1$$

$$\frac{\partial \phi}{\partial t} + \kappa\, n \cdot \nabla \phi = 0.$$

$$\kappa = \nabla \cdot n$$

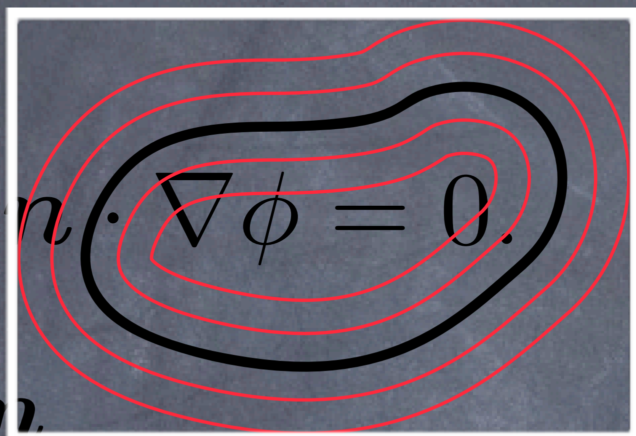

$$\Phi_\epsilon^h(x,t) = \sum_{p=1}^{N_p} h_p^d \, \Phi_p(t) \, \zeta_\epsilon(x - x_p(t))$$

$$\frac{D\Phi_p}{Dt} = 0 \qquad \frac{dx_p}{dt} = \mathbf{u}$$

Particle Approximation

A Lagrangian Particle Level Set Method, Hieber and Koumoutsakos, J. Comp. Phys. 2005

Benchmark: Rigid Body Motion

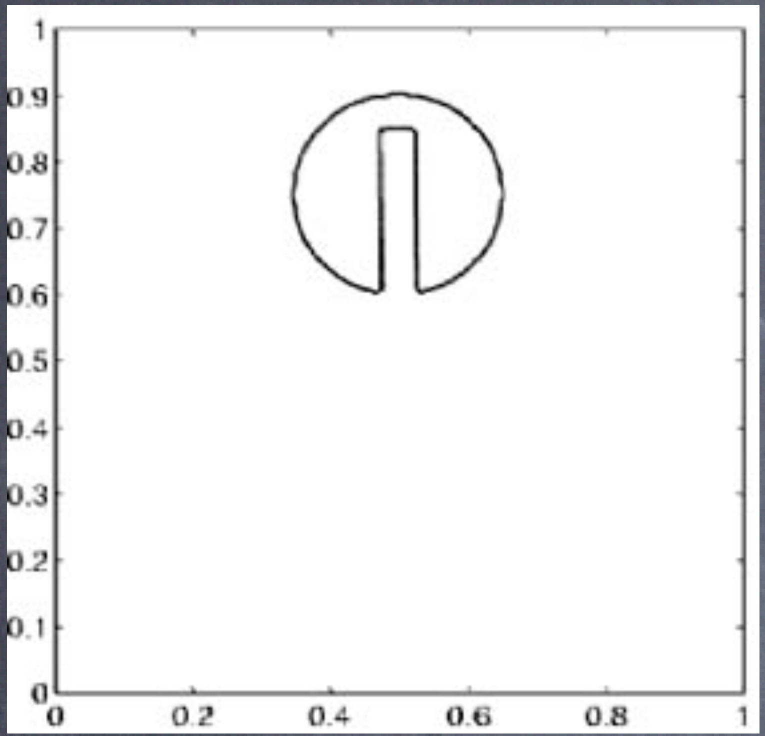

- Problem of rotating slotted disk/sphere
- Particle level sets exact for rigid body motion

Particle level set method

(800 particles)

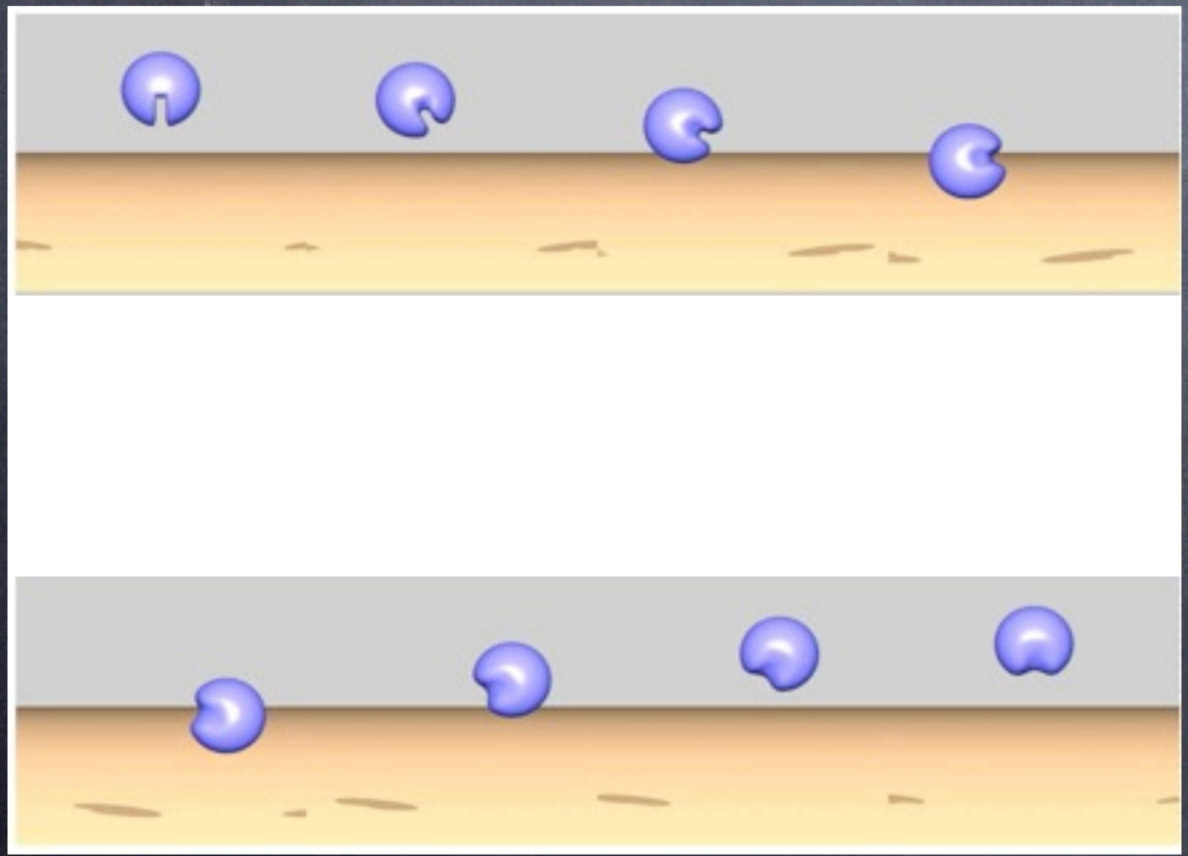

Particle Level Sets (exact !)

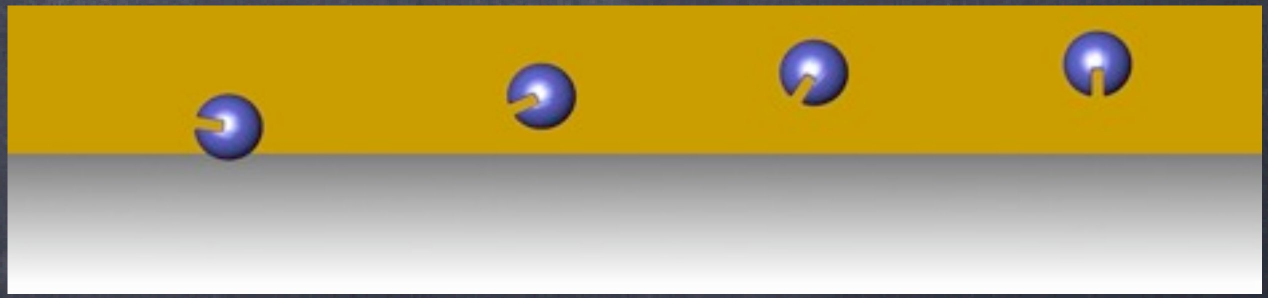

Are grid-free Particle Methods Accurate ?

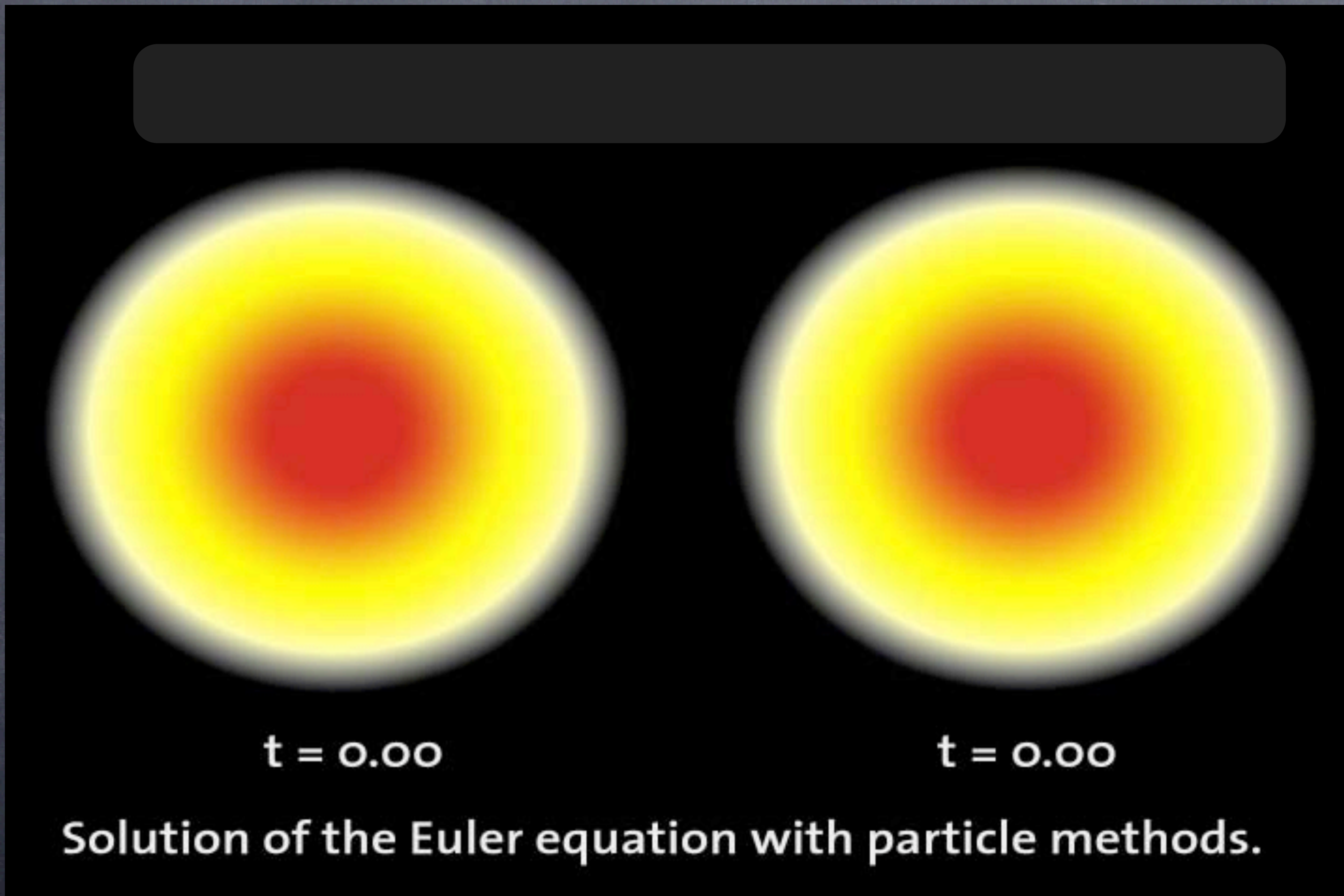

Smooth Particles must Overlap

Particle Approximation =

Mollification

$$\Phi_\epsilon(x) = \int \Phi(y)\,\zeta_\epsilon(x-y)\,dy$$

+

Quadrature

$$\Phi_\epsilon^h(x,t) = \sum_{p=1}^{N_p} h_p^d\,\Phi_p(t)\,\zeta_\epsilon(x - x_p(t))$$

$$||\Phi - \Phi_\epsilon^h|| \leq ||\Phi - \Phi_\epsilon|| + ||\Phi_\epsilon - \Phi_\epsilon^h||$$

$$\leq (C_1\,\epsilon^r + C_2 (\frac{h}{\epsilon})^m)\,||\Phi||_\infty$$

NOTES :

- **Must have** $h/\varepsilon < 1$ for the quadrature to be accurate **i.e. PARTICLES MUST OVERLAP.**
- References : J. Raviart (1970's), O. Hald (1980's), T. Hou (1990's), G.H. Cottet (1990's)

Lagrangian distortion and REMESHING

Particles follow flow trajectories

- distortion of particle locations
- loss of overlap
- loss of convergence

Preventive action: remeshing

Reinitialize particles on a regular grid.

$$Q_{\boldsymbol{i}}^{\text{new}} = \sum_p Q_p \, \zeta^h(\boldsymbol{i}h - \boldsymbol{x}_p)$$

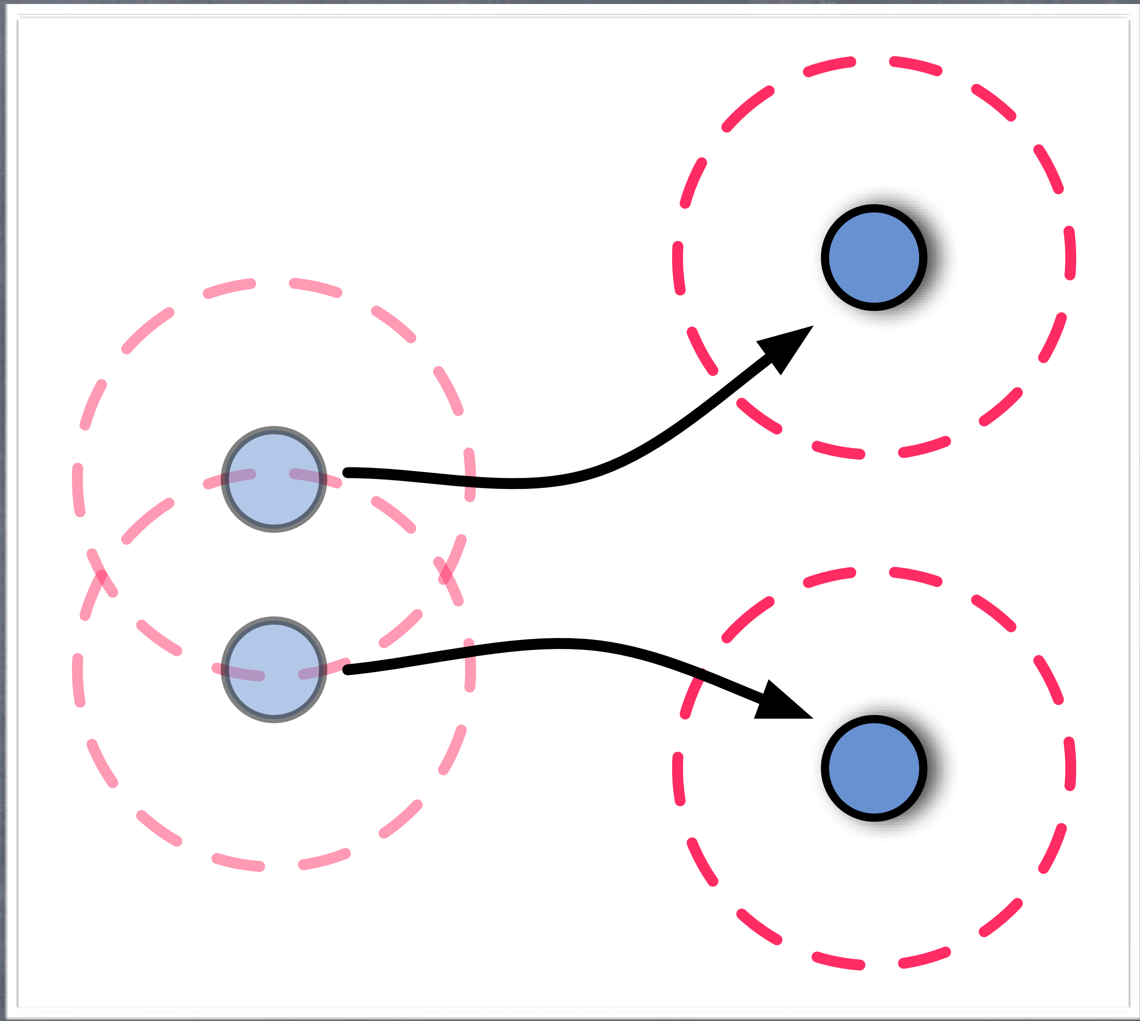

Limiting: Introduction of a grid

Enabling:

- Fast Poisson solvers
- Access versatility of finite differences
- Enabling efficient multiresolution adaptivity

Remeshing = Regularization = Resampling

A new **regularized** particle set from the old one

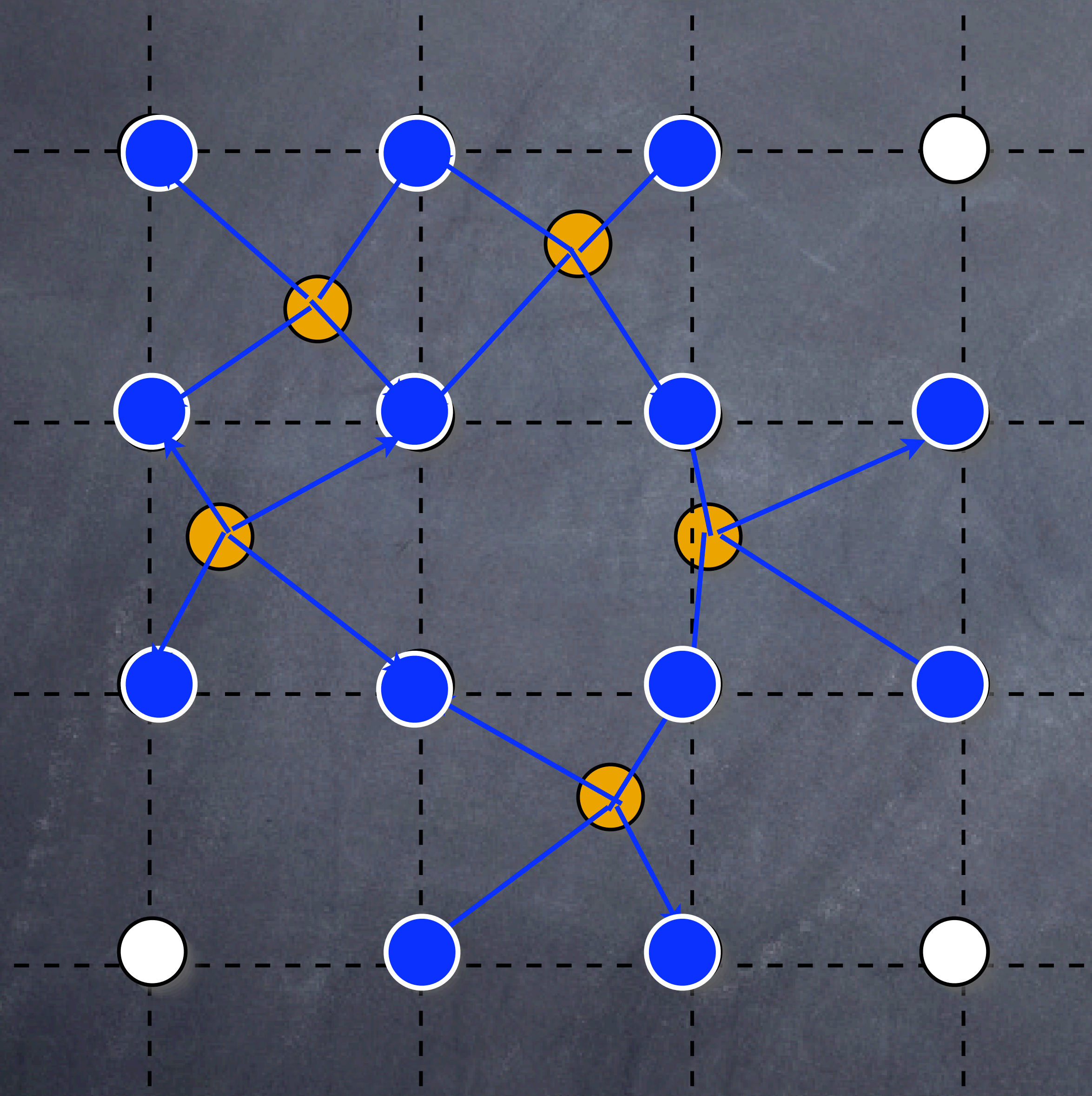

$$Q_p^{\text{new}} = \sum_{p'} Q_{p'} M(j\,h - x_{p'})$$

Interpolation Kernel $M(x)$

- **Moment conserving**
- Tensorial Product of 1D kernels

REFERENCES :

Vortex Methods : PK and Leonard , JFM, 1995, and PK, JCP, 1997

SPH : Chaniotis, Poulikakos and PK, JCP, 2002

Hybrid Particle Mesh Techniques

step 1 : ADVECT : Particles

step 2 : REMESH : Particles to Mesh nodes

step 3 : SOLVE : field equations / Derivatives on Mesh

step 4 : RESAMPLE : Mesh Nodes BECOME Particles

Particle Methods are adaptive yet Inefficient

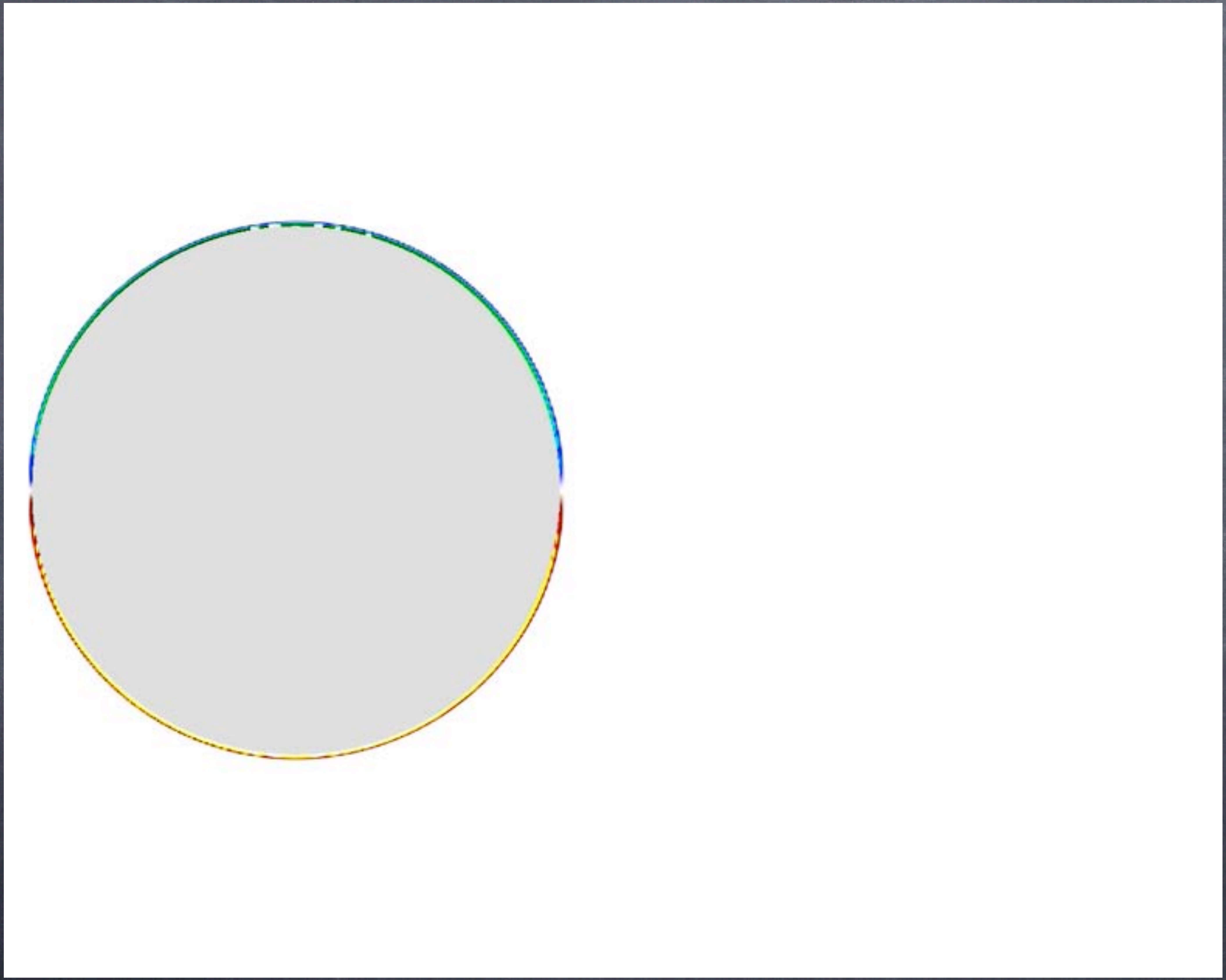

Koumoutsakos and Leonard, JFM,1994

Particles and Multiple Scales/Physics

Wavelet - Particle Method

Keypoints: Wavelets guide particle refinement.
Lagrangian convection of small scales

Multi-Particle Methods

Keypoints: Coupling Discrete and Smooth Particle Methods
Interface of different physics and numerics

While particles are on grid locations

Wavelet-particle method

mollification kernel ⟷ basis/scaling function

Multiresolution analysis (MRA) $\{\mathcal{V}^l\}_{l=0}^{L}$ of particle quantities

Refineable kernels as basis functions of $\mathcal{V}^l$

$$\zeta_k^l = \sum_j h_{j,k}^l \, \zeta_j^{l+1}$$

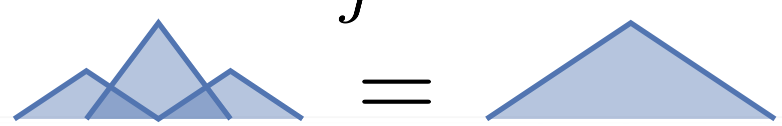

Wavelets as basis functions of the complements $\mathcal{W}^l$

$$\zeta_k^{l+1} = \sum_j \tilde{h}_{j,k}^l \, \zeta_j^l + \sum_j \tilde{g}_{j,k}^l \, \psi_j^l$$

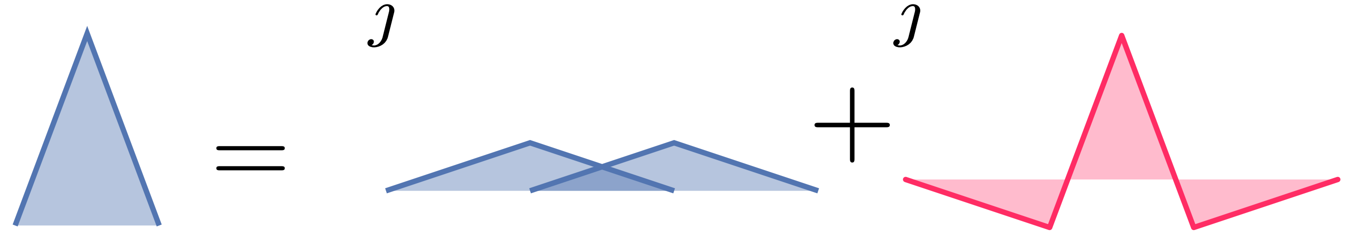

M. Bergdorf, P. Koumoutsakos. A Lagrangian Particle-Wavelet Method. Multiscale Modeling and Simulation: A SIAM Interdisciplinary Journal, 5(3), 980-995, 2006

Multiresolution function representation:

Analysis (collocation): d^l_k ~ | fine - Prediction(coarse) |

$$q^L = \sum_k c^0_k \, \zeta^0_k + \sum_{l<L} \sum_k d^l_k \, \psi^l_k$$

GROUND LEVEL

DETAIL COEFFICIENTS

WAVELETS

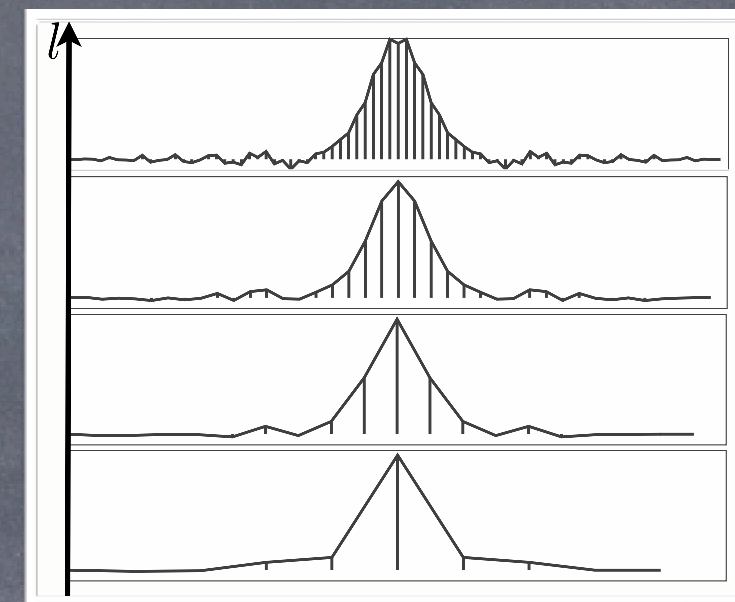

Each wavelet is associated with a specific grid point/particle (2D)

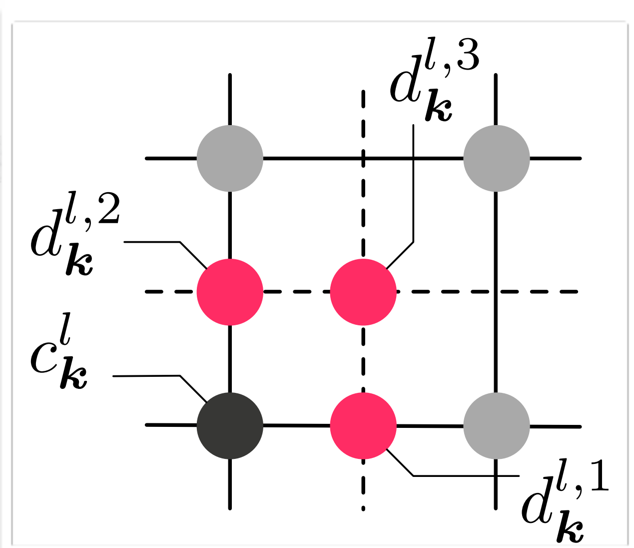

Compression/Adaptation:

Discard insignificant detail coefficients: $|d^{l,m}_{\boldsymbol{k}}| < \varepsilon$

Compressed → Adapted grid

$$\|q^L - q^L_{\geq}\| < \varepsilon$$

Remeshing + MultiResolution Analysis

1. Remesh
2. Wavelets- Compress/Adapt
3. Convect
4. Wavelets Reconstruct
5. GOTO 1

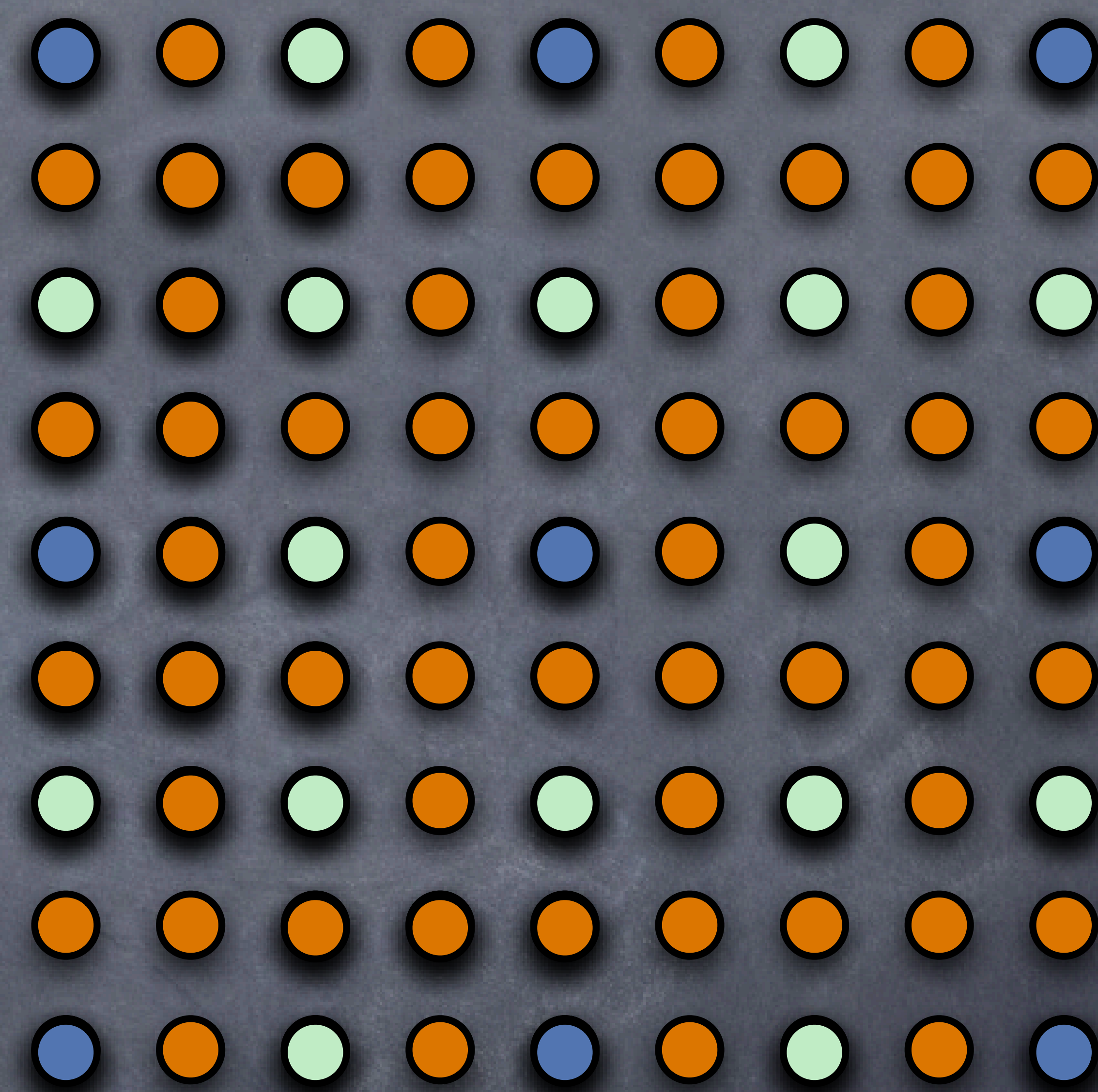

$$q^L = \sum_k c_k^0 \, \zeta_k^0 + \sum_{l<L} \sum_k d_k^l \, \psi_k^l$$

"ground" level

detail coefficients

wavelets

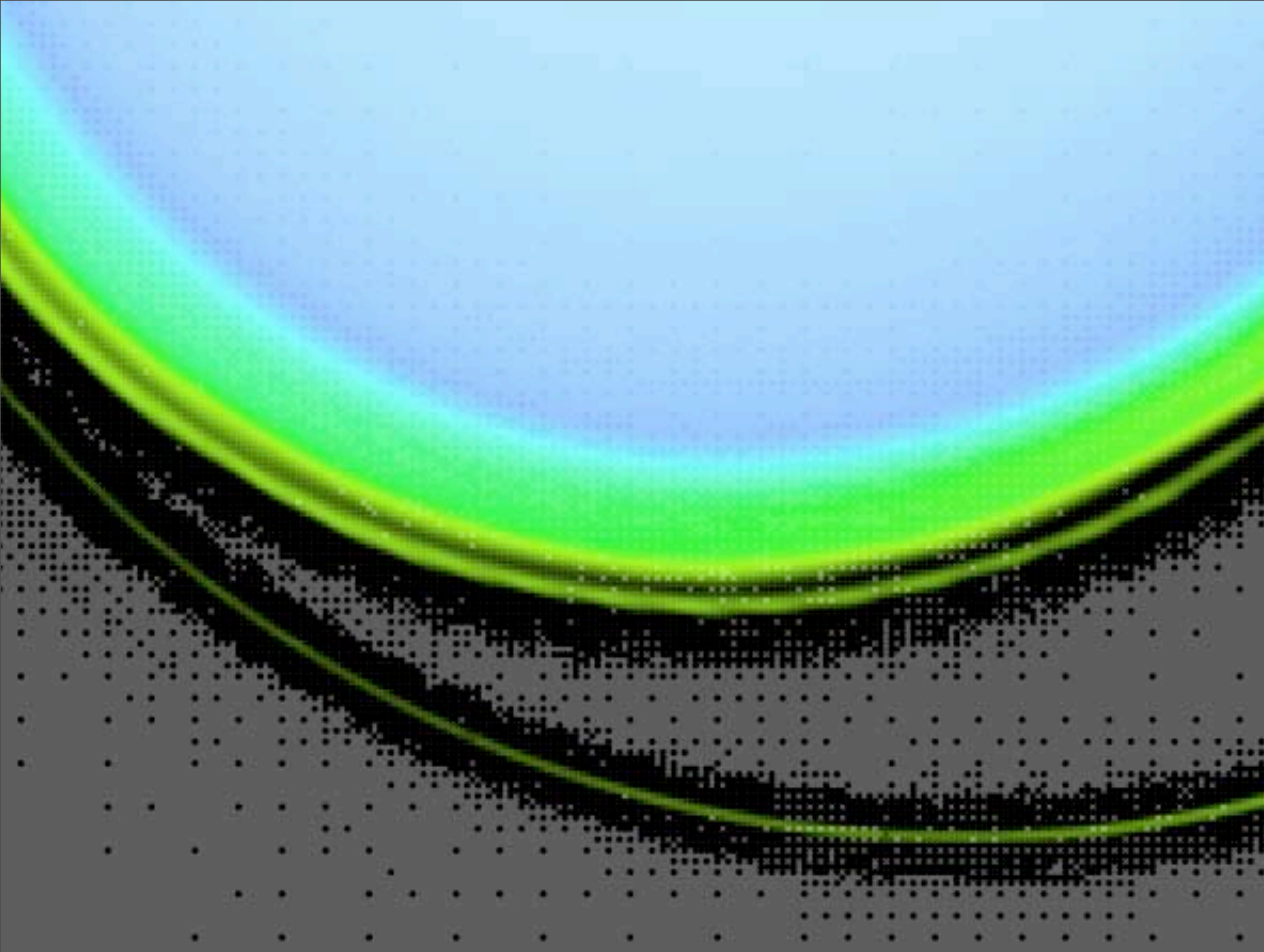

Wavelet - Particle Level sets

$$\frac{\partial \Phi}{\partial t} + \mathbf{u} \cdot \nabla \Phi = 0$$

$$\mathbf{u} = \mathbf{n} \nabla \cdot \mathbf{n}$$

$$\Gamma(t) = \{\mathbf{x} \in \Omega \mid \phi(\mathbf{x}, t) = 0\}$$

$$|\nabla \phi| = 1$$

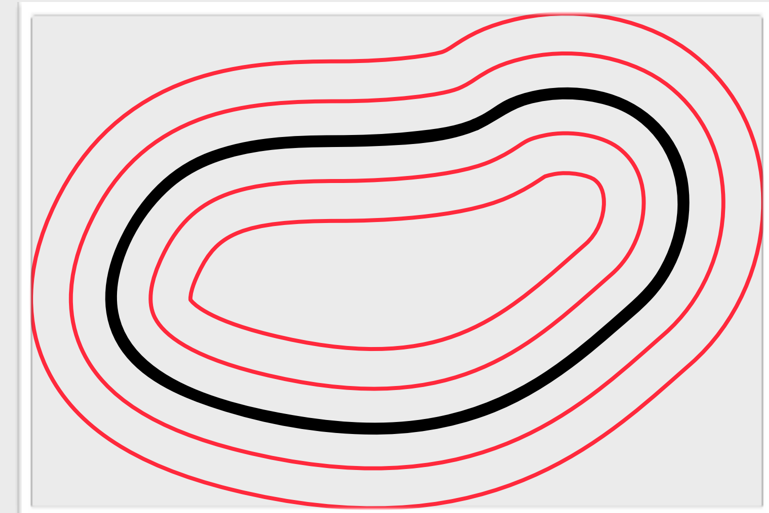

Solve with particles:

$$\Phi_\epsilon^h = \sum_{p=1}^{N_p} h_p^d \, \Phi_p(t) \, \zeta_\epsilon(x - x_p(t))$$

$$\frac{dx_p}{dt} = \mathbf{u}_p \qquad \frac{d\Phi_p}{dt} = 0$$

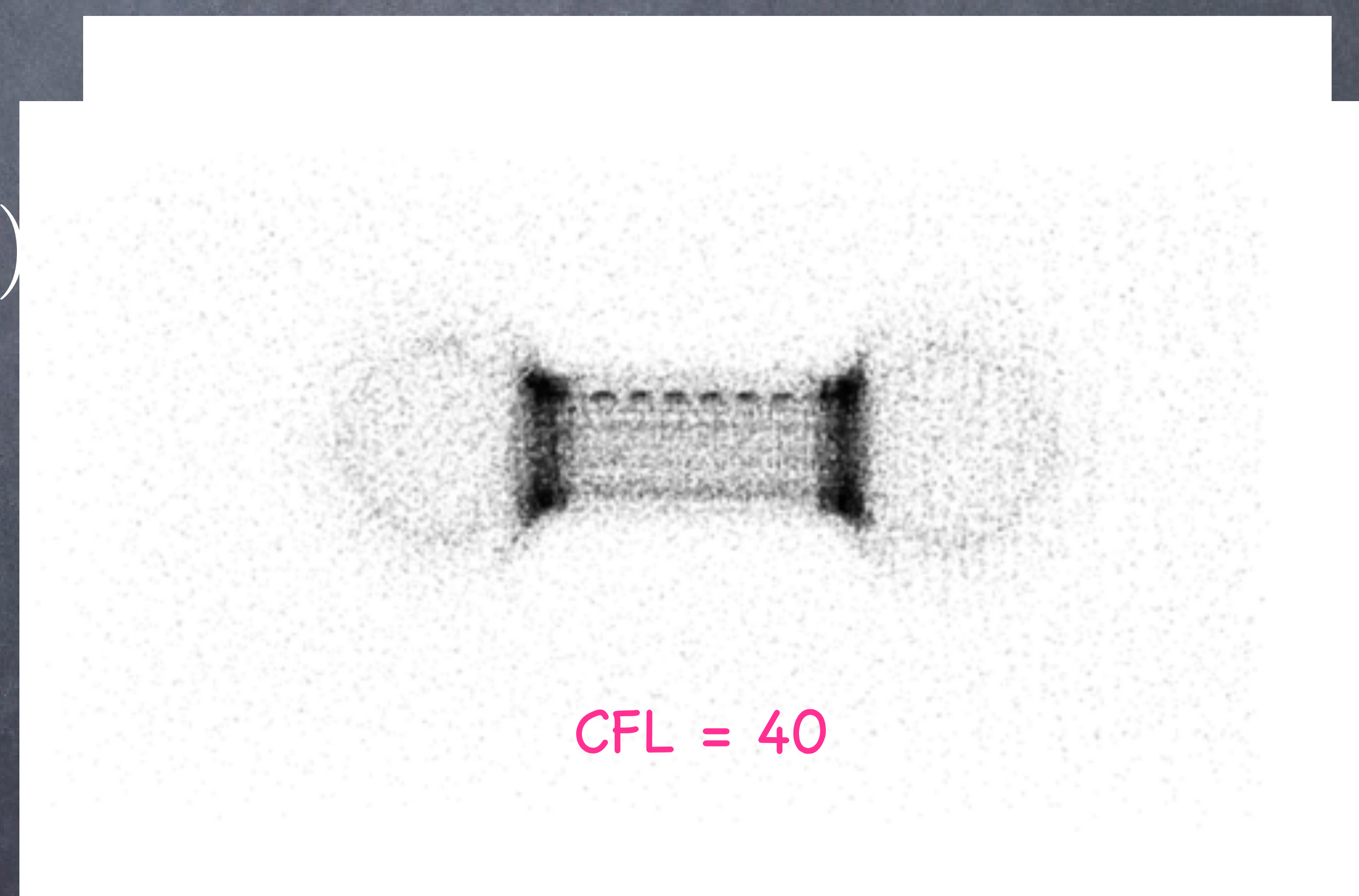

Hieber and Koumoutsakos, J. Comp. Phys. 2005
Bergdorf and Koumoutsakos, SIAM Multisc. Mod. Simul., 2007

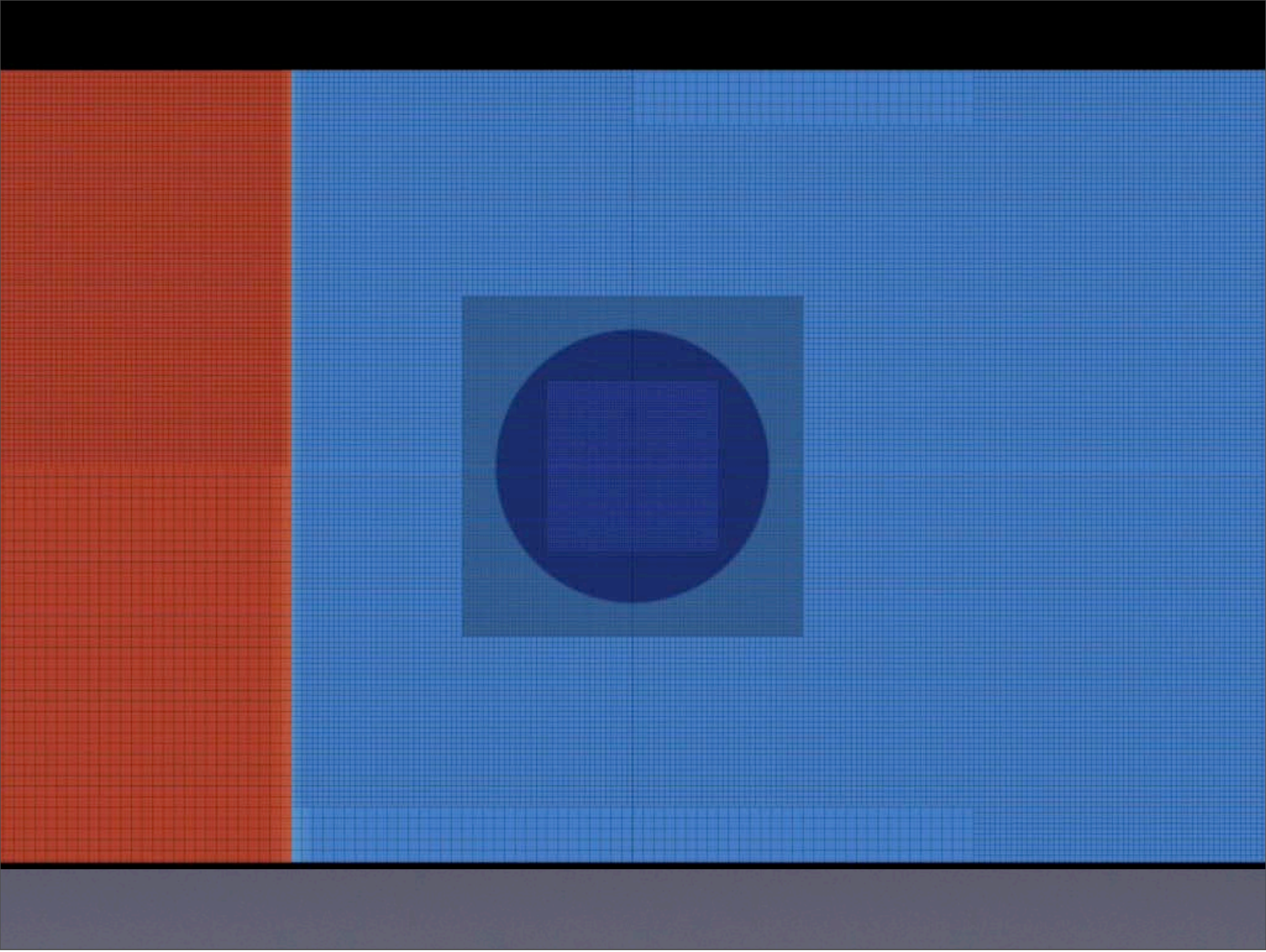

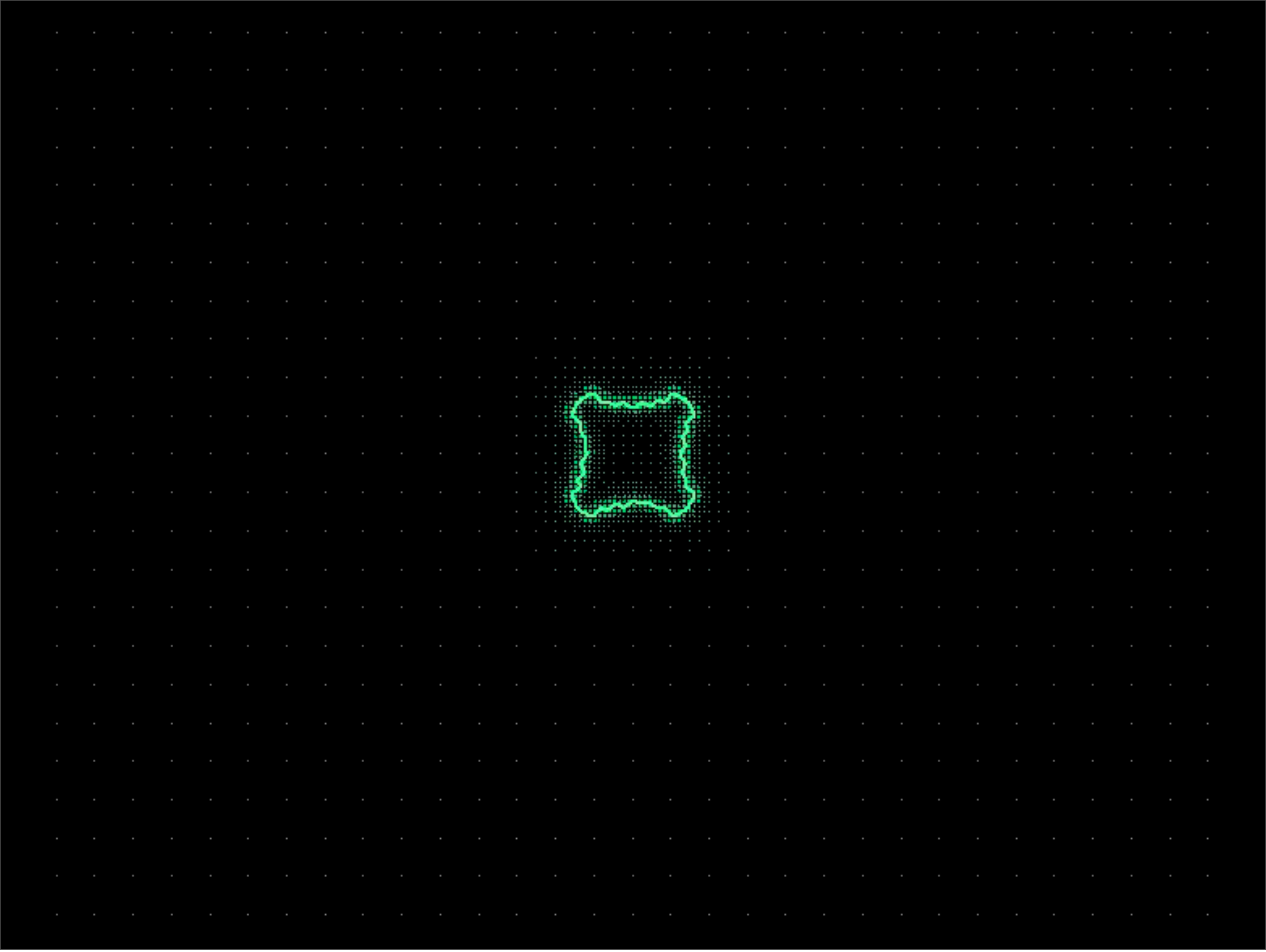

Wavelet Particle Level sets - 3D

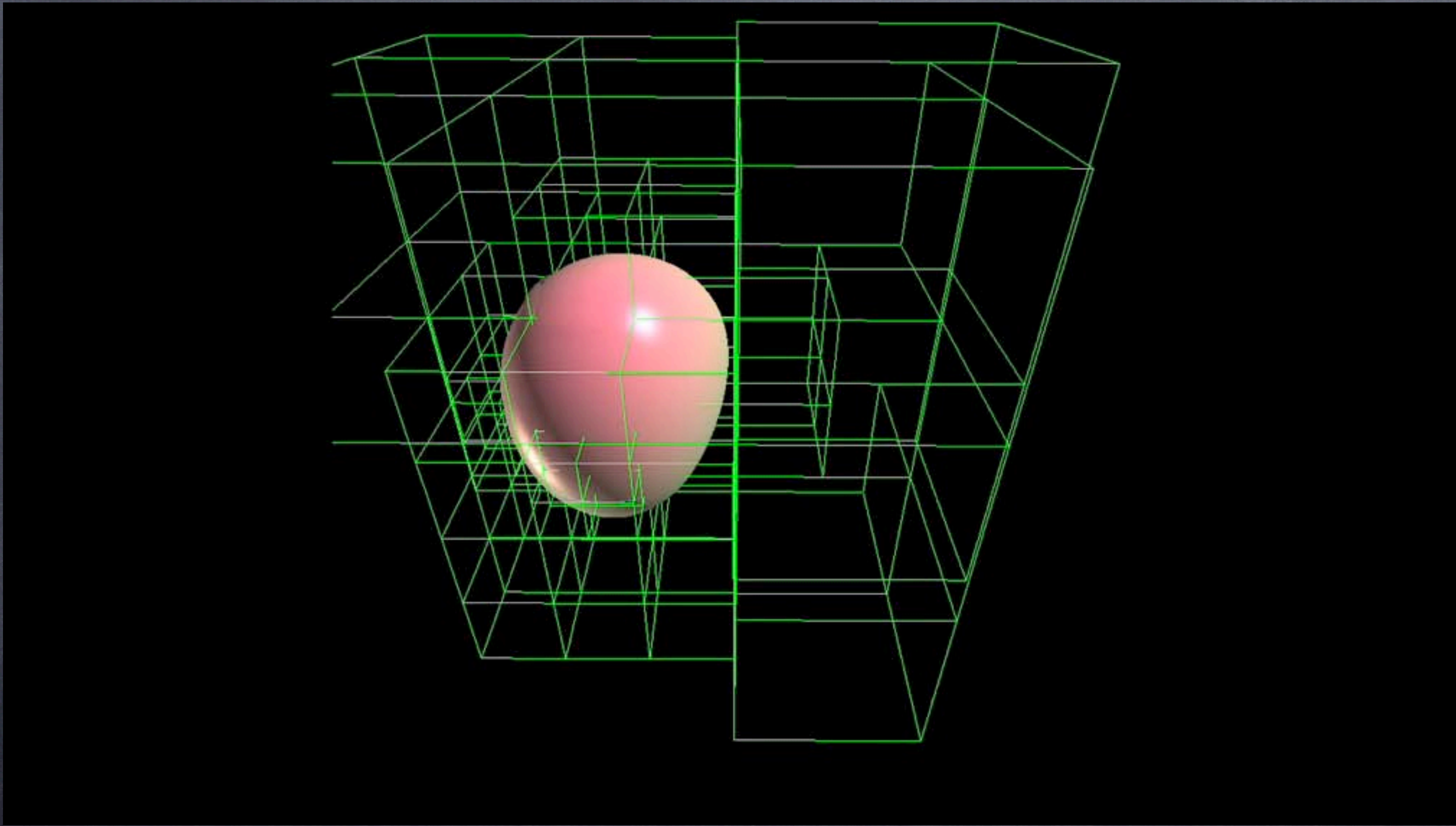

Key Issues : Data Structures & Software Engineering

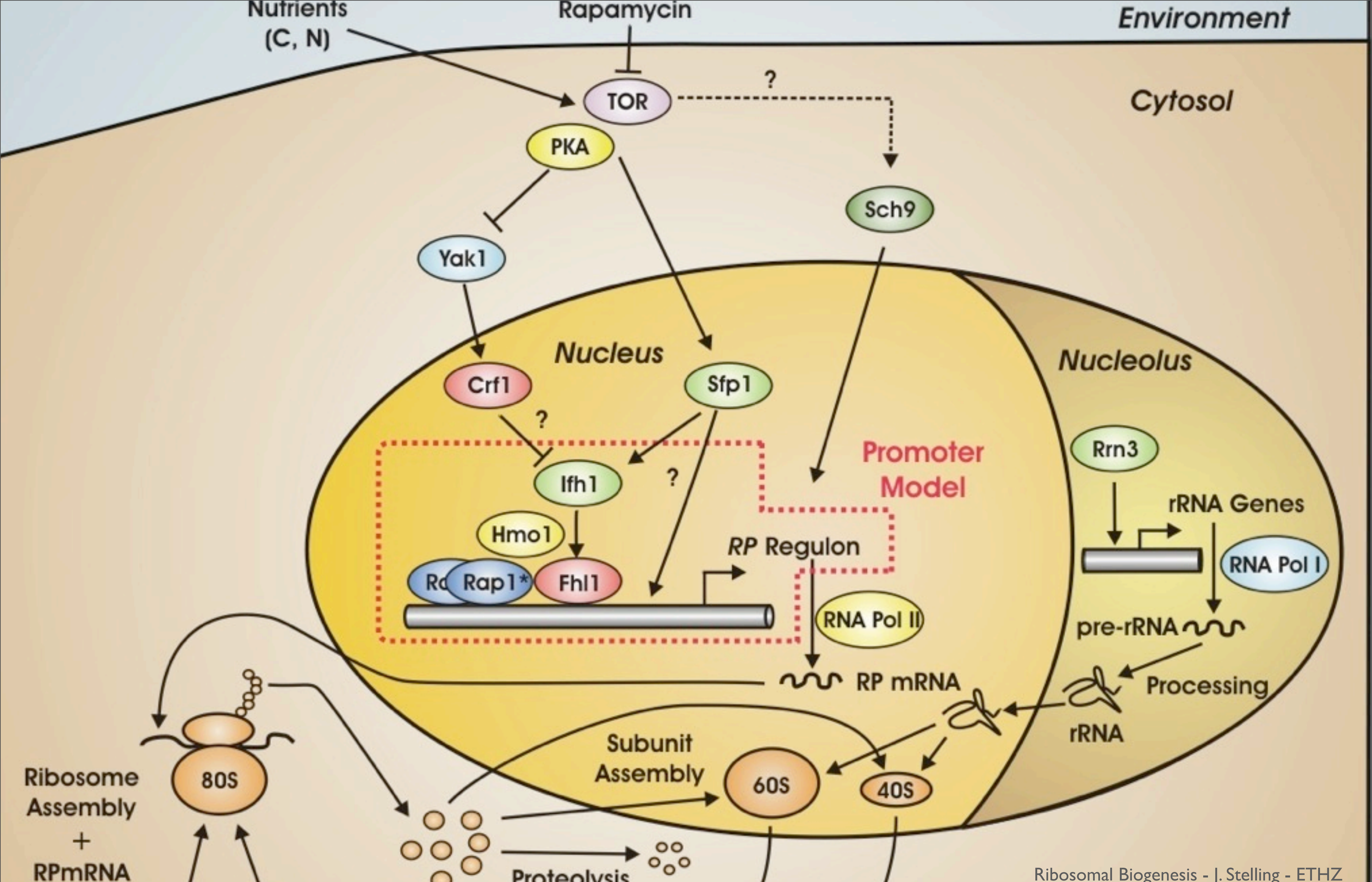

Stochastic Simulation Algorithms

Stochastic Simulation Algorithm

Gillespie,J. Comp. Phys. 1977

- For **M reactions**, time until any reaction

$$\tau \sim \mathcal{E}(1/a_0) \qquad a_0 = \sum_{j=1}^{M} a_j$$

- Reaction index : point-wise distribution $p(j = l) = \frac{a_l}{a_0}$

- One timestep:
  - Sample **τ**
  - Sample the index j
  - Update the X_i, t=t+**τ**

exact BUT slow

- The SSA simulates every reaction event !

SSA : acceleration in time

Gillespie,J. Chem. Phys. 2001

- **τ-leaping** : several reaction events over one time step,

- **Assumption** : reaction propensities a_i remain essentially constant over τ, in spite of several firings

  - Over this given τ, the number of reaction firings K^{P}_{j} is governed by a Poisson distribution

$$K_j^{\mathcal{P}} \sim \mathcal{P}(a_j \tau)$$
$$\mathbf{X}(t+\tau) = \mathbf{X}(t) + \sum_{j=1}^{M} K_j^{\mathcal{P}} \boldsymbol{\nu}_j .$$

Cost ~ M Poisson samplings

τ leaping : Fast BUT Inexact

- τ leaping : Can generate negative populations

- Binomial τ leaping : Approximate the unbounded Poisson distributions with Binomial ones

  Tian & Burrage, J. Chem. Phys. 2004

  Chatterjee et al., J. Chem. Phys. 2005

- Modified τ leaping

  Cao et al., J. Chem. Phys. 2005

  - Critical reactions, i.e. those likely to drive some populations negative, handled by SSA
  - Other reactions advanced by τ leaping

R-leaping : Accelerate SSA by reaction leaps

Leaps : **prescribe number of firings L across all channels**

- Time increment τ_L is Gamma-distributed $\tau_L \sim \Gamma(L, 1/a_0(\mathbf{x}))$
- In this interval we will have K_m firings of channel R_m
- with : $$\sum_{m=1}^{M} K_m = L$$
- In R-leaping, (as in SSA), the index j of every firing obeys a point-wise distribution

$$P(j = l) = \frac{a_l(\mathbf{x})}{a_0(\mathbf{x})} \quad \text{for } l = 1, \ldots, M.$$

Auger, Chatelain, Koumoutsakos, **R-leaping: Accelerating the stochastic simulation algorithm by reaction leaps**.
J. Chem. Phys. , 125, 84103, 2006

R-leaping : One step

Auger, Chatelain, Koumoutsakos
J. Chem. Phys. 125, 84103, 2006

- Define L

$$\tau_L \sim \Gamma(L, 1/a_0(\mathbf{x}))$$

- Sample the index j

$$P(j = l) = \frac{a_l(\mathbf{x})}{a_0(\mathbf{x})} \quad \text{for } l = 1, \dots, L.$$

- Number of reactions for channel m

$$K_m = \sum_{l=1}^{L} \delta_{l,m}$$

- Update species and time :

$$\mathbf{X}(t + \tau_L) = \mathbf{X}(t) + \sum_{j=1}^{M} K_j \boldsymbol{\nu}_j$$

R-leaping : Accelerate SSA by reaction leaps

- L firings distributed across M reaction channels
  - In τ leaping: K^{P}_{j} are independent Poisson variables.
  - In R-leaping, K_j are not independent.
- L as a control parameter
  - System can be brought to a desired state X
  - Time is not a-priori specified
  - New approaches to controlling negative species

R-leaping : How to Sample the the M K_j

R_0 `Algorithm`

- Pointwise Sampling of **L** *independent* reaction indices

$$p(j = l) = \frac{a_l}{a_0}$$

  - Simple BUT scales with L - close to the work load of SSA!

Reaction index →

Firing ↓

	1	2	3	...	M
1	x				
2			x		
3					x
...			x		
L	x				
K	2		2		1

Ro-sampling scales with L and, in particular when compared with τ -leaping that scales with M, the method is inefficient for large leap sizes, L ≫ M.

R-Leaping Theorem

The distribution of K_1 is a binomial distribution :

$$\mathcal{B}(L, a_1(\mathbf{x})/a_0(\mathbf{x}))$$

and for every $m \in \{2, \ldots, M\}$ the conditional distribution of K_m

given the event $\{(K_1, \ldots, K_{m-1}) = (k_1, \ldots, k_{m-1})\}$ is

$$K_m \sim \mathcal{B}\left(L - \sum_{i=1}^{m-1} k_i, \frac{a_m(\mathbf{x})}{a_0(\mathbf{x}) - \sum_{i=1}^{m-1} a_i(\mathbf{x})}\right).$$

This result is invariant under any permutation of the indices

R-leaping : How to Sample the the M K_j

R_0 Algorithm

- Pointwise Sampling of **L** *independent* reaction indices

$$p(j = l) = \frac{a_l}{a_0}$$

  - Simple BUT scales with L - close to the work load of SSA!

Ro-sampling scales with L and, in particular when compared with τ -leaping that scales with M, the method is inefficient for large leap sizes, L ≫ M.

Reaction index →

Firing ↓

	1	2	3	...	M
1	x				
2			x		
3					x
...			x		
L	x				
K	2		2		1

R_1 Algorithm

- Sampling **M** *correlated* binomial variables

$$\mathcal{B}(L, a_j/a_0)$$

  - Create correlations with conditional distributions

$$\text{If } K_i = k_i, \forall i < m,$$

$$K_m \sim \mathcal{B}\left(L - \sum_{i=1}^{m-1} k_i, \frac{a_m}{a_0 - \sum_{i=1}^{m-1} a_i}\right)$$

Reaction index →

Firing ↓

	1	2	3	...	M
1	x				
2			x		
3					x
...			x		
L	x				
K	2		2		1

R-leaping : Efficient Sampling / Sorting

- **Sampling the M K_j efficiently (SORT the reactions)**
  - **M** can be large (~10²) for bio-chemical systems!
  - Efficient sampling effectively loops over a fraction of **M**.

Number of binomial samples per time step
LacYLacZ activities in E. Coli., M=22

- The larger the system, the bigger the payoff.
- The more disparate the reaction rates are, the smaller the fraction.
- Price to pay: carry out re-ordering often enough (cheap!)

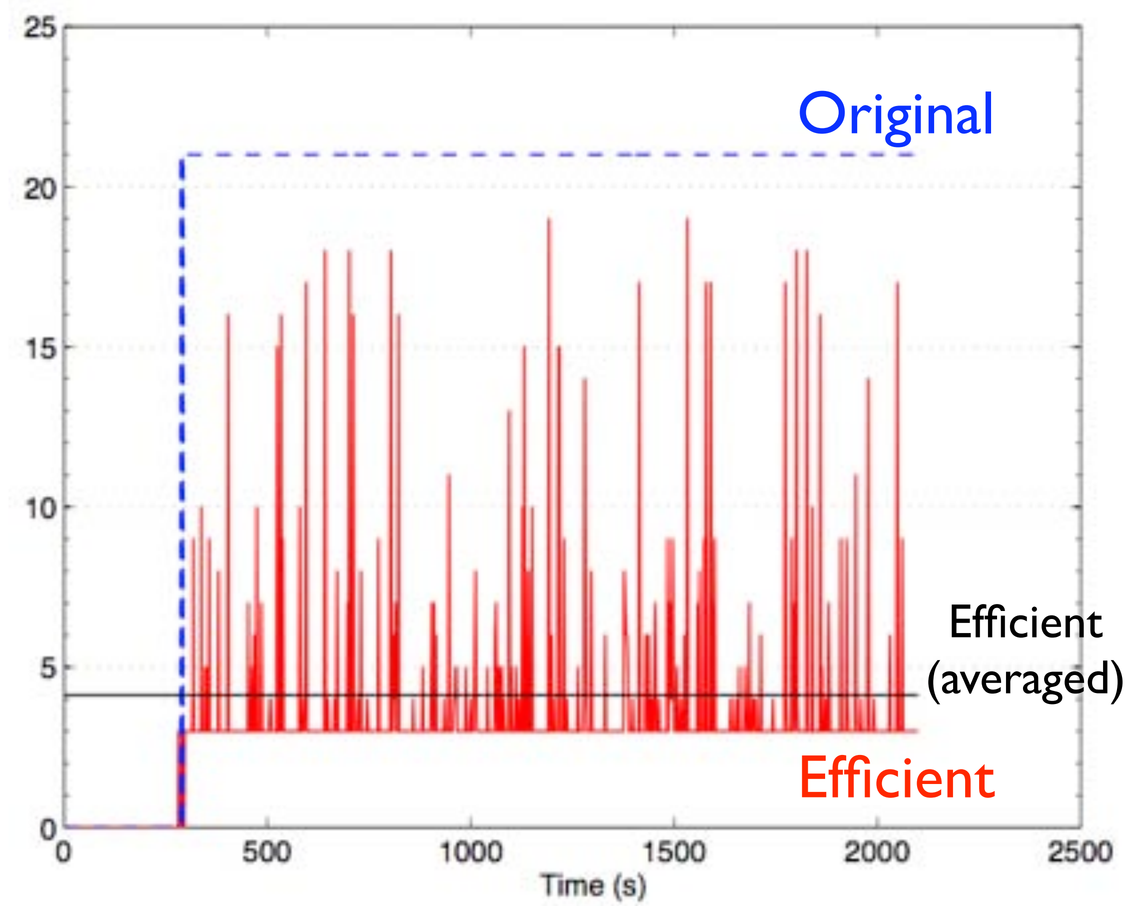

Stochastic simulation: R-leaping

- **Controlling the leap approximation**
  - All three methods of τ leaping are transposable to R-leaping
    - Absolute change of a_j
    - Relative change of a_j
    - Relative change of a_j but efficiently through the relative changes in populations

Results

- **LacZ/LacY genes expression and enzymatic/ transport activities of LacZ/LacY proteins in E. Coli**

Kierzek, Bioiformatics 2002

  - Moderately large system (M = 22)
  - Disparate rates
  - Scarce reactants and negative species

	Reaction Channel	Reaction rate
R_1	PLac + RNAP → PLacRNAP	0.17
R_2	PLacRNAP → PLac + RNAP	10
R_3	PLacRNAP → TrLacZ1	1
R_4	TrLacZ1 → RbsLacZ + PLac + TrLacZ2	1
R_5	TrLacZ2 → TrLacY2	0.015
R_6	TrLacY1 → RbsLacY + TrLacY2	1
R_7	TrLacY2 → RNAP	0.36
R_8	Ribosome + RbsLacZ → RbsRibosomeLacZ	0.17
R_9	Ribosome + RbsLacY → RbsRibosomeLacY	0.17
R_{10}	RbsRibosomeLacZ → Ribosome + RbsLacZ	0.45
R_{11}	RbsRibosomeLacY → Ribosome + RbsLacY	0.45
R_{12}	RbsRibosomeLacZ → TrRbsLacZ + RbsLacZ	0.4
R_{13}	RbsRibosomeLacY → TrRbsLacY + RbsLacY	0.4
R_{14}	TrRbsLacZ → LacZ	0.015
R_{15}	TrRbsLacY → LacY	0.036
R_{16}	LacZ → dgrLacZ	$6.42x10^{-5}$
R_{17}	LacY → dgrLacY	$6.42x10^{-5}$
R_{18}	RbsLacZ → dgrRbsLacZ	0.3
R_{19}	RbsLacY → dgrRbsLacY	0.3
R_{20}	LacZ + lactose → LacZlactose	$9.52x10^{-5}$
R_{21}	LacZlactose → product + LacZ	431
R_{22}	LacY → lactose + LacY	14

Results

- **LacZ/LacY genes expression and enzymatic/ transport activities of LacZ/LacY proteins in E. Coli**
  - Histogram errors vs CPU time

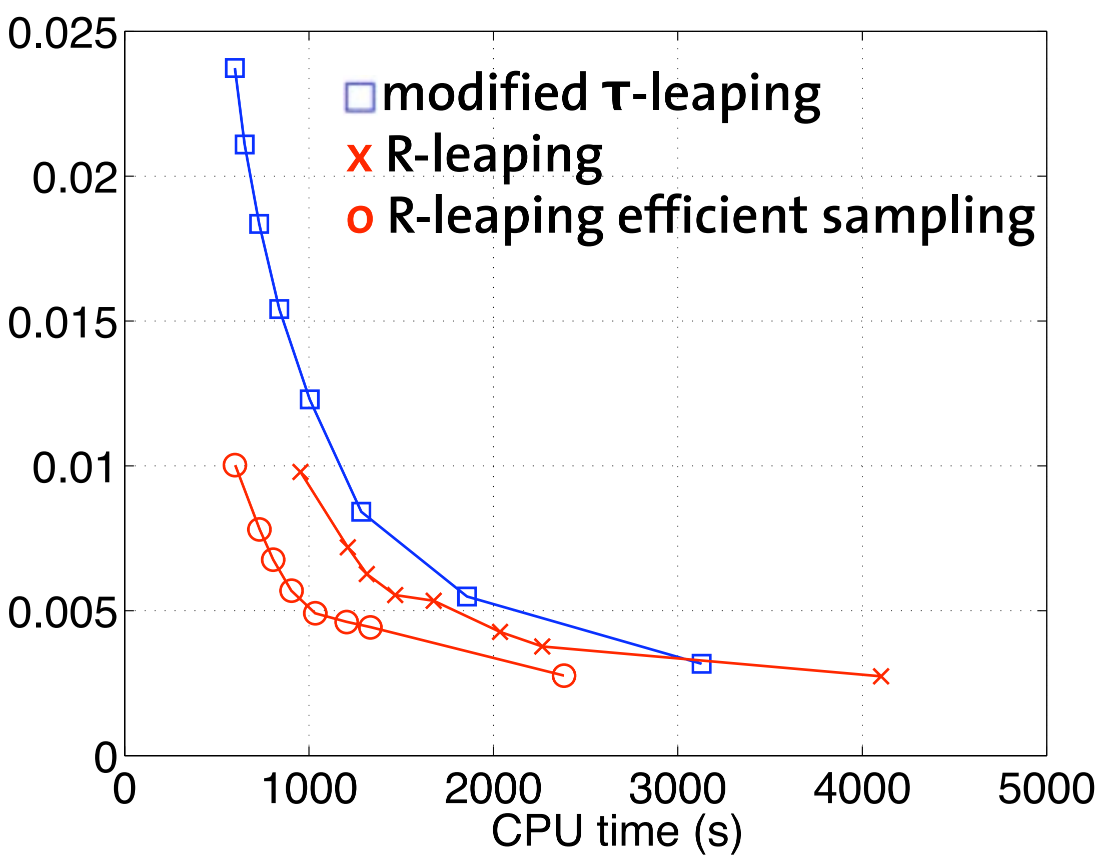

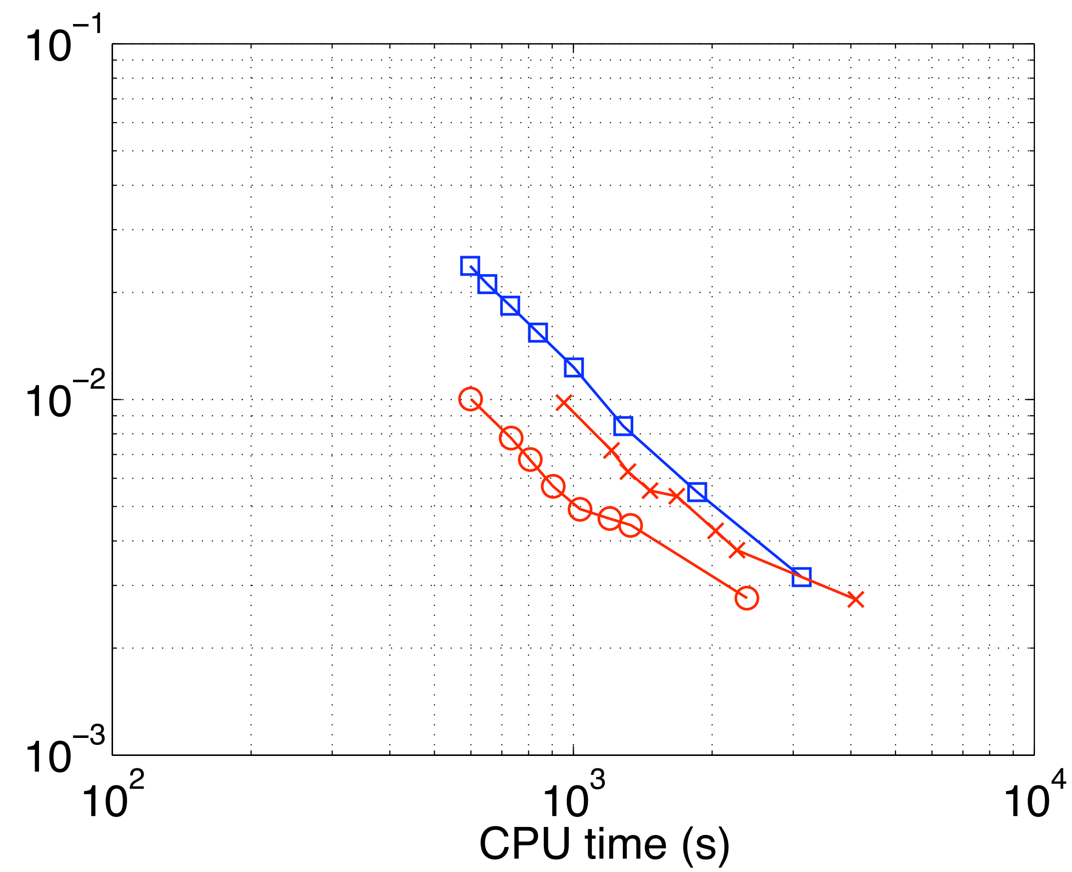

  - Efficient sampling offers factor 2 in speed w.r.t. modified τ-leaping!

R-LEAP for Stochastic Diffusion on Non-uniform Discretizations

Diffusion events between cells, i.e. propensity for diffusion from cell i to cell j: $a_{i,j}(\mathbf{x}) = X_i \cdot k_{i,j}$

Uniform Cells: $k_{i,j} = \dfrac{D}{h^2}$

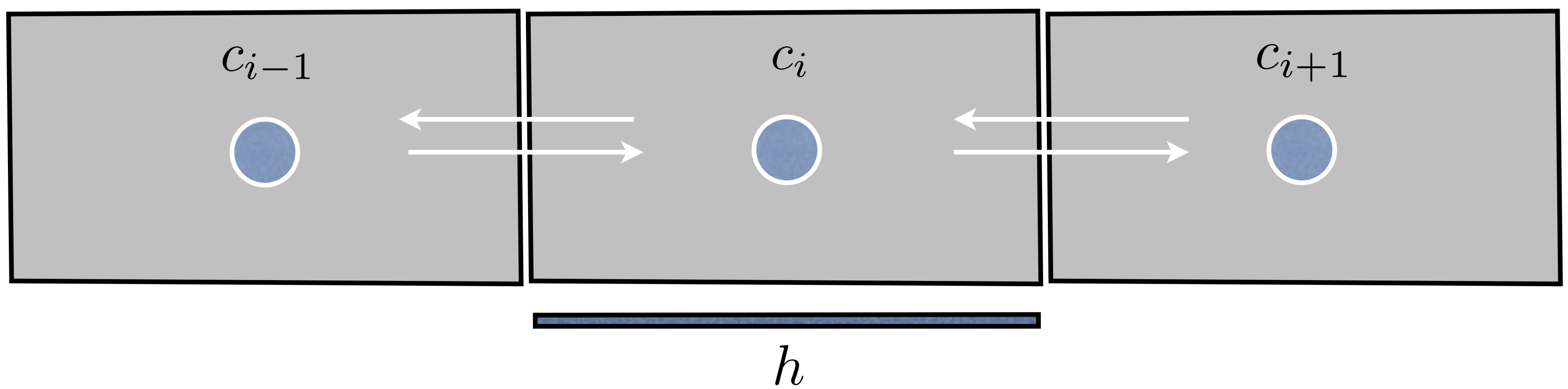

Non-uniform Cells: $k_{i,j} = ?$

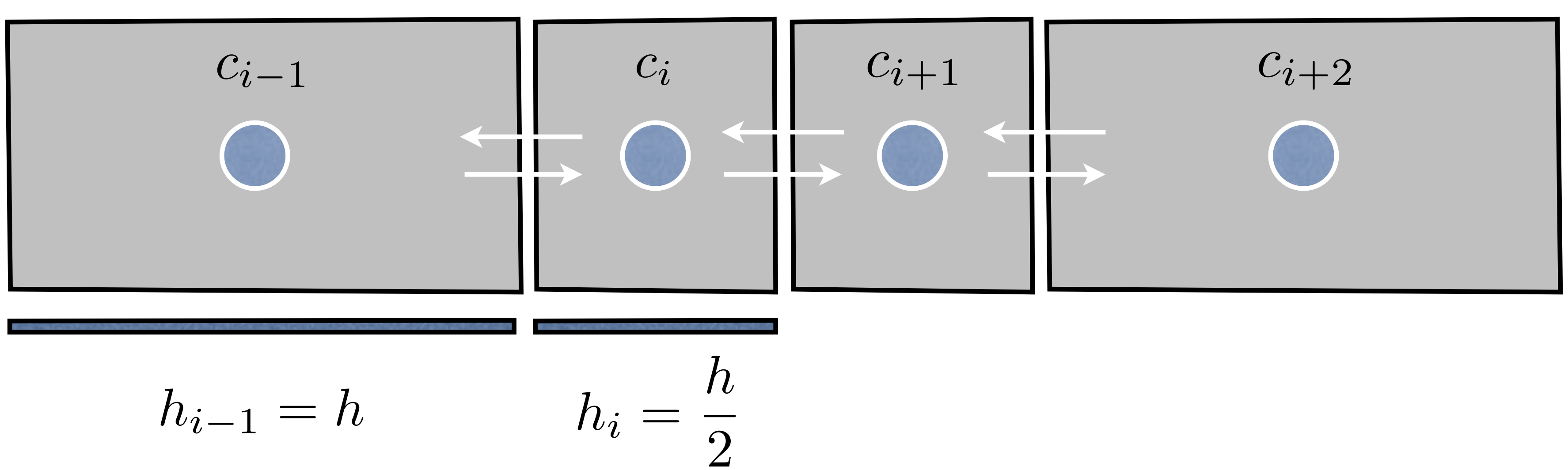

Stochastic Diffusion on Non-Uniform Mesh Using a Finite Volume [1]

Continuum

$$\frac{\partial u}{\partial t} = -\nabla \cdot J$$

$$J = -D(x)\nabla u$$

Diffusion Process

$$\frac{dU_i}{dt} = -(k_{i,i+1} + k_{i,i-1})U_i + k_{i+1,i}U_{i+1} + k_{i-1,i}U_{i-1}$$

$$\frac{\partial U_i}{\partial t} = -\int_i \nabla \cdot J \; dx$$

Using the Divergence Theorem

$$\frac{\partial U_i}{\partial t} = J(c_i - \frac{h_i}{2}) - J(c_i + \frac{h_i}{2})$$

Approximating the Gradient in Fick's Law

$$\nabla u(c_i - \frac{h_i}{2}) \approx \frac{u(c_i) - u(c_{i-1})}{c_i - c_{i-1}} = \frac{1}{c_i - c_{i-1}}\left(\frac{U_i}{h_i} - \frac{U_{i-1}}{h_{i-1}}\right)$$

$$\frac{dU_i}{dt} = -\left(\frac{D_{i,i+1}}{h_i|c_i - c_{i+1}|} + \frac{D_{i,i-1}}{h_i|c_i - c_{i-1}|}\right)U_i + \left(\frac{D_{i+1,i}}{h_{i+1}|c_i - c_{i+1}|}\right)U_{i+1} + \left(\frac{D_{i-1,i}}{h_{i-1}|c_i - c_{i-1}|}\right)U_{i-1}$$

Reaction Rates for Diffusion Events:

$$k_{i,j} = \begin{cases} \frac{D_{i,j}}{h_i|c_i - c_j|} & \text{if } |i-j| = 1 \\ 0 & \text{otherwise} \end{cases}$$

[1] D. Bernstein. Simulating mesoscopic reaction-diffusion systems using the gillespie algorithm. *Phys. Rev. E*, 2005.

SSA using AMR

- Inhomogeneous volume
- random collisions and reactions in each volume element
- different species in each volume element
- Validity of spatial discretization lies in the assumption that:

$$\frac{\tau_R}{\tau_D} \gg 1$$

Kuramato, Prog. Theor. Phys. 1974

- τ_R is the mean free time with respect to reactive collisions in a volume element and τ_D is the mean time during which a molecule will remain in a volume element.
- For a bimolecular reaction with rate k and diffusion coefficient D, this can be estimated by

$$\frac{\hat{\tau}_R}{\hat{\tau}_D} = \frac{D}{h^2 k}$$

Bayati et al., PCCP. 2008

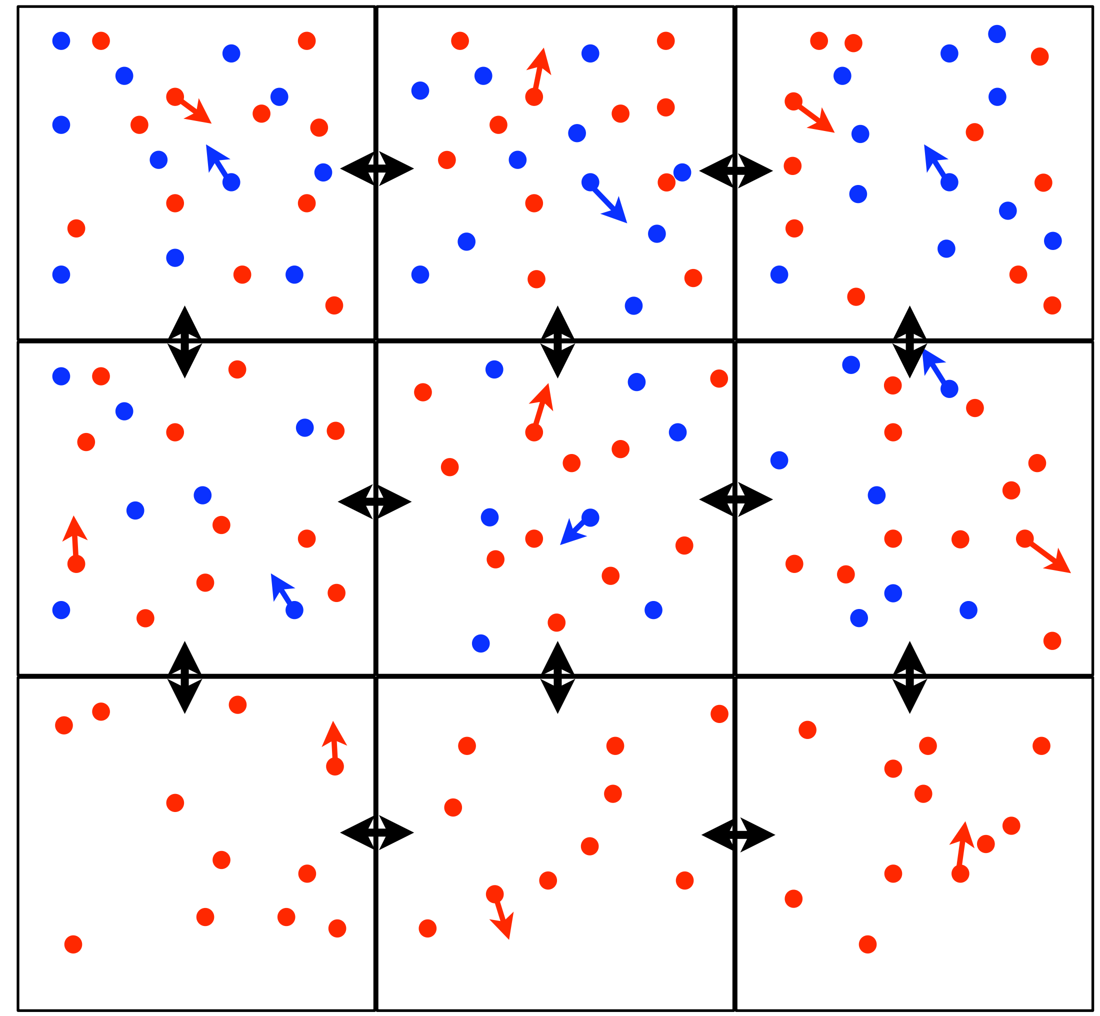

- h must therefore be small for the discretization to be valid

SSA using AMR

- Diffusion in 2-D (3-D similar derivation)

$$u^{(s)} \triangleq u^{(s)}(x,y,t)$$
- concentration of species *s*

$$\bar{u}_i^{(s)} \triangleq h^{-2} \int_i u_i^{(s)} \, \mathrm{d}V$$
- average concentration of species *s* in volume element *i*

$$U_i^{(s)} \triangleq \int_i \bar{u}_i^{(s)} \, \mathrm{d}V = \bar{u}_i^{(s)} h^2$$
- number of molecules

- start with macroscopic equations for diffusion

$$\frac{\partial u^{(s)}}{\partial t} = -\nabla \cdot \mathbf{J}$$

$$\mathbf{J} = -D \nabla u^{(s)}$$

- Integrating the conservation equation over a volume element *i*, applying the divergence theorem on the right-hand-side, and decomposing the surface integral into faces yields:

$$\frac{\mathrm{d}U_i^{(s)}}{\mathrm{d}t} = -\sum_{a=1}^{4} \int_{\gamma_a} \mathbf{J} \cdot \mathbf{n} \, \mathrm{d}S$$

Bernstein, PRE. 2005

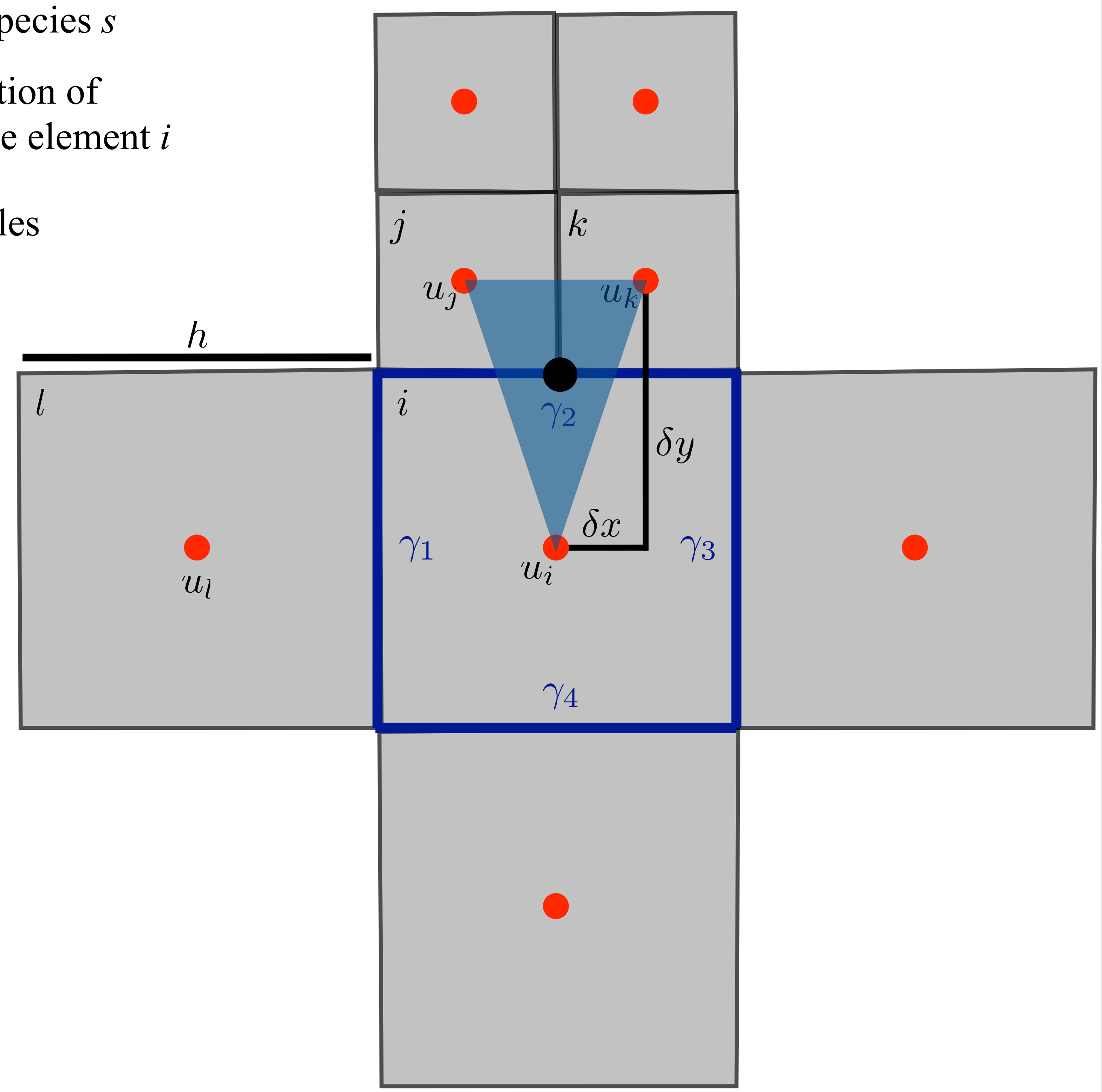

SSA using AMR

- Gray-Scott Reaction-Diffusion System in 2-D

Pearson, Science. 1993

$$U + 2V \rightarrow 3V \qquad V \rightarrow \emptyset \qquad U \rightarrow \emptyset \qquad \emptyset \rightarrow U$$

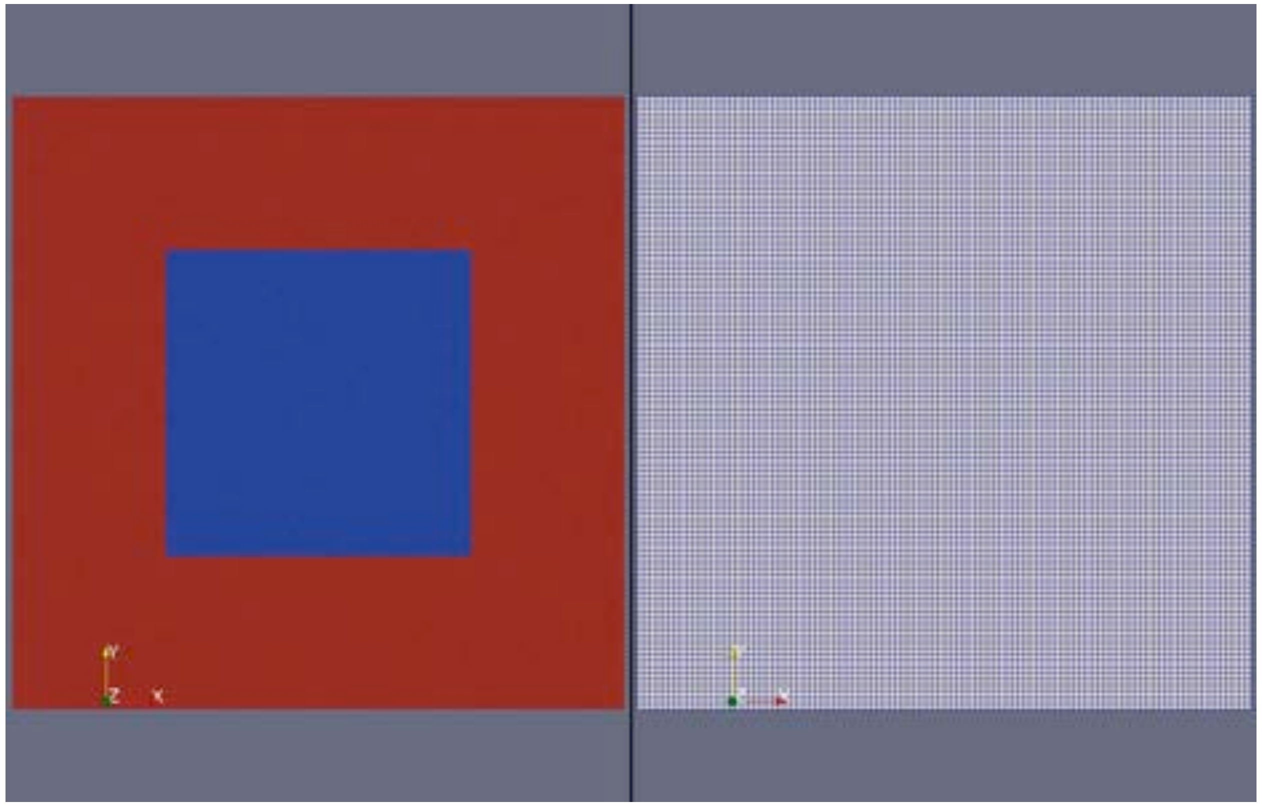

- Stochastic
- *Imperfect* refinement criterion -some fluctuations are tagged as gradients

$$h_{min} = \frac{1}{400} \qquad h_{max} = \frac{1}{100}$$

- Deterministic
- Gradient-based AMR - finite differences

Henshaw et al., J. Comp. Phys. 2008

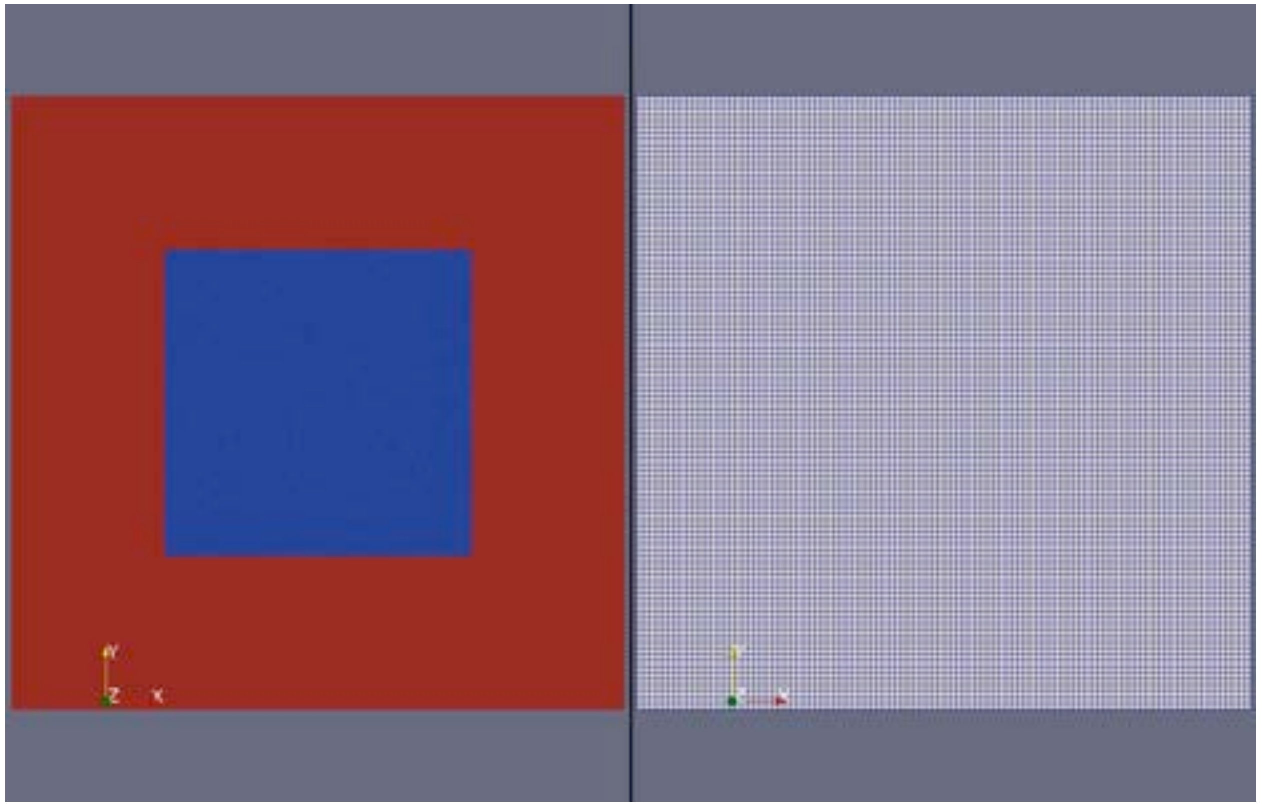

SSA using AMR

- Fisher-Kolmogorov Reaction-Diffusion System in 2-D

$$U + V \xrightarrow{k} 2U$$

Fisher, Ann. Eugenics 1937

- Fluctuations are stronger in smaller cells
- Not mesh effects
- < U > = 15

different physics

- Weak fluctuations in coarse region
- < U > = 960

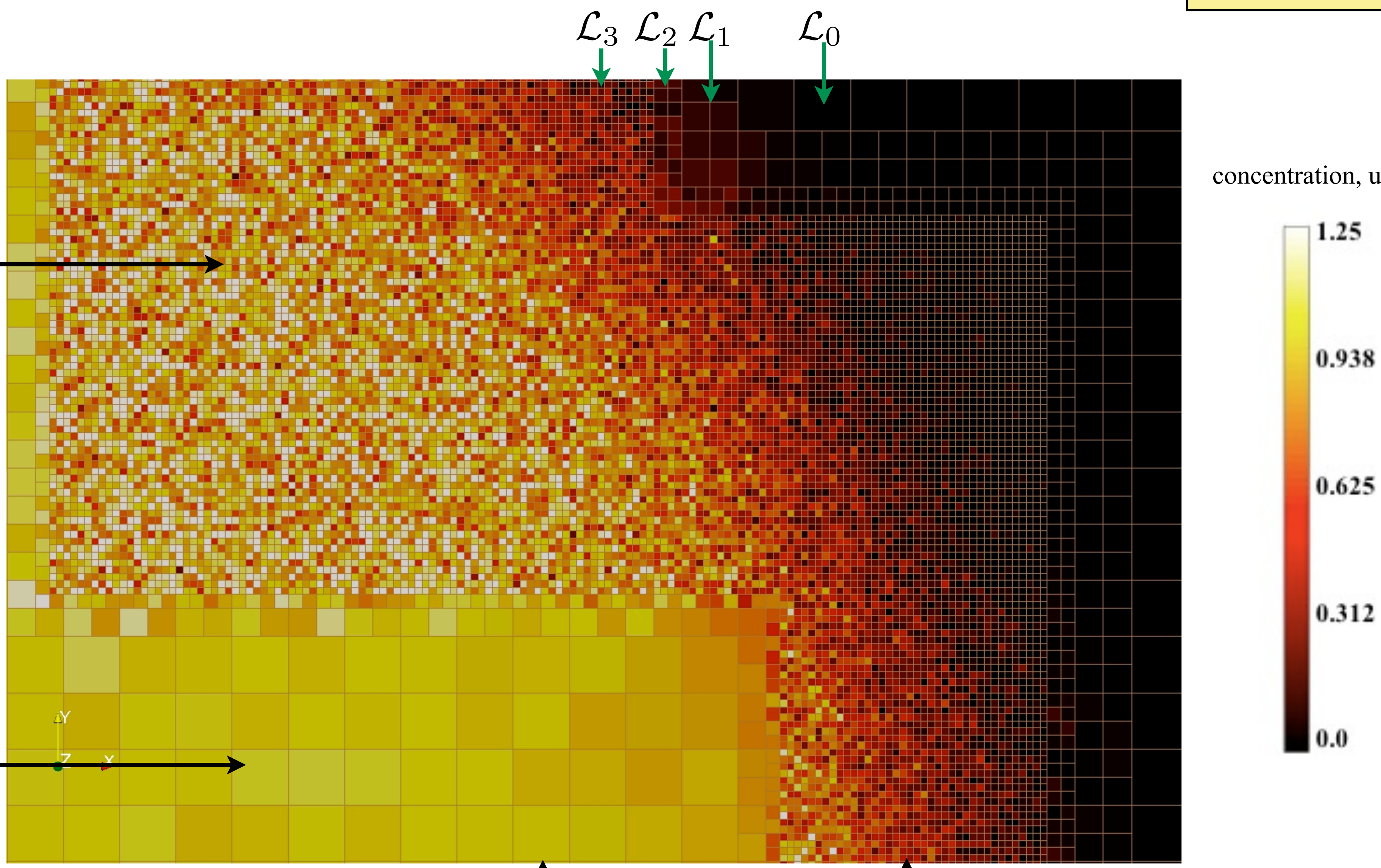

$$h_{max} = \frac{1}{100} \qquad h_{min} = \frac{1}{800}$$

$$\frac{\hat{\tau}_R}{\hat{\tau}_D} = 25$$

SSA using AMR

- Fisher-Kolmogorov Reaction-Diffusion System in 2-D

$$U + V \xrightarrow{k} 2U$$

Fisher,
Ann. Eugenics
1937

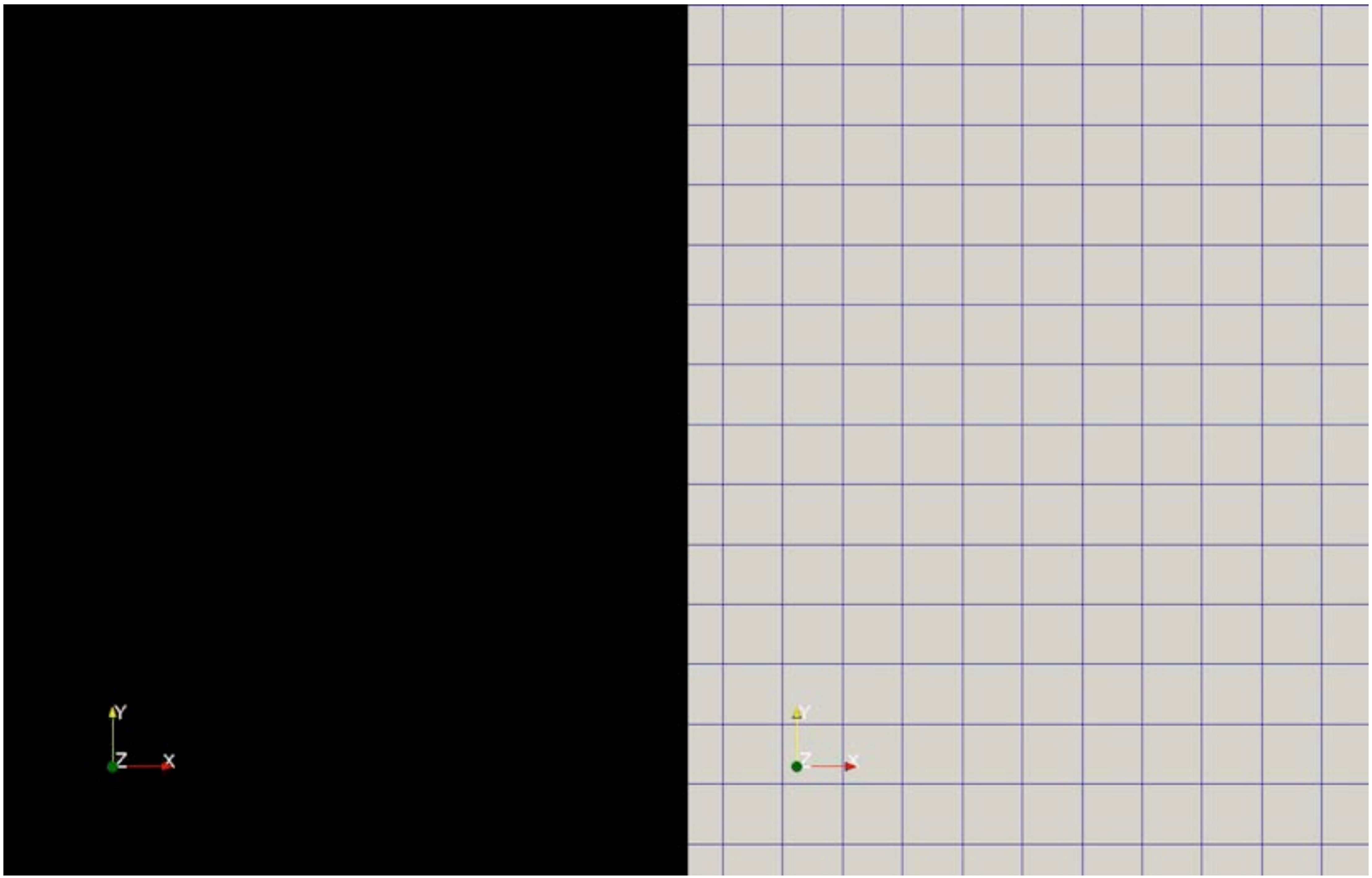

SSA using AMR

- Fisher-Kolmogorov Reaction-Diffusion System in 2-D

$$U + V \xrightarrow{k} 2U$$

Fisher,
Ann. Eugenics
1937

- *halo* is projected 1-D analytical solution

$u \in [0.45, 0.55]$

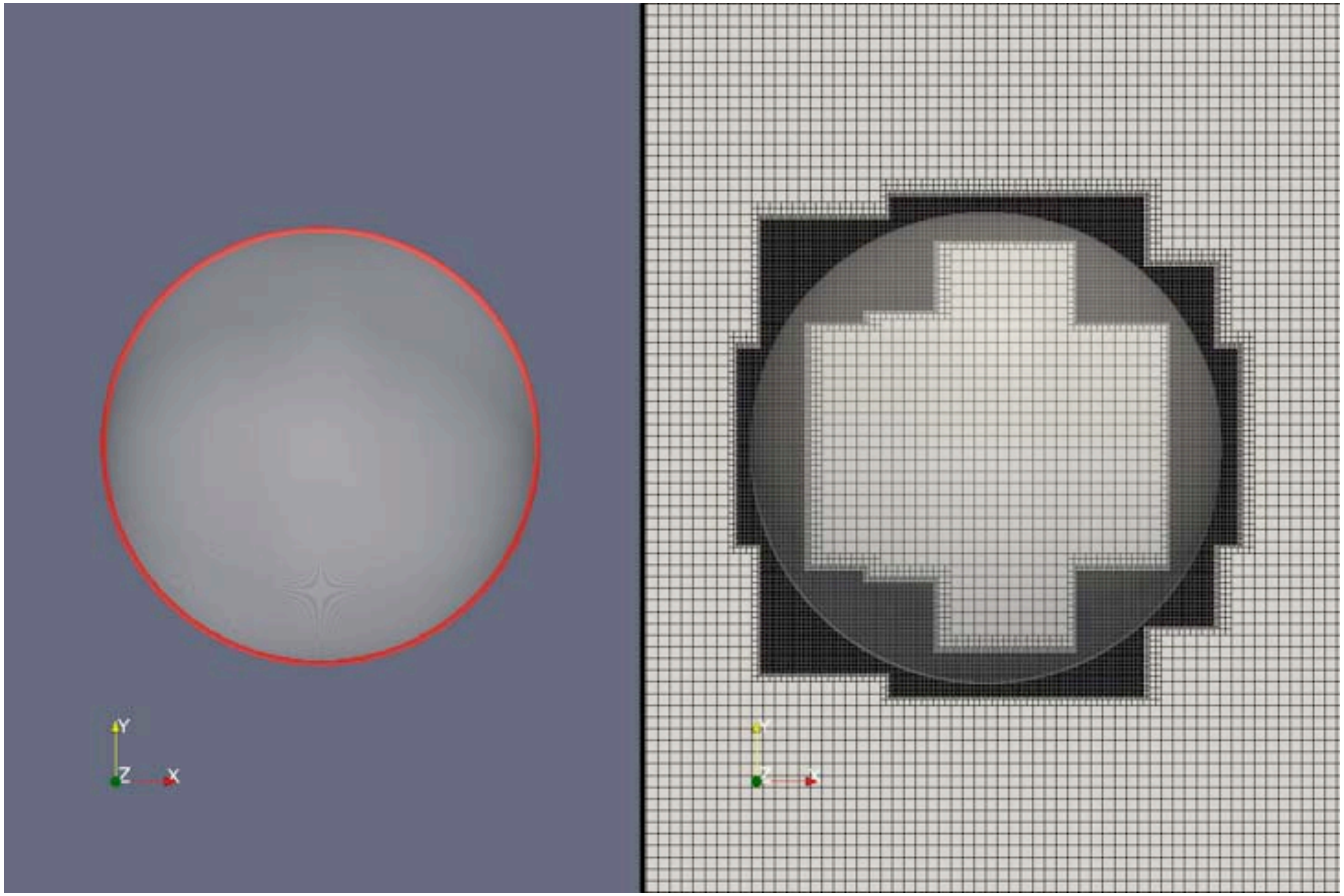

Vorticity $\omega = \nabla \times \mathbf{u}$

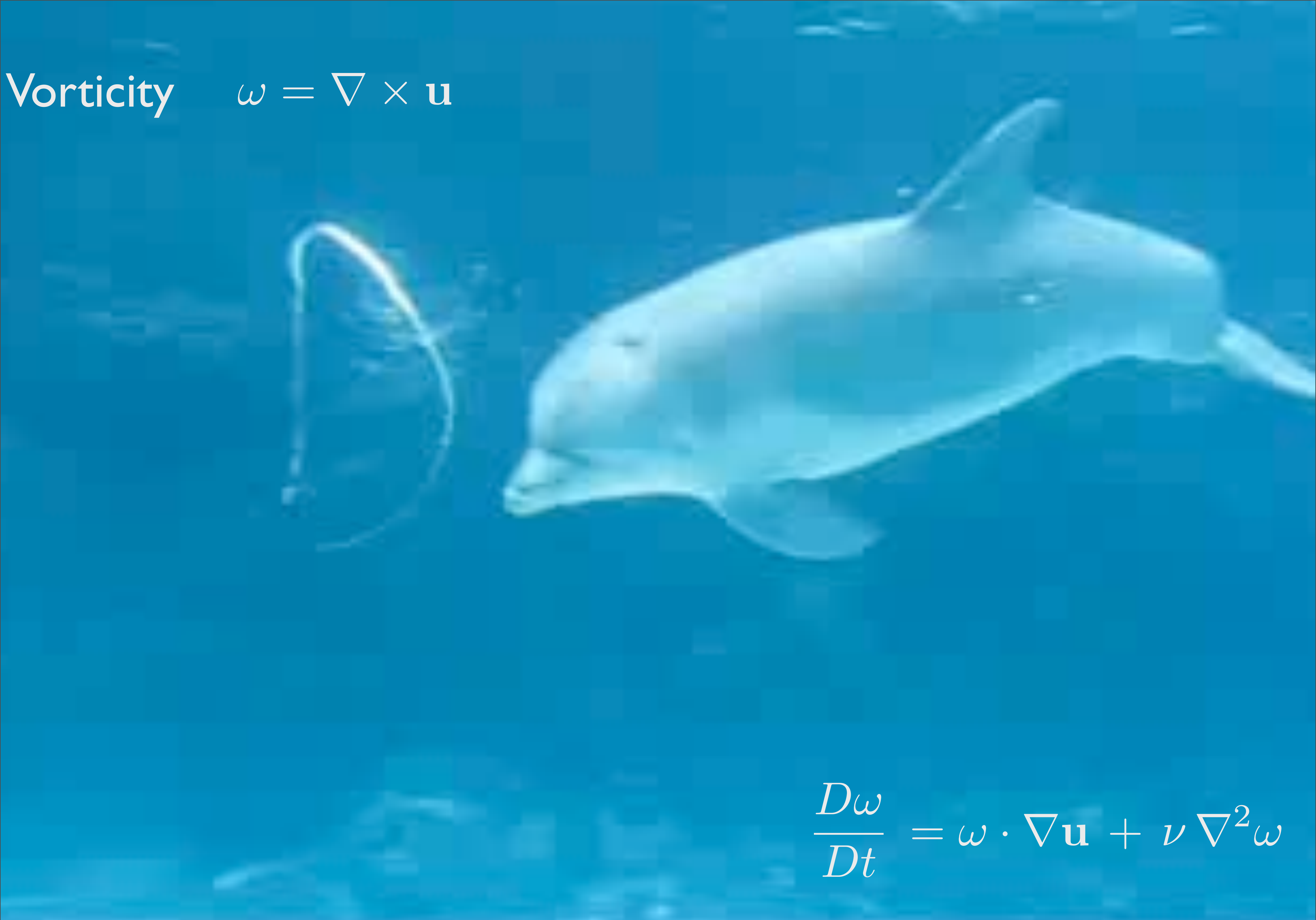

$$\frac{D\omega}{Dt} = \omega \cdot \nabla \mathbf{u} + \nu \nabla^2 \omega$$

Fluids and Biology

Vorticity $\omega = \nabla \times \mathbf{u}$

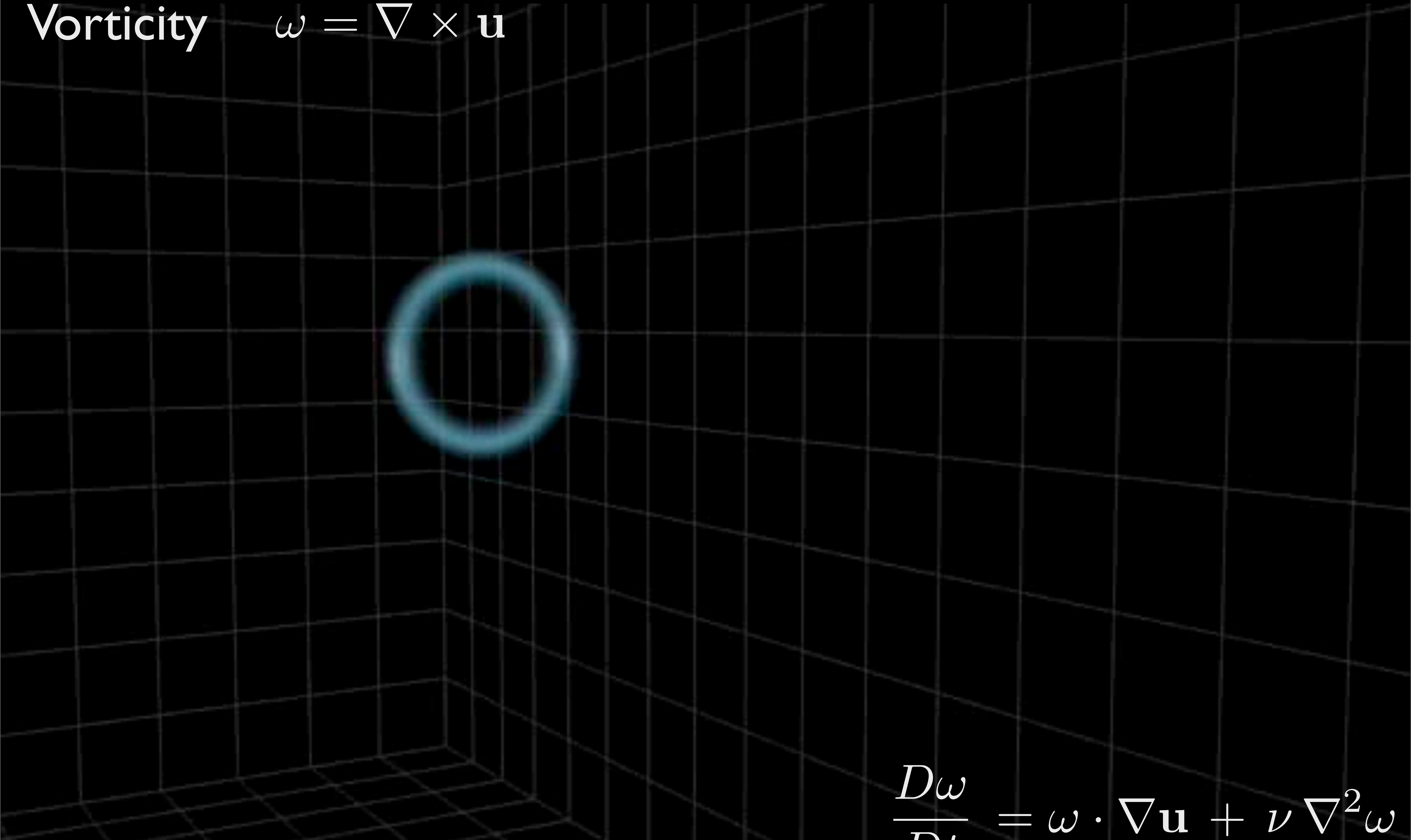

$$\frac{D\omega}{Dt} = \omega \cdot \nabla \mathbf{u} + \nu \, \nabla^2 \omega$$

FLUIDS - Macroscale Conservation Laws

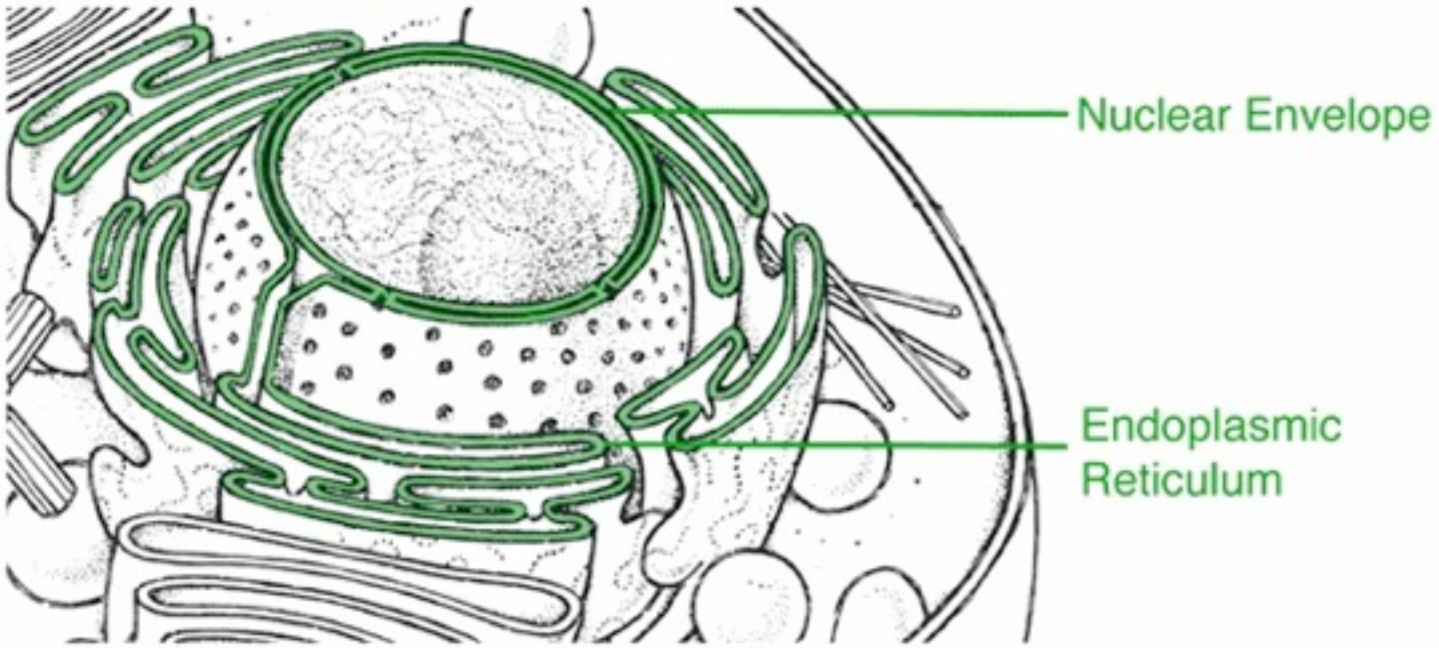

Figure: De Duve, Une visite guidée de la cellule vivante, 1987.

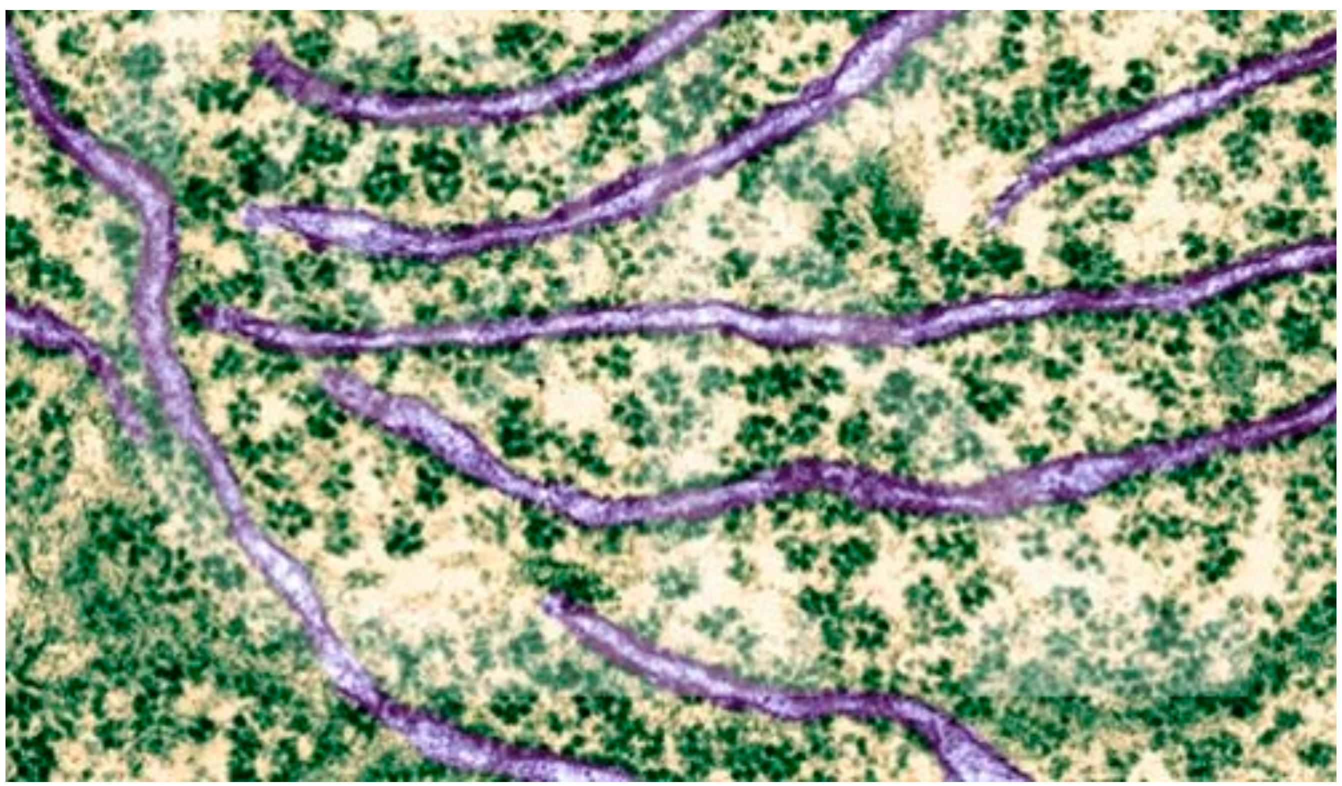

Figure: D. Kunkel, (c) www.DennisKunkel.com

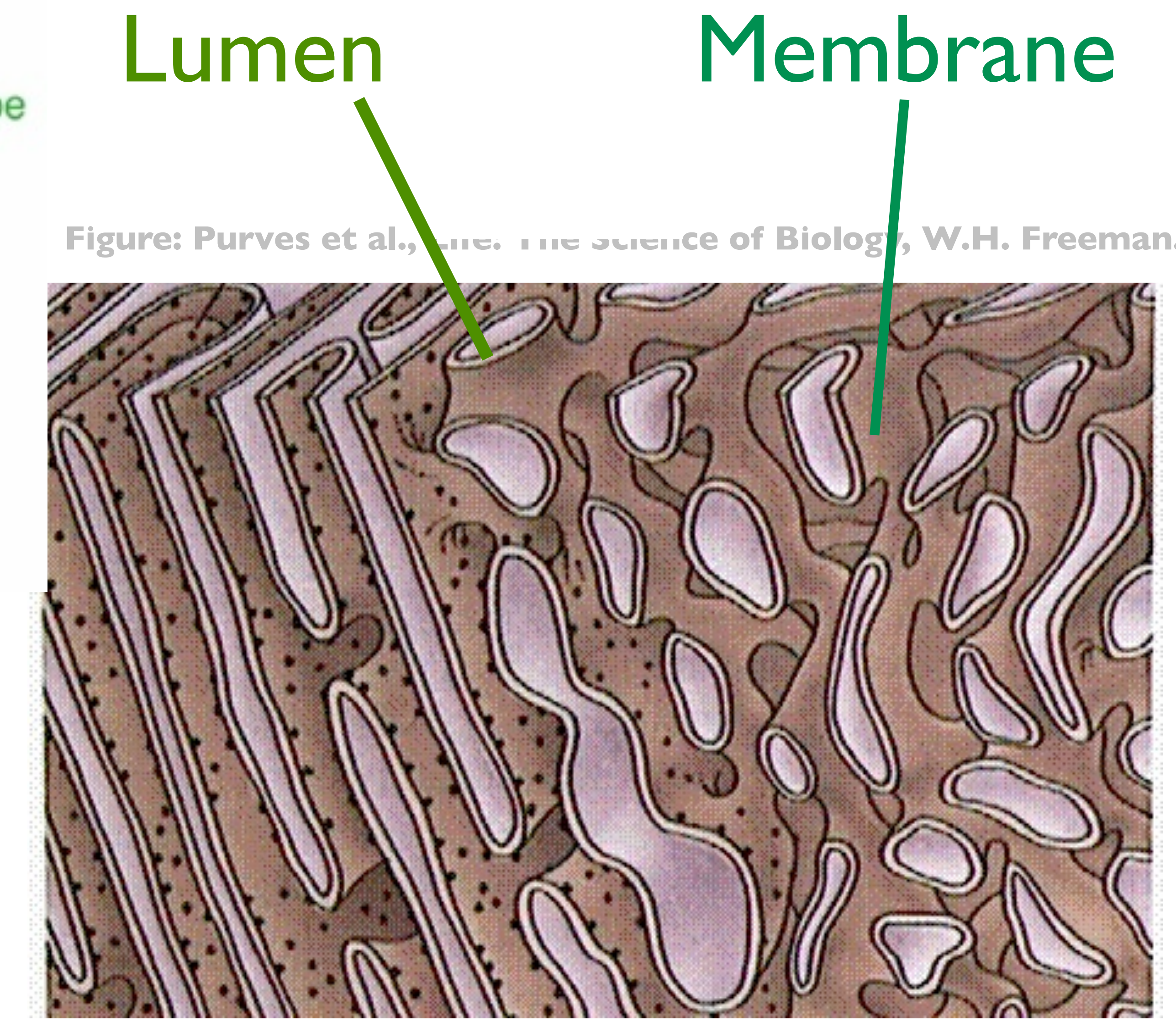

Figure: Purves et al., Life: The Science of Biology, W.H. Freeman.

The main **biosynthetic organelle** in Eukaryotes: Protein and lipid synthesis. Enclosed by a **contiguous** membrane

COMPLEX GEOMETRIES : Diffusion in the ER

FRAP : Fluorescence Recovery After Photobleaching

- Tag protein fluorescently
- Laser Bleach **region of interest**
- Monitor influx of unbleached protein

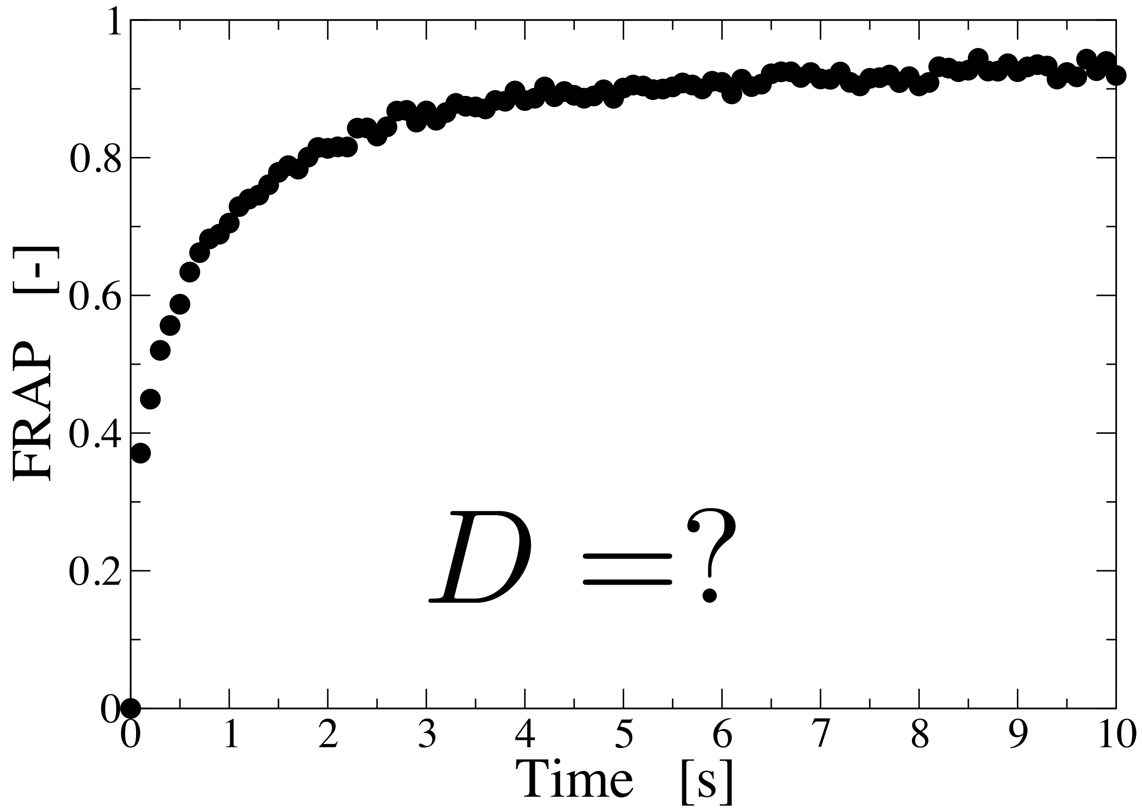

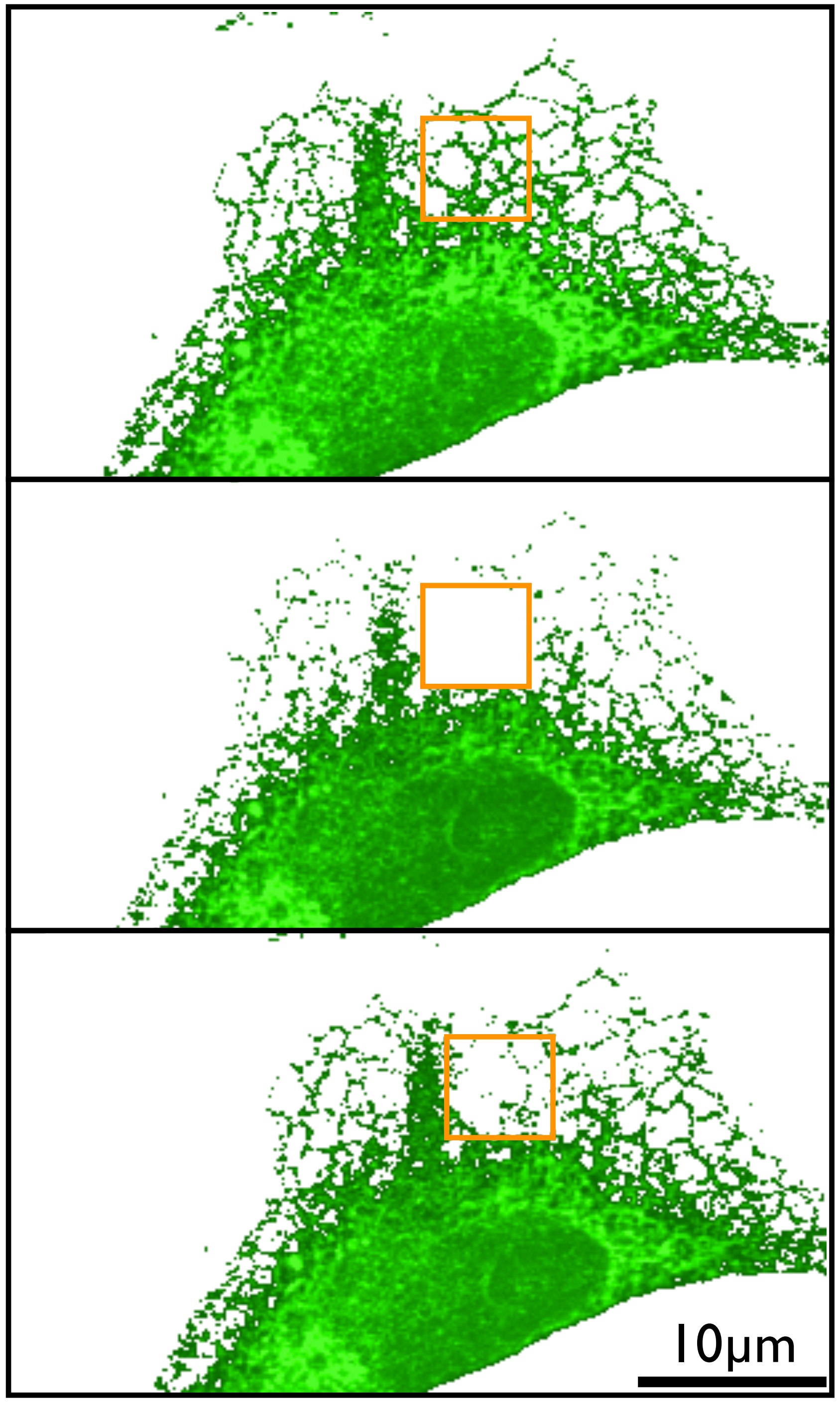

Helenius group (ETHZ)

Diffusion

Continuum assumption $$\frac{\partial u(\boldsymbol{x},t)}{\partial t} = \nabla \cdot \left(\boldsymbol{D}(\boldsymbol{x},t)\nabla u(\boldsymbol{x},t)\right)$$

Cases:

$\boldsymbol{D}(\boldsymbol{x},t) = \boldsymbol{D}(\boldsymbol{x})$	$\boldsymbol{D}(\boldsymbol{x},t) = \boldsymbol{D}$	$\boldsymbol{D}(\boldsymbol{x},t) = \nu(\boldsymbol{x},t)\mathbb{1}$
Normal	Homogeneous	Isotropic

Recall CFD : "Vorticity" becomes "Concentration"

$$\frac{D\omega}{Dt} = \omega \cdot \nabla \mathbf{u} + \nu \nabla^2 \omega$$

$$\frac{dx_p}{dt} = \mathbf{u}$$

Diffusion Approximations

Diffusion

$$\frac{\partial c}{\partial t} = \nu \, \Delta \mathbf{c}$$

Particles

$$C_\epsilon^h(x,t) = \sum_{p=1}^{N_p} h_p^d \, c_p(t) \, \zeta_\epsilon(x - x_p(t))$$

Particle Strength Exchange

$$\frac{dc_q}{dt} = \frac{\nu}{\epsilon^2} \sum_{p=1}^{N_p} (h_p^d \, c_p - h_q^d \, c_q) \, \zeta_\epsilon(x_q - x_p)$$

Degond & Mas-Gallic, Math. Comput. 53:509. 1989.

Accuracy ~ $\frac{1}{N^4}$

Cost ~ N

Extendable to any diffusion operator

PSE is Orders of magnitude better than random walk

Diffusion in the Endoplasmic Reticulum

representation of complex geometries using Lagrangian Particle Level Sets

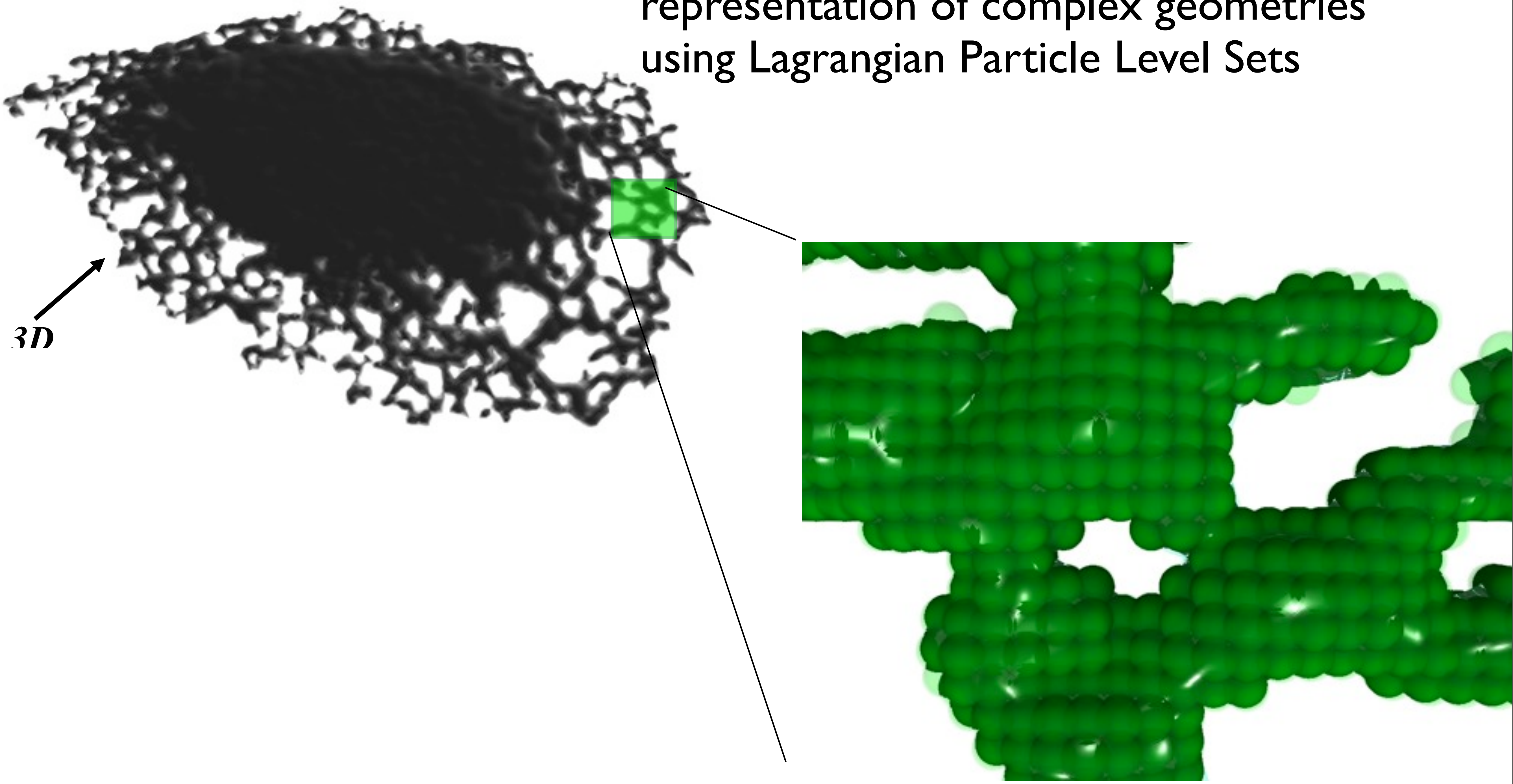

Simulation of diffusion in the lumen of reconstructed real biological geometries

Integrate Imaging and Simulations

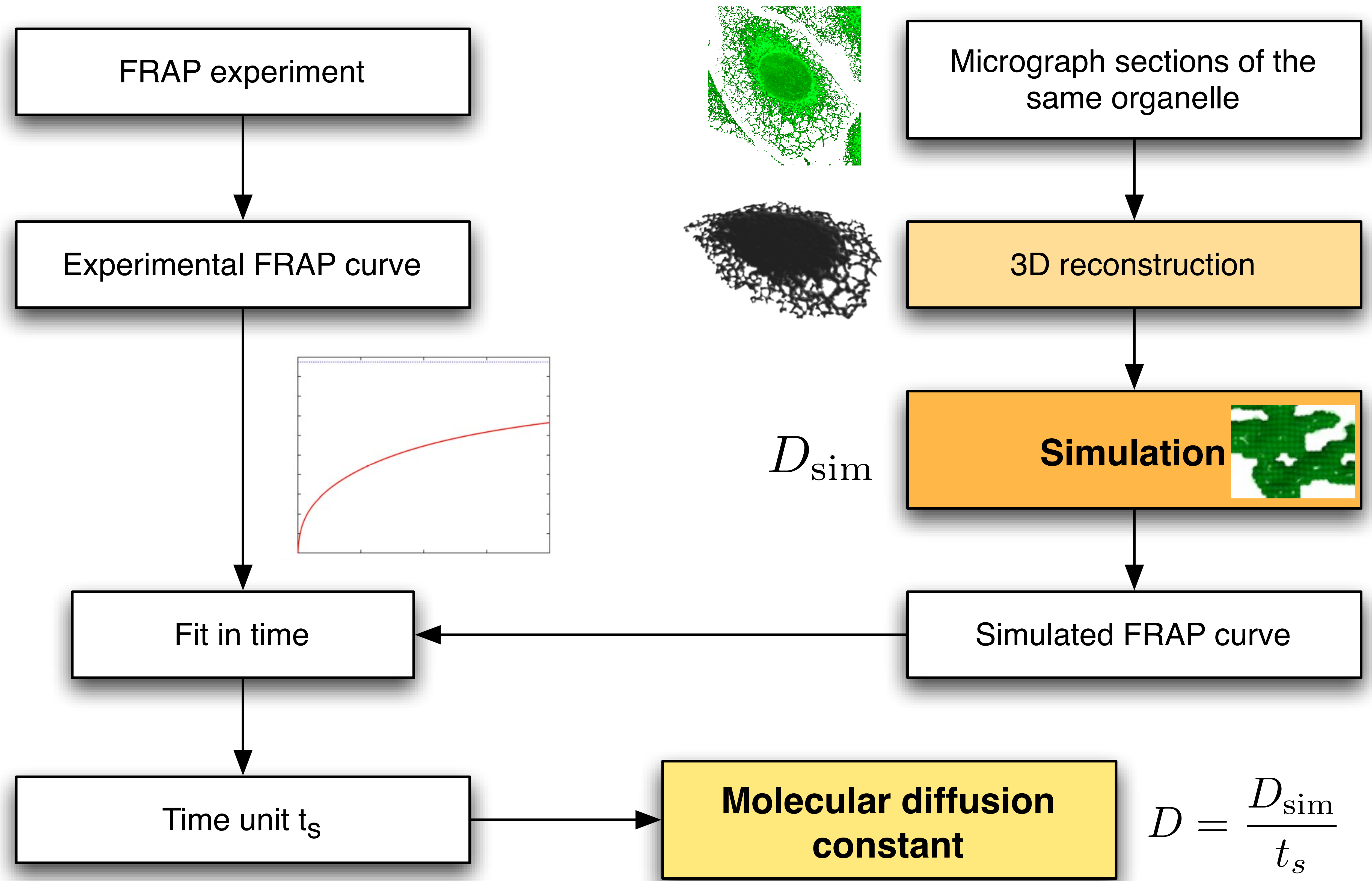

Diffusion in the Real Endoplasmic Reticulum - LUMEN

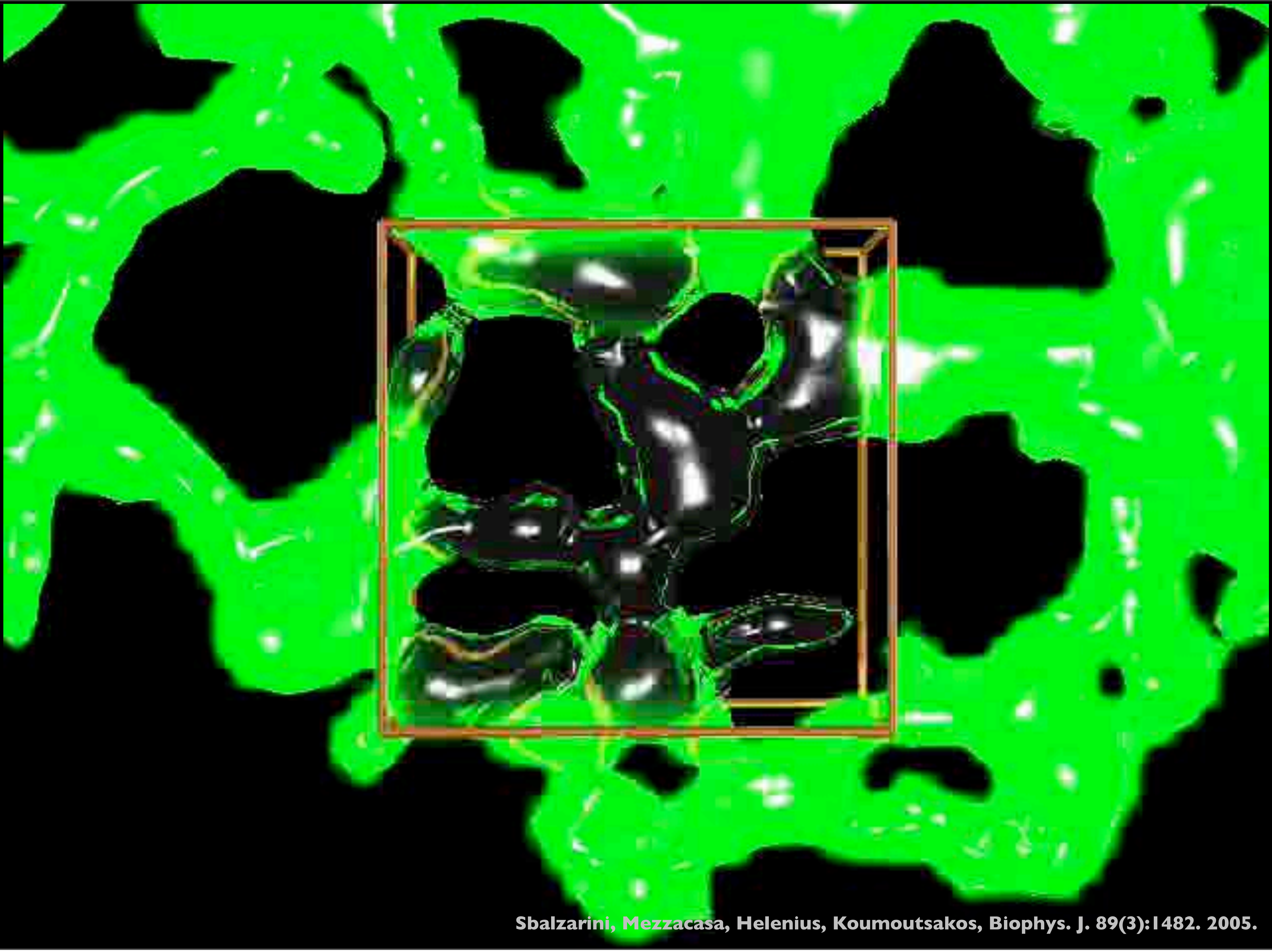

Sbalzarini, Mezzacasa, Helenius, Koumoutsakos, Biophys. J. 89(3):1482. 2005.

Simulations and Experiments in the same Geometry

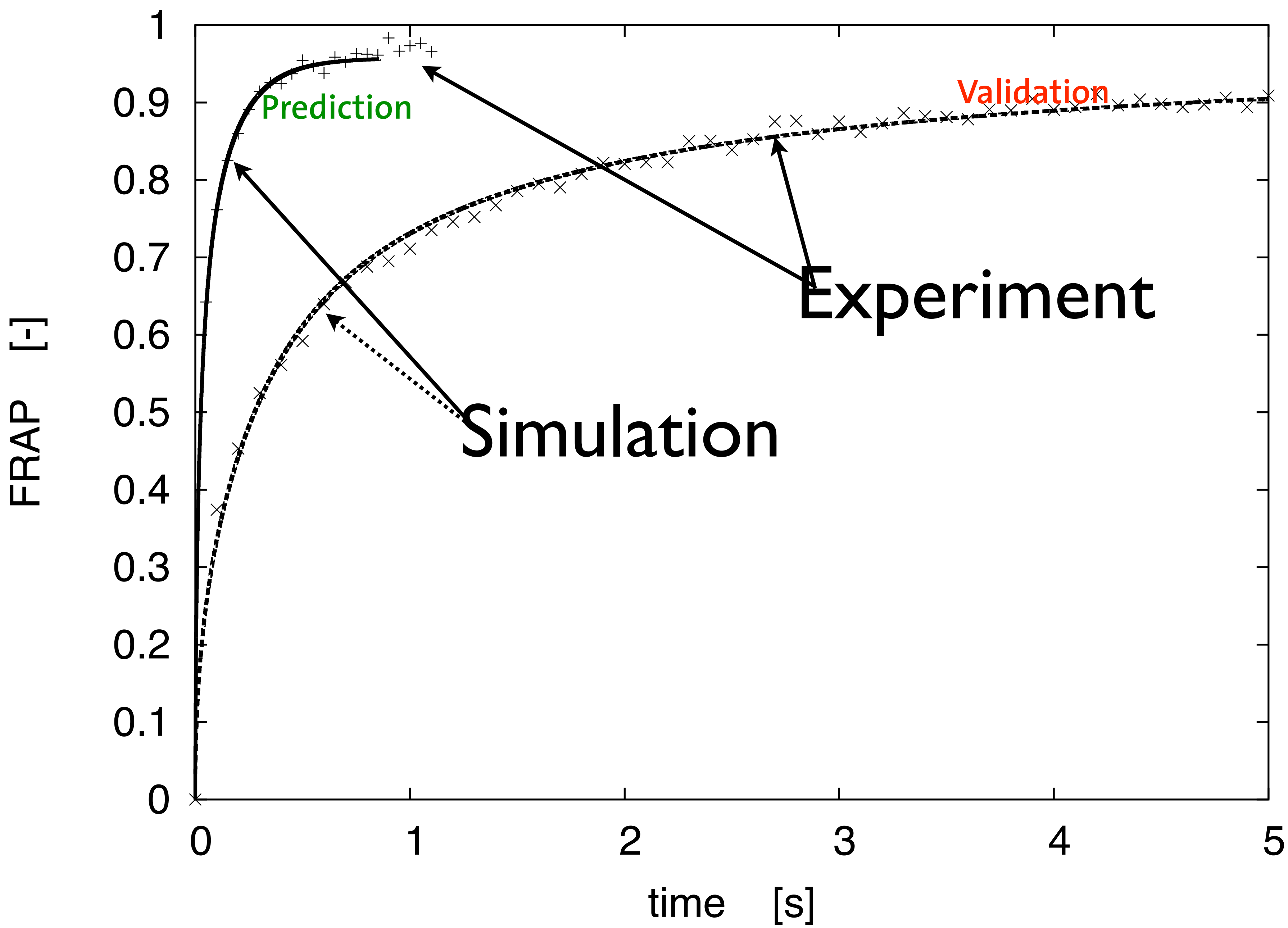

Simulation and Experiment in the **same** ER

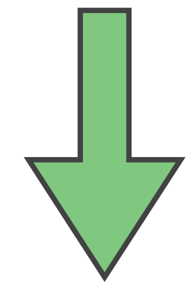

in vivo diffusion constant from fit

"...but, can you do this on a surface ?" - A. Helenius

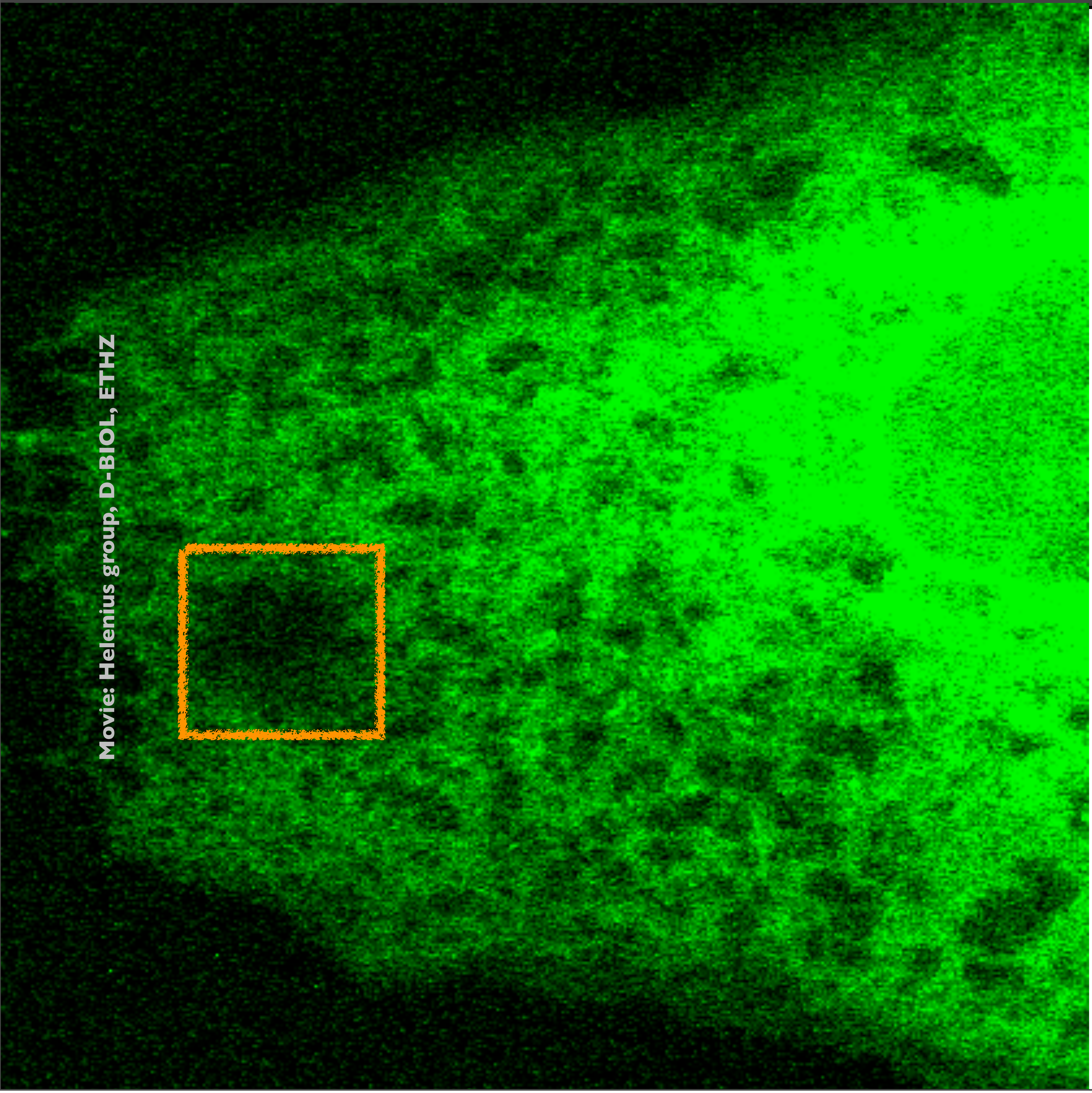

Membrane:

ts045-VSVG-GFP

Diffusion in the Real Endoplasmic Reticulum - SURFACE

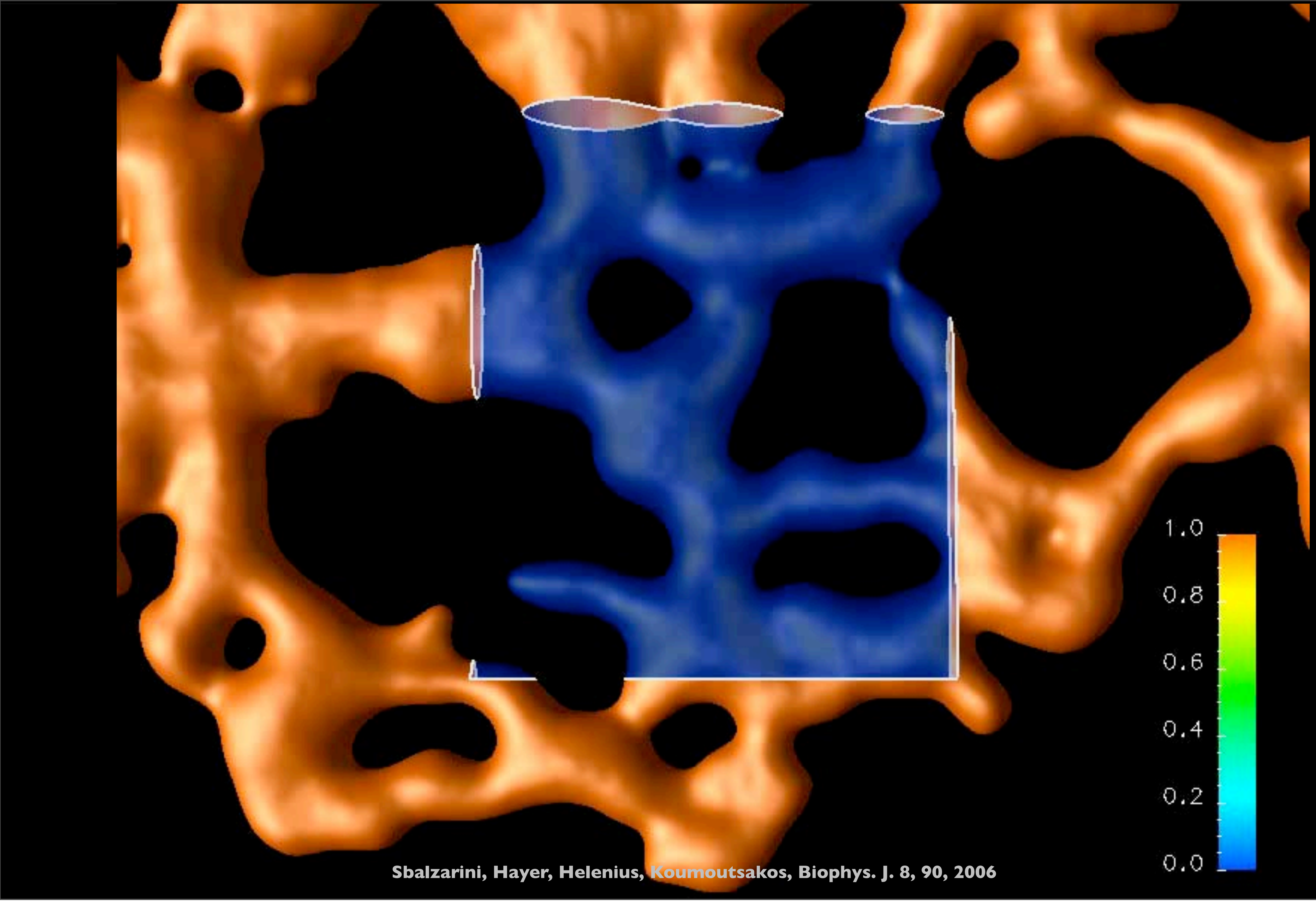

Diffusion on reconstructed ER of VERO cells

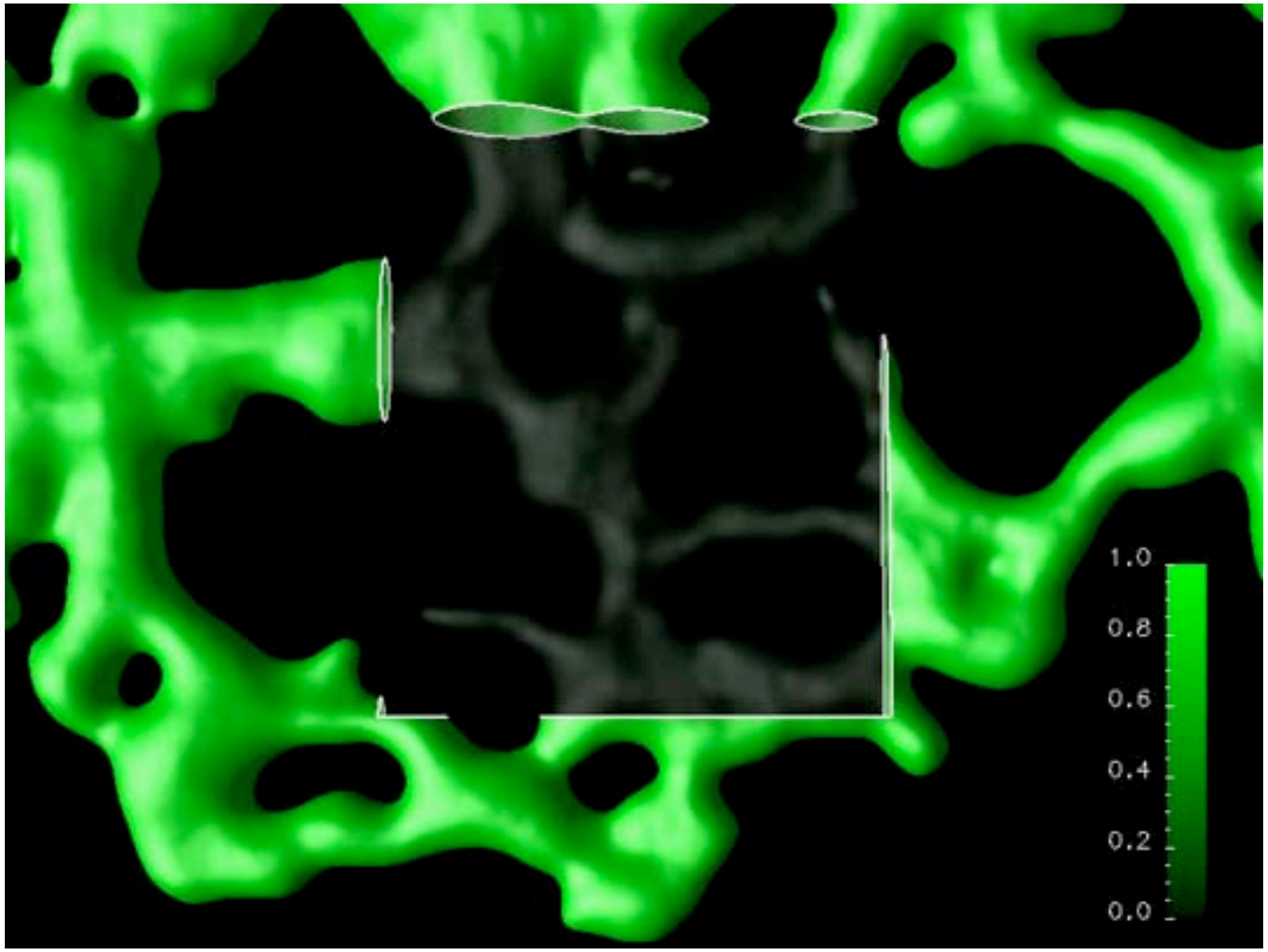

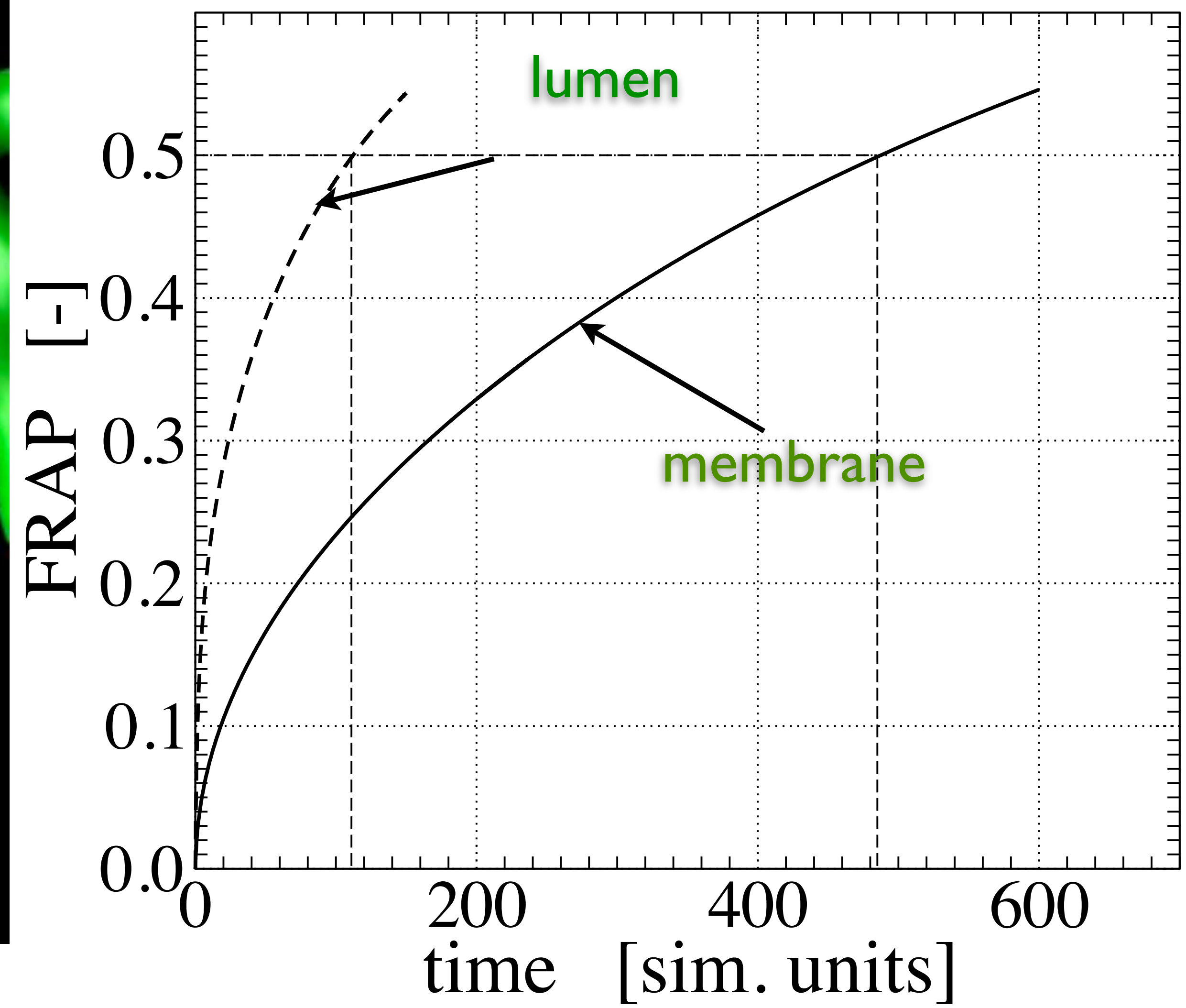

ssGFP-KDEL in the ER lumen $\nu = 34 \pm 0.95\,\mu\mathrm{m}^2/\mathrm{s}$

tsO45-VSVG-GFP in the ER membrane $\nu = 0.16 \pm 0.07\,\mu\mathrm{m}^2/\mathrm{s}$

Using the *same diffusion constant* recovery speed varies by ***>400%***.

Gray Scott system

$$\begin{aligned} U + 2V &\to 3V, \\ V &\to P \end{aligned}$$

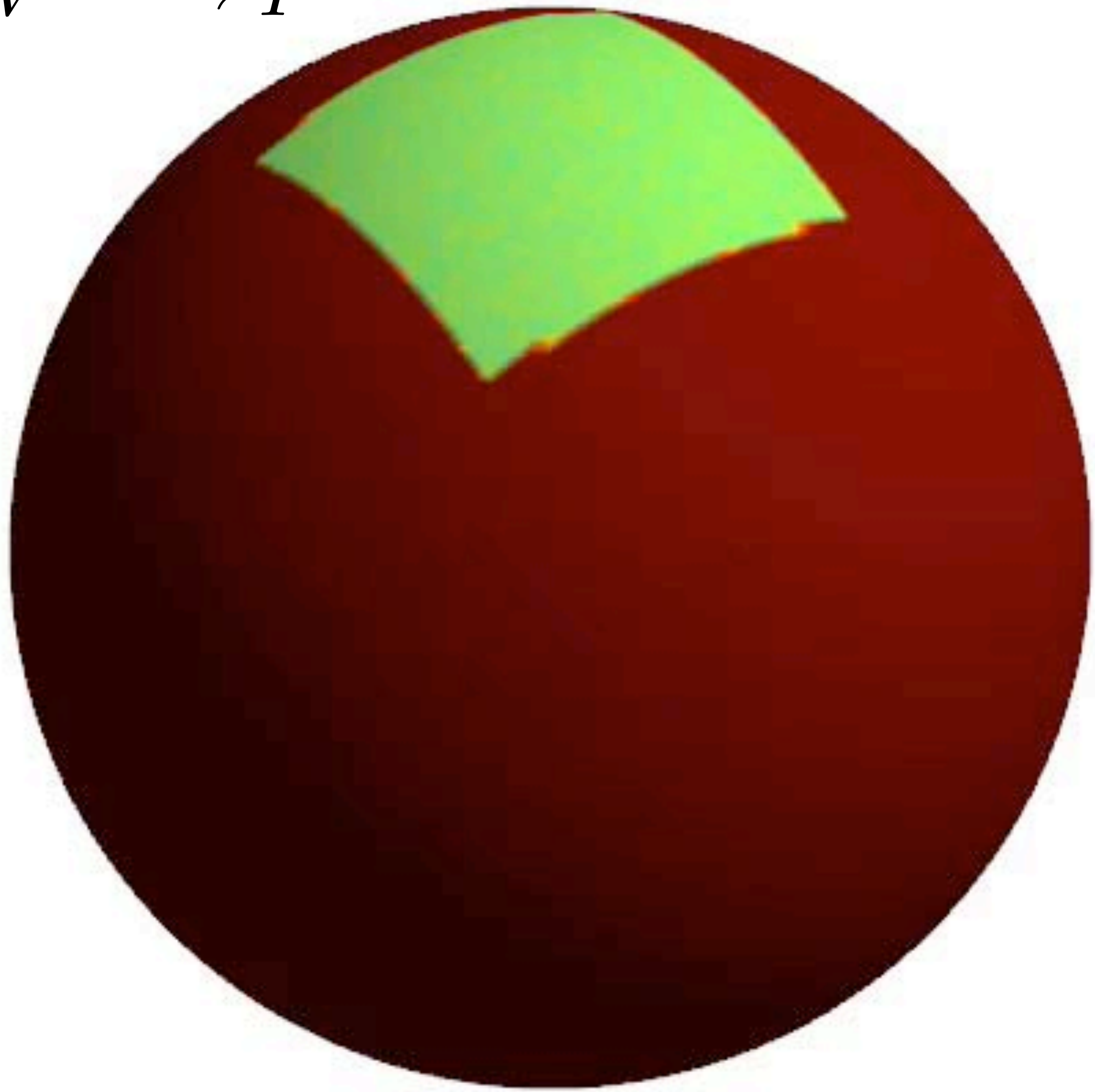

Deterministic

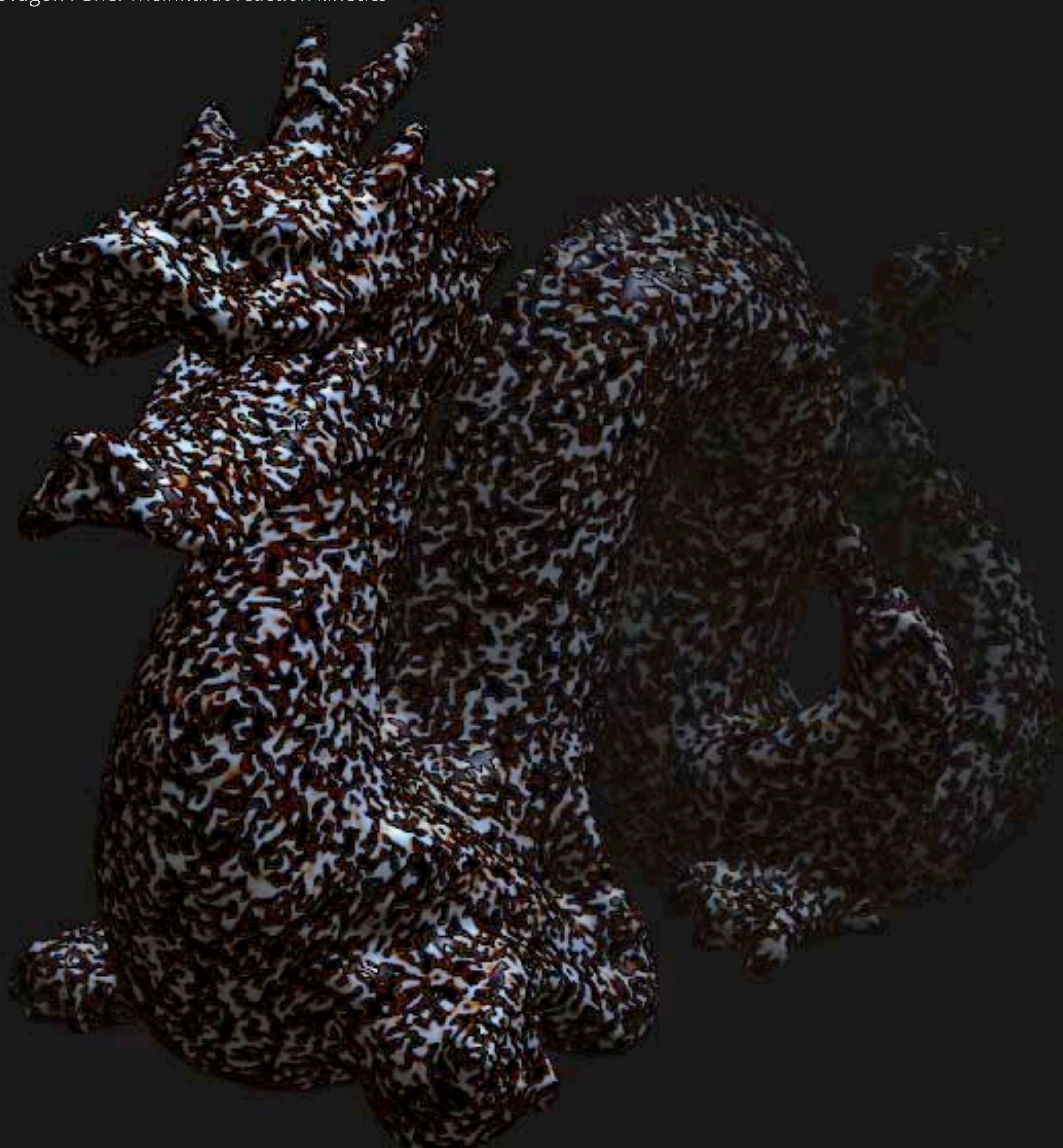

The Dragon : Grier-Meinhardt reaction kinetics

"Well, the stripes are easy, but what about the horse part " ?

Turing

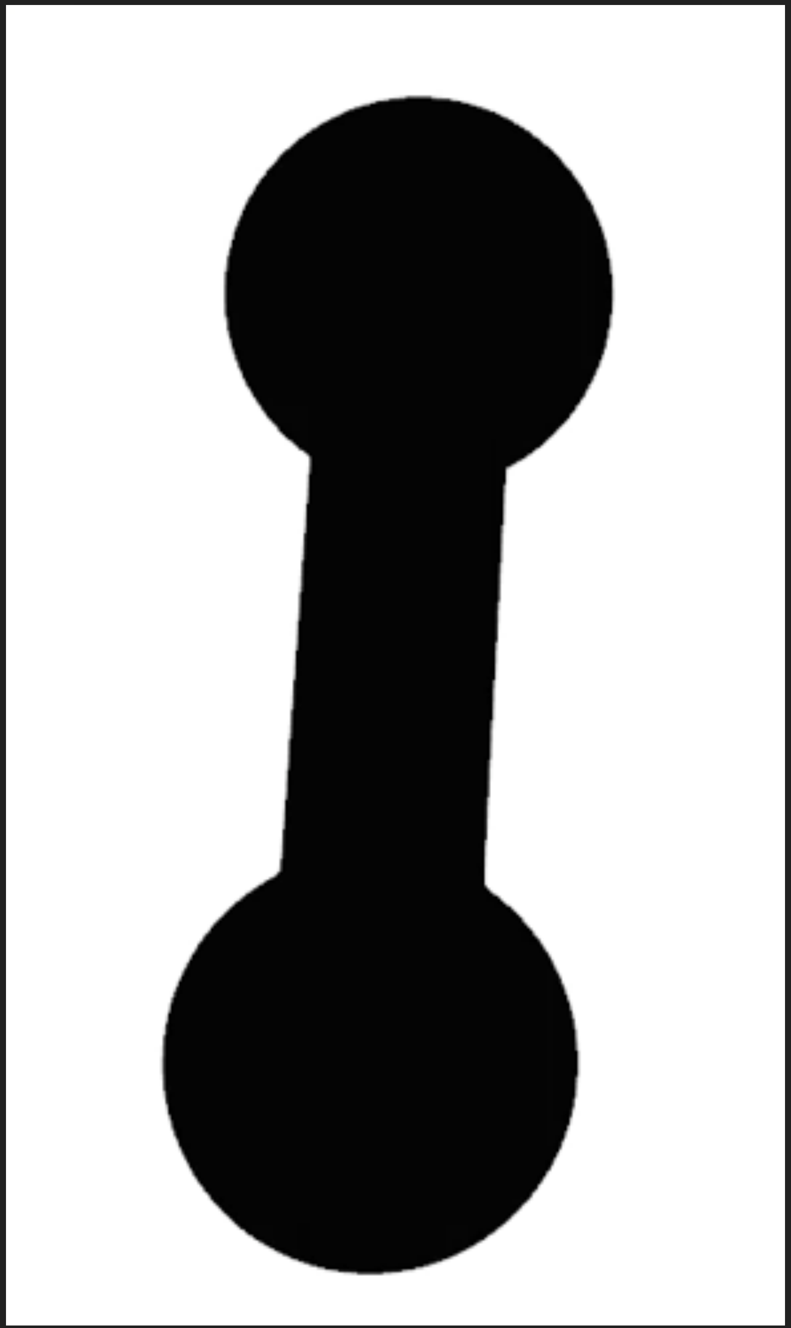

Hieber and Koumoutsakos, Lagrangian Particle Level Sets, **J. Comput. Phys.,** 2005

GROWTH : Reaction-Diffusion on Deforming Geometries

RDG - Equations

- Reaction-Diffusion on growing surface

$$\frac{\partial c_i}{\partial t} + \nabla_{\Gamma(t)} \cdot (c_i \mathbf{u}) = D_i \Delta_{\Gamma(t)} c_i + R_i(\mathbf{c}) \quad \text{on } \Gamma(t), i = 1 \ldots N,$$

$$N = \text{Number of species},$$

$$\mathbf{c} = \left[c_1, \ldots, c_N\right] = \text{Concentrations},$$

$$D_i = \text{Diffusion constant for species } i,$$

$$R_i(\mathbf{c}) = \text{Reaction terms for species } i.$$

- Surface changes over time

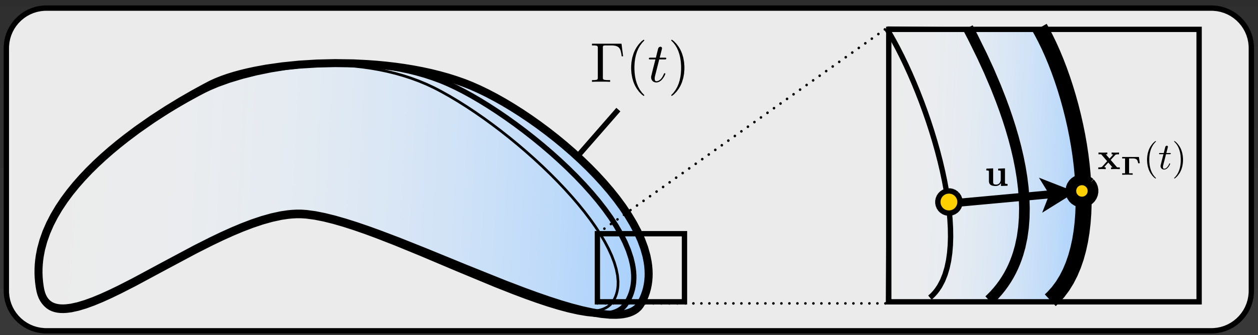

$$\Gamma(t) = \{\mathbf{x_\Gamma}(t)\},$$

$$\frac{d\mathbf{x_\Gamma}}{dt} = \mathbf{u}(\mathbf{x_\Gamma}, \mathbf{c_s}).$$

References:

Bergdorf, M., Sbalzarini, I. F., and Koumoutsakos, P. (2009). A Lagrangian particle method for reaction-diffusion systems on deforming surfaces, Journal of Mathematical Biology (submitted)

Extended domain

- Species given in narrow band around surface

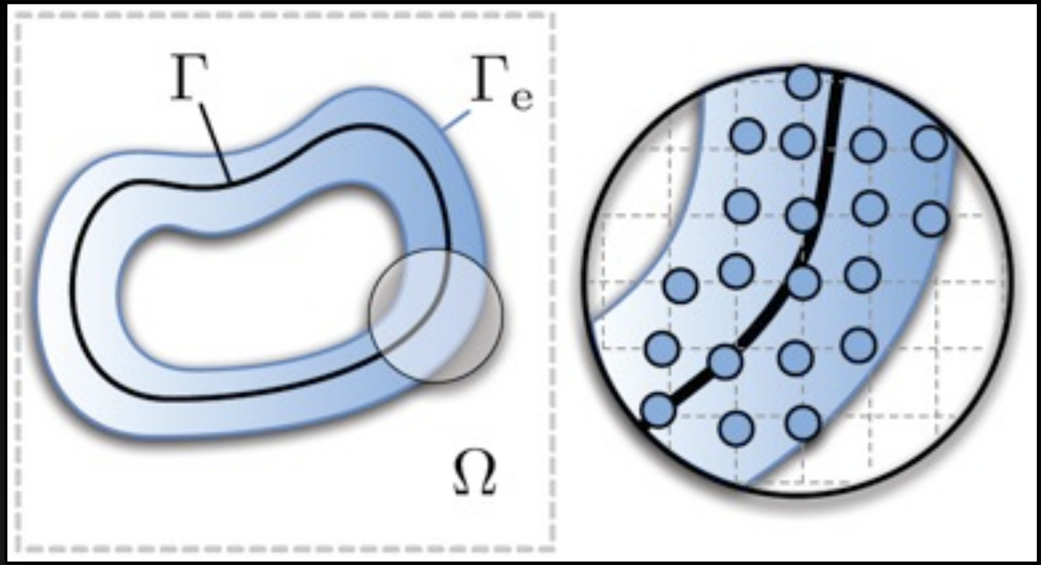

- Use level set for surface

$$\Gamma = \{ \mathbf{x} \mid \varphi(\mathbf{x}) = 0 \},$$
$$\mathbf{n} = \nabla\varphi / \|\nabla\varphi\|$$

- Replace diffusion operator

$$D_s \nabla \cdot ((\mathbb{I} - \mathbf{n} \otimes \mathbf{n}) \nabla c)$$

- Extend concentration
  - simplifies surface growth

$$\frac{\partial c}{\partial n} = \nabla c \cdot \mathbf{n} = 0$$

Plant growth with Brusselator

$$X > X_{th}: \quad \begin{aligned} \partial X/\partial t &= D_X \nabla^2 X + aA - bBX + cX^2Y - dX, \\ \partial Y/\partial t &= D_Y \nabla^2 Y + bBX - cX^2Y, \end{aligned}$$

$$X \leq X_{th}: \quad \begin{aligned} \partial X/\partial t &= D_X \nabla^2 X - dX, \\ \partial Y/\partial t &= D_Y \nabla^2 Y, \end{aligned}$$

A given as prepattern based on spherical harmonics Y_l^m,

Initial condition based on A: $X_0 = \dfrac{aA}{d}$, $Y_0 = \dfrac{bB}{cX_0}$,

Surface growth starting at $t = t_{move}$ by $\mathbf{u} = vX\mathbf{n}$,

$D_X, D_Y, a, bB, c, d, X_{th}, t_{move}, v$ given as parameters.

Holloway, D. M. and Harrison, L. G. (2008). Pattern selection in plants: Coupling chemical dynamics to surface growth in three dimensions, Annals Of Botany, 101(3), 361--374

Results (stronger A)

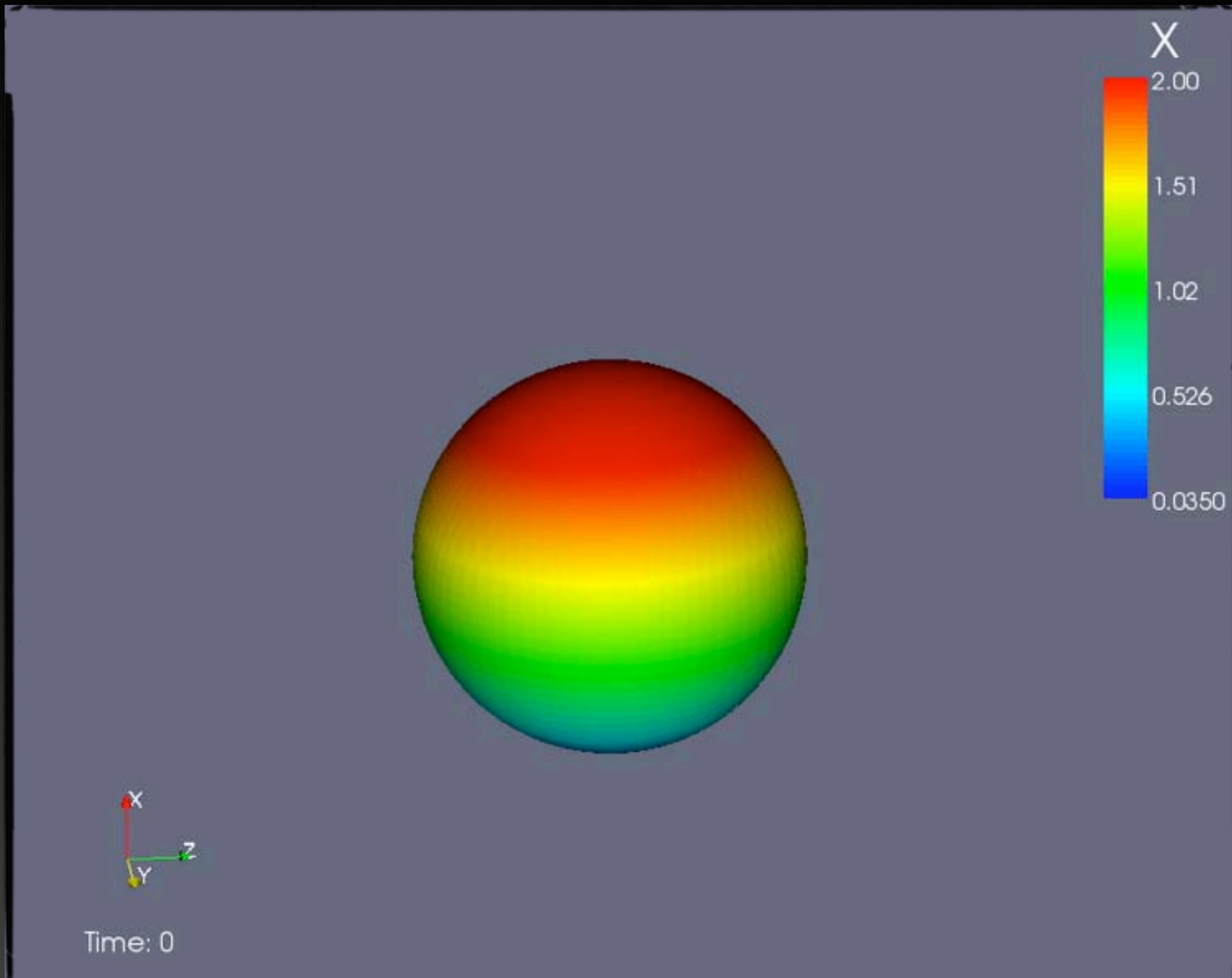

Settings:

$A = Y_1^0$ in $[1, 16]$,

$D_X = 0.008, D_Y = 0.16$,

$a = 0.01, bB = 1.5$,

$c = 1.8, d = 0.07$,

$X_{th} = 0.035, v = 0.01$,

$t_{move} = 20$,

Species here are growing with surface.

Results (mass conservation)

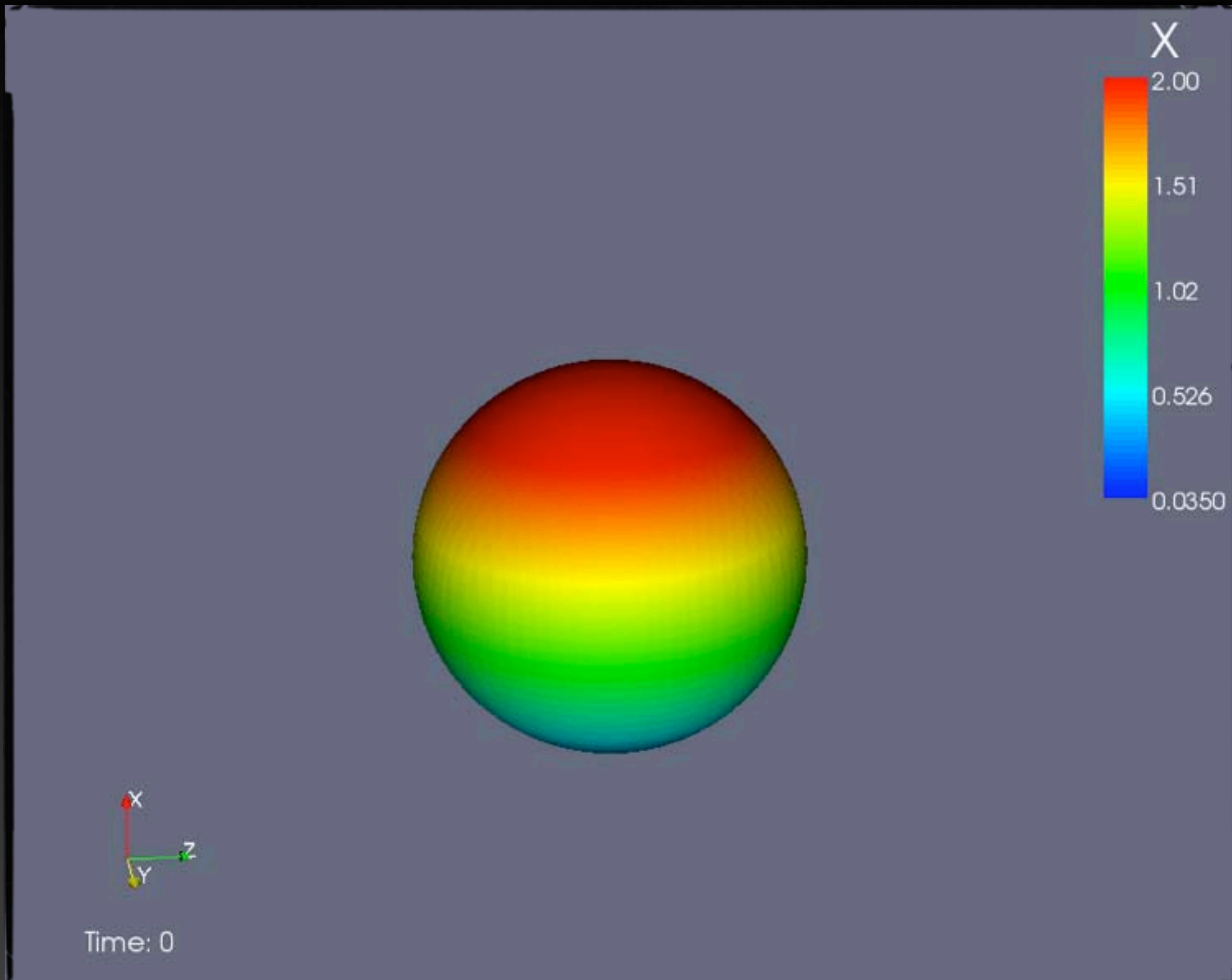

Settings:

$A = Y_1^0$ in $[1, 16]$,

$D_X = 0.008, D_Y = 0.16$,

$a = 0.01, bB = 1.5$,

$c = 1.8, d = 0.07$,

$X_{th} = 0.035, v = 0.01$,

$t_{move} = 20$.

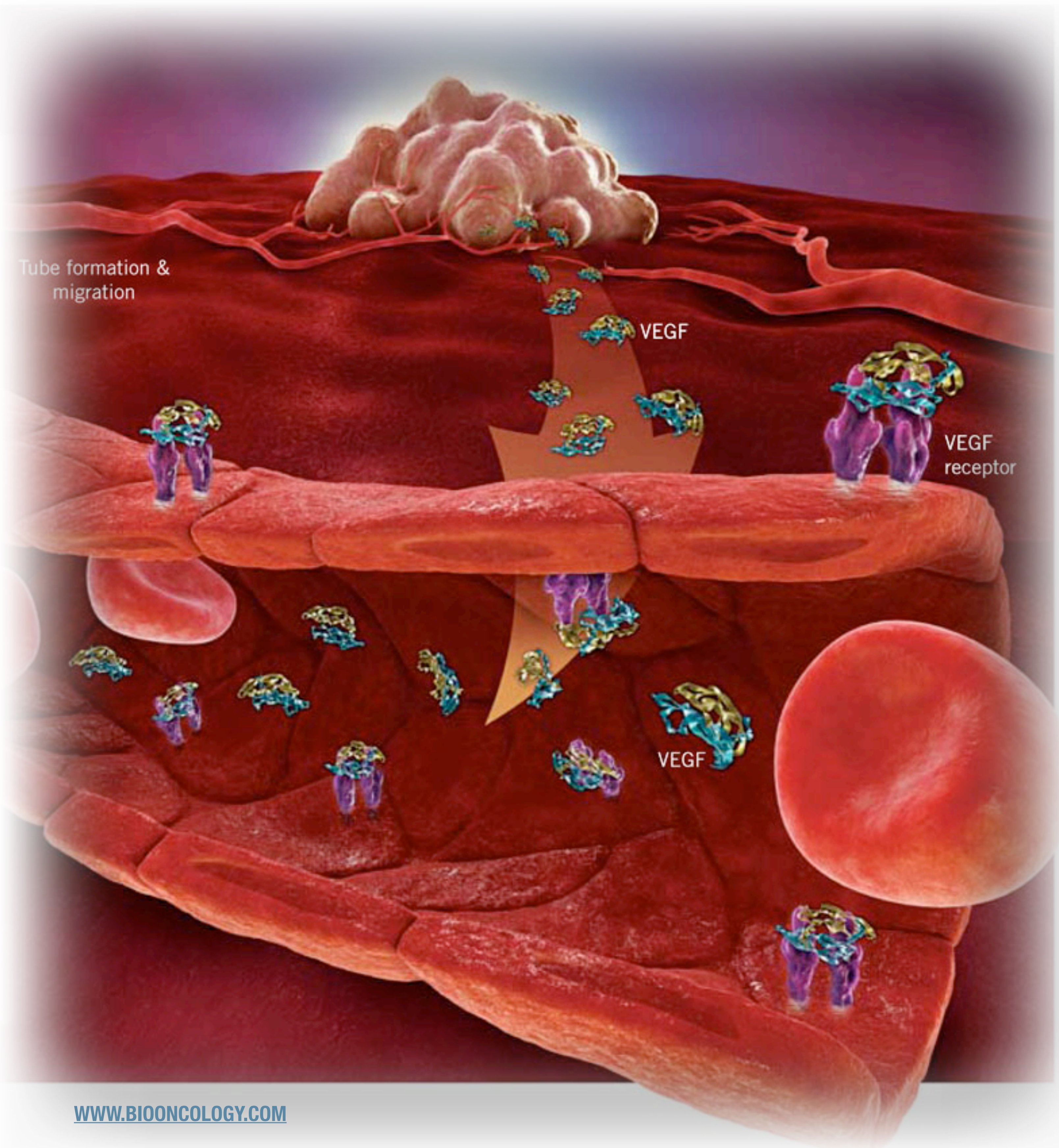

WWW.BIOONCOLOGY.COM

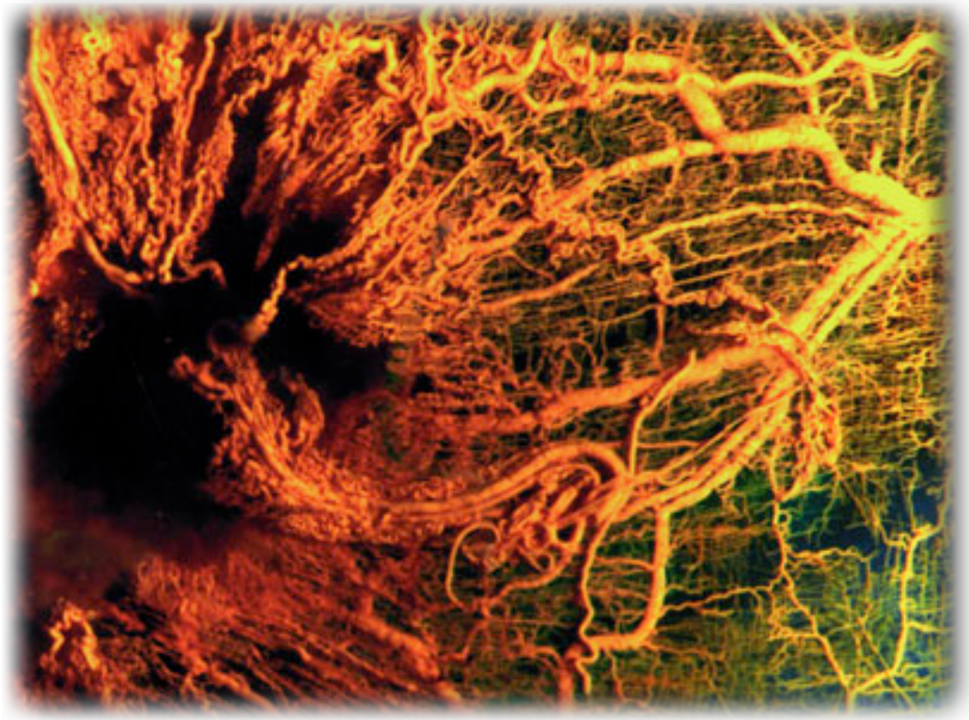

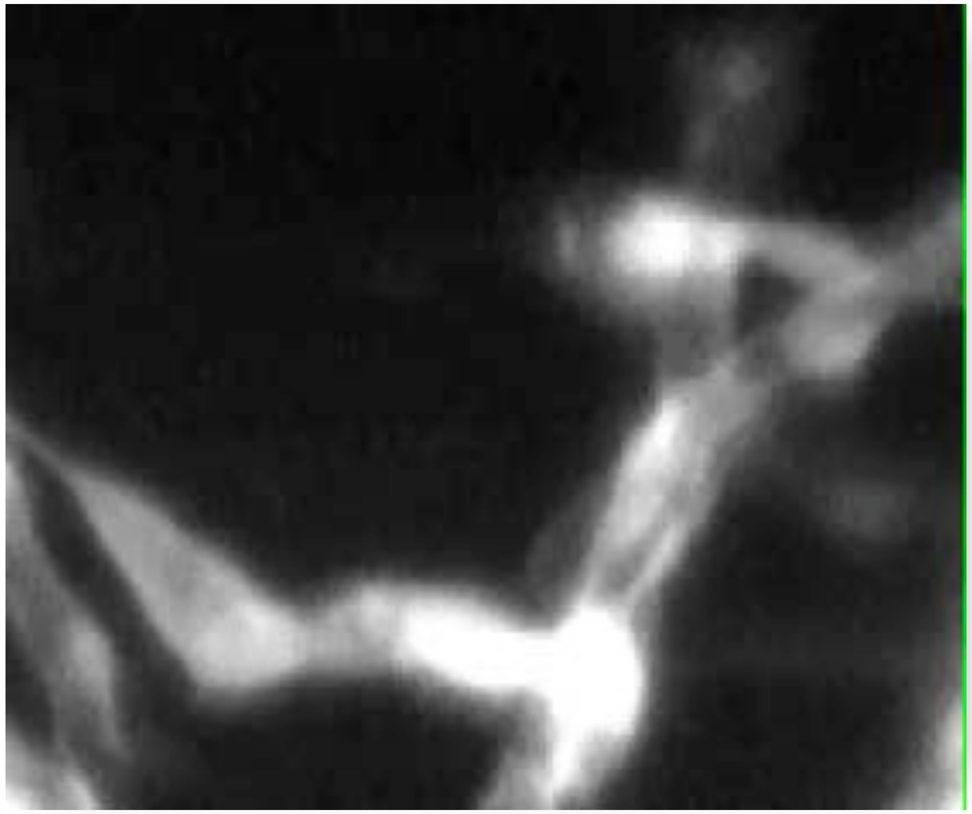

CRANIAL VESSEL ANGIOGENESIS IN ZEBRAFISH
HTTP://ZFISH.NICHD.NIH.GOV/ZFATLAS/FLI-GFP/FLI_MOVIES.HTML

Example of Deterministic Models : **Angiogenesis**

Tumor-Induced Angiogenesis

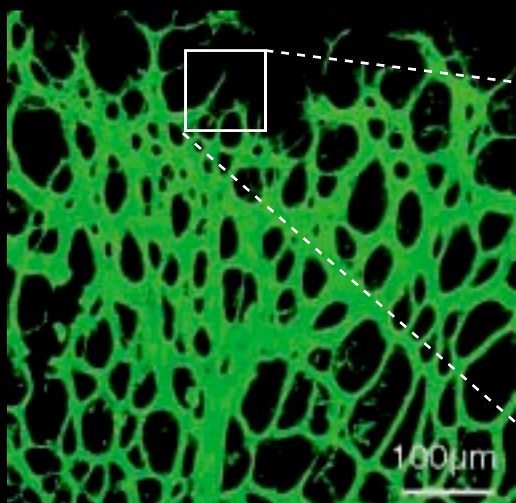

Tissue

Vessel Network

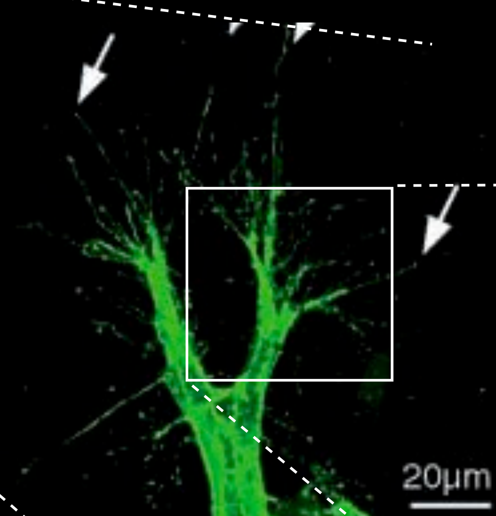

Cellular

Filopodia

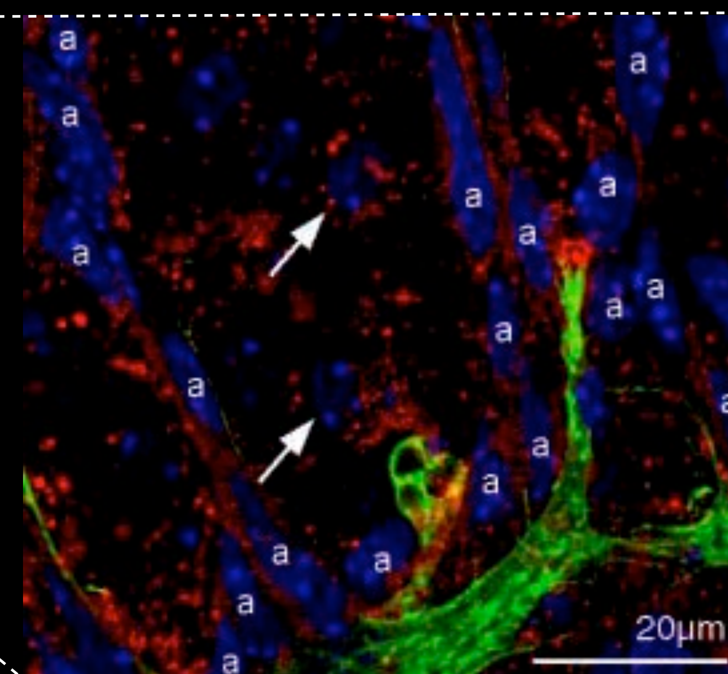

Molecular

Growth factors

A Model of Sprouting Angiogenesis

Mechanism:

endothelial cells migrate towards source of growth factors

- form cords
- proliferate
- branch / fuse

Growth factor: VEGF

exists in two forms:

- soluble
- bound to the matrix (bVEGF)

Release of bVEGF

endothelial cells secrete proteinases

proteinases cleave bVEGF → soluble

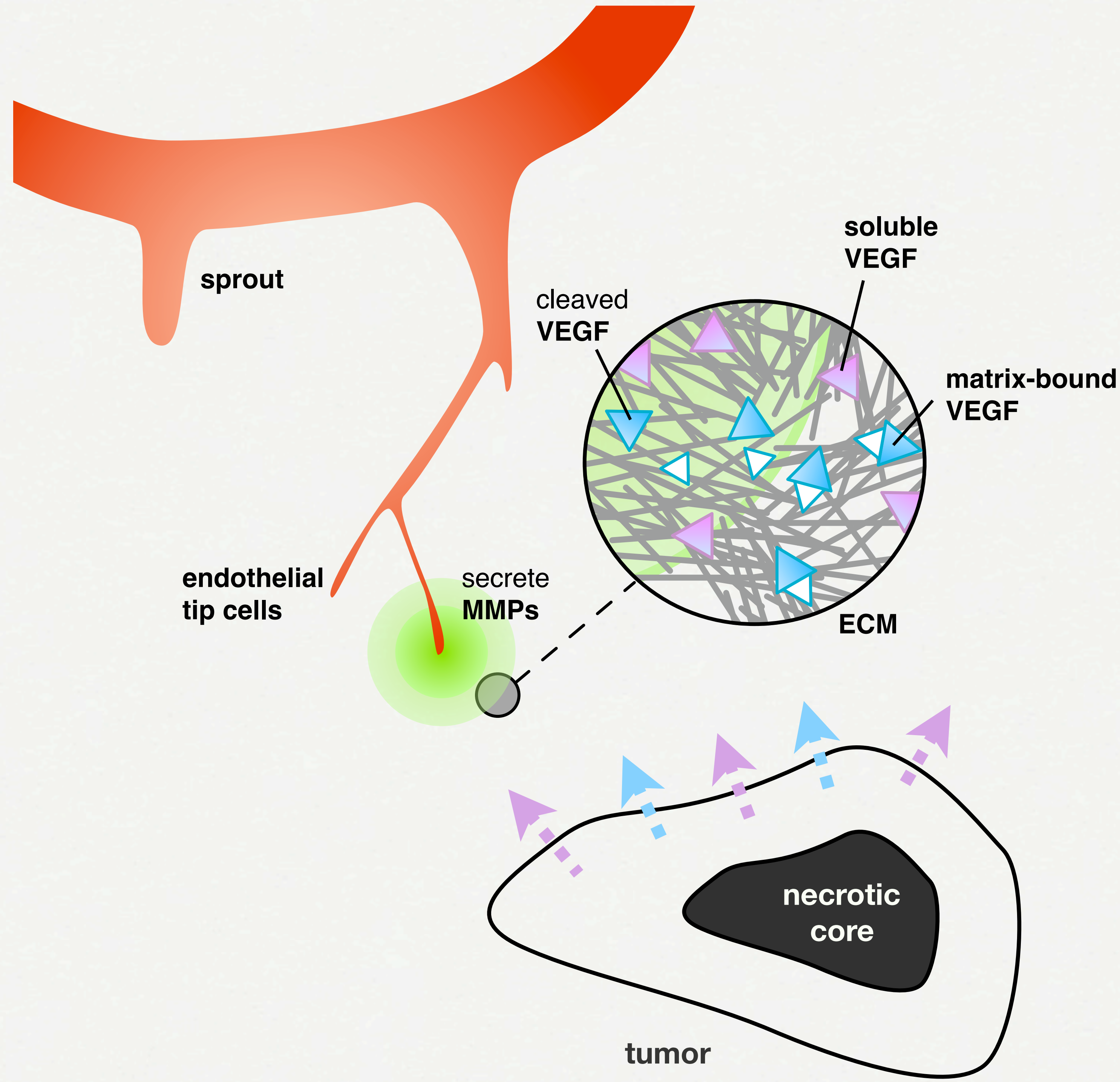

Particle-mesh models for mesenchymal motion / PM4

The Cell

- confined by semipermeable membrane
- inside: cytosol (fluid) & organelles
- cell adhesion molecules on the membrane
- extends filopodia for sensing

Extracellular Matrix

- fibrous proteins
- gels of polysaccharides
- sticky scaffolding
- structural support

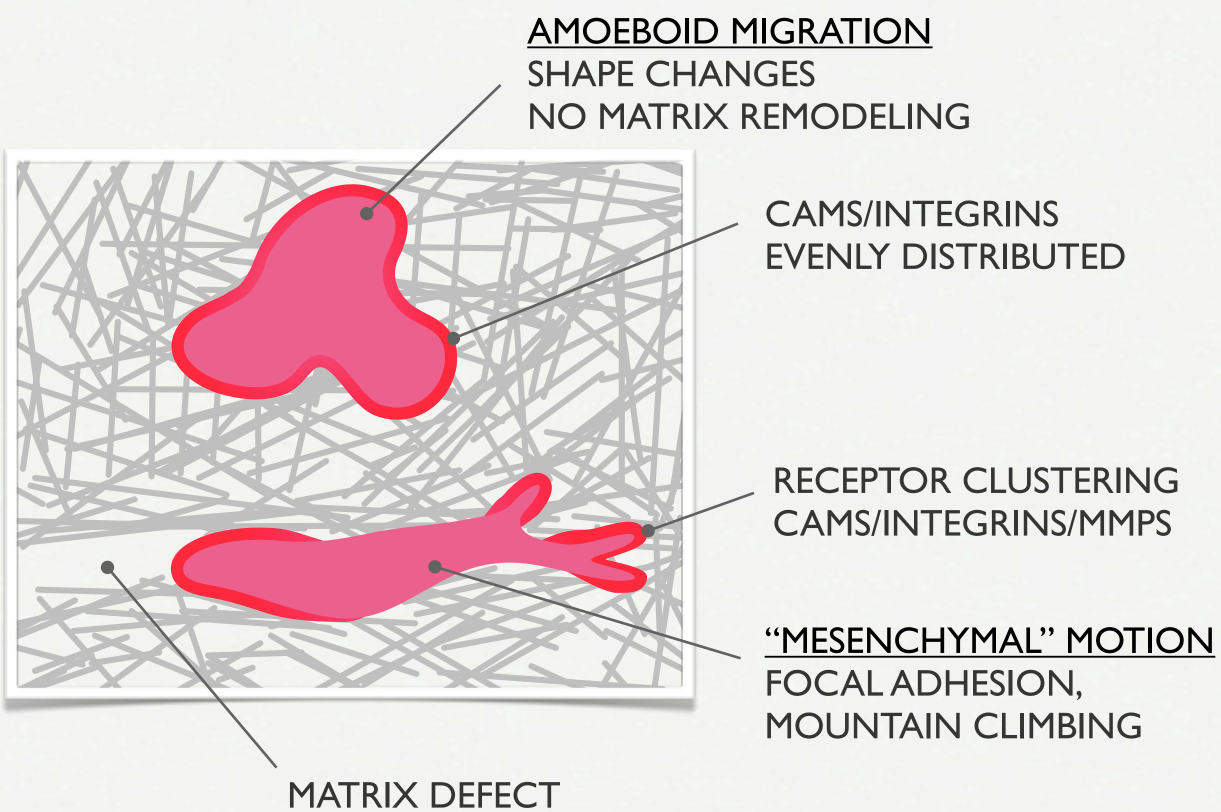

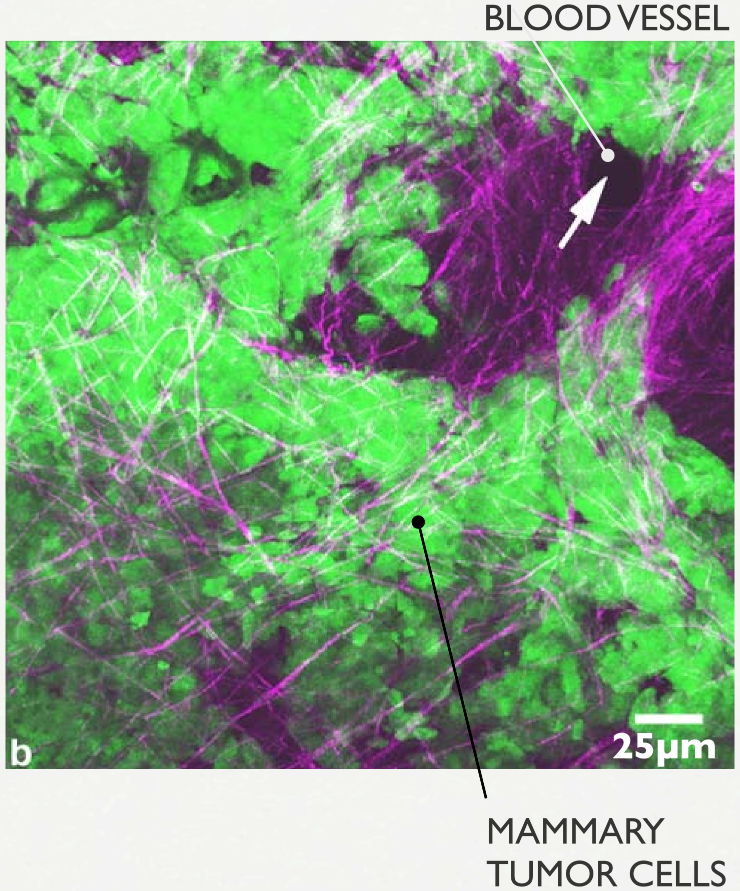

[1] M. Sidani, J. Wyckoff, C. Xue, J. E. Segall, and J. Condeelis. Probing the microenvironment of mammary tumors using multiphoton microscopy. *Journal of Mammary Gland Biology and Neoplasia*, v11(2):151–163, 2006.

Representing Cells:

About scale:

Cellular Potts
- shape optimization
- interaction energies

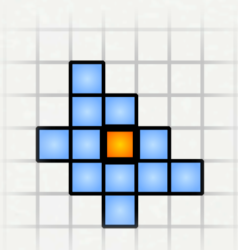

Cellular automaton
- intuitive
- behavioral rules
- one “cell” = one cell

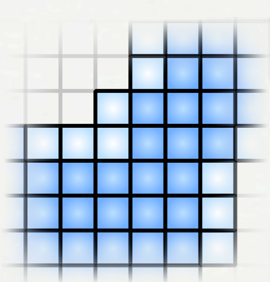

Continuum
- cell density (= no individuals)
- PDEs

Continuum modeling of cells
Primary implications:

Cell density: $\rho(\boldsymbol{x}, t)$

$$\frac{\partial \rho}{\partial t} = -\nabla(\boldsymbol{u}\,\rho) + k\,\rho$$

MIGRATION PROLIFERATION

Continuum cell-cell adhesion:

Existing continuum models:

either expensive (large radius of interaction), [1]
or expensive (leading to stiff PDEs) [2]

Cell-cell adhesion as cell “signaling”:

cells secrete adhesion molecules
cells **follow gradient** of these CAMs (autocrine signal)
the CAMS:

- **diffuse** (slow)
- **decay** (fast)

$$\boldsymbol{a}_{\mathrm{c2c},\rho} = \kappa \nabla f$$ CELL-CELL ADHESION CONTRIBUTION TO MIGRATION

$$\frac{\partial f}{\partial t} = \alpha\,\rho - \mu\, f + D\,\Delta f$$

SECRETION DECAY DIFFUSION

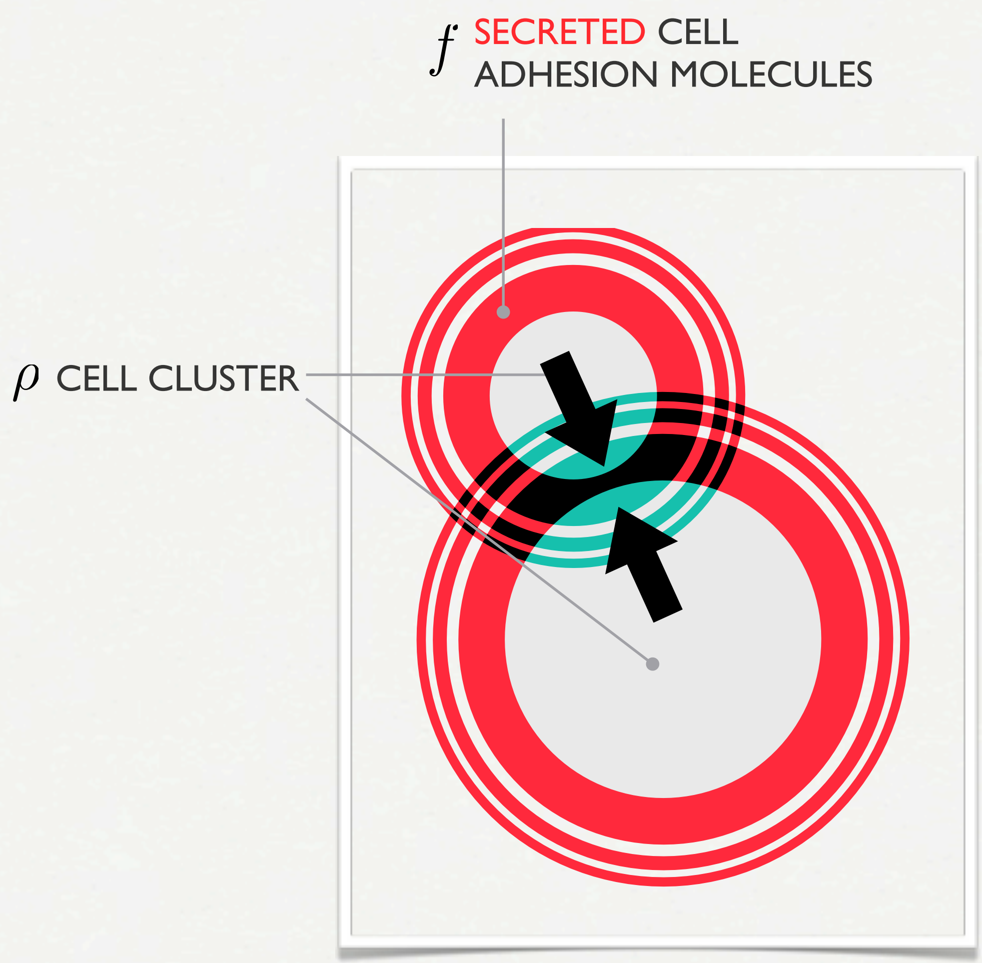

[1] N. J. ARMSTRONG, K. J. PAINTER, AND J. A. SHERRATT. A CONTINUUM APPROACH TO MODELLING CELL-CELL ADHESION. *J. THEOR. BIOL.*, 2006.

[2] J. KIM. A CONTINUOUS SURFACE TENSION FORCE FORMULATION FOR DIFFUSE-INTERFACE MODELS. *J. COMPUT. PHYS.*, 204(2):784–804, 2005.

The “differential adhesion hypothesis”

Cell sorting by differential adhesion

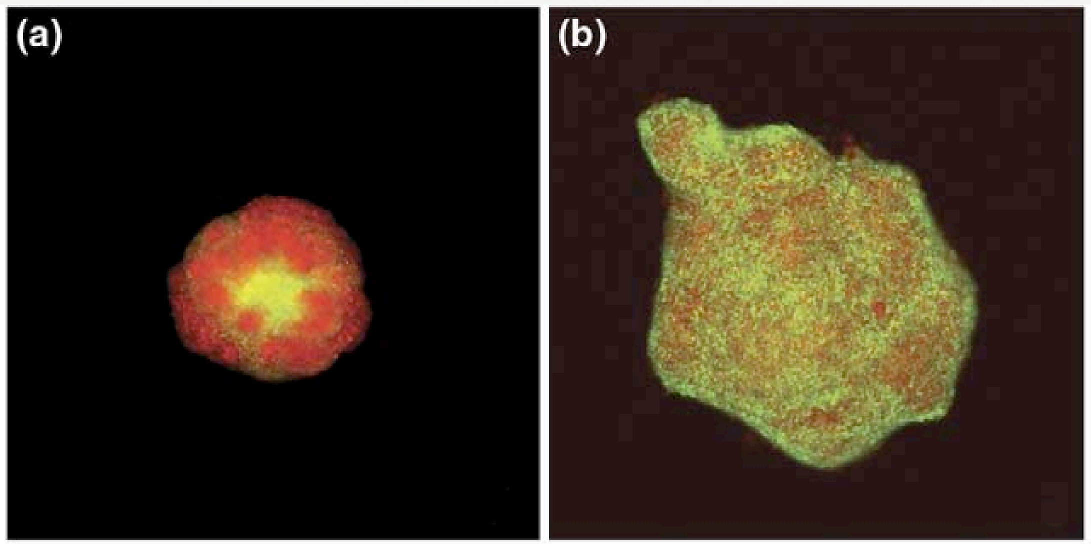

CELL SORTING a) VERSUS INTERMIXING b) IN PROSTATE CANCER [1]

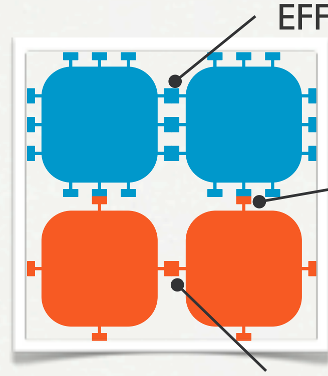

$$\boldsymbol{a}_{ij} = \kappa_{ij} \nabla f_j$$

e.g. sorting:

κ_{11} LARGE

$\kappa_{12} = \kappa_{21}$ SMALL

κ_{22} LARGE

$$\frac{\partial \rho_i}{\partial t} = -\nabla \cdot \left(\sum_j \boldsymbol{a}_{ij}\, \rho_i \right) + d_i\, \Delta \rho_i$$

i=1,2 CELL DENSITIES, DISCRETIZED WITH PARTICLES

$$\frac{\partial f_i}{\partial t} = -\mu_i\, f_i + \alpha_i\, \rho_i + D_i \Delta f_i$$

ARTIFICIAL CAM CONCENTRATIONS

$\kappa_{11} = 0.25$, $\kappa_{22} = 0.025$, $\kappa_{12} = \kappa_{21} = 0.05$ + pressure due to close packing

$\kappa_{11} = 0.25$, $\kappa_{22} = 0.25$, $\kappa_{12} = 0.0$, $\kappa_{21} = 0.0$

$\kappa_{11} = 0.25$, $\kappa_{22} = 0.09$, $\kappa_{12} = 0.2$, $\kappa_{21} = 0.2$

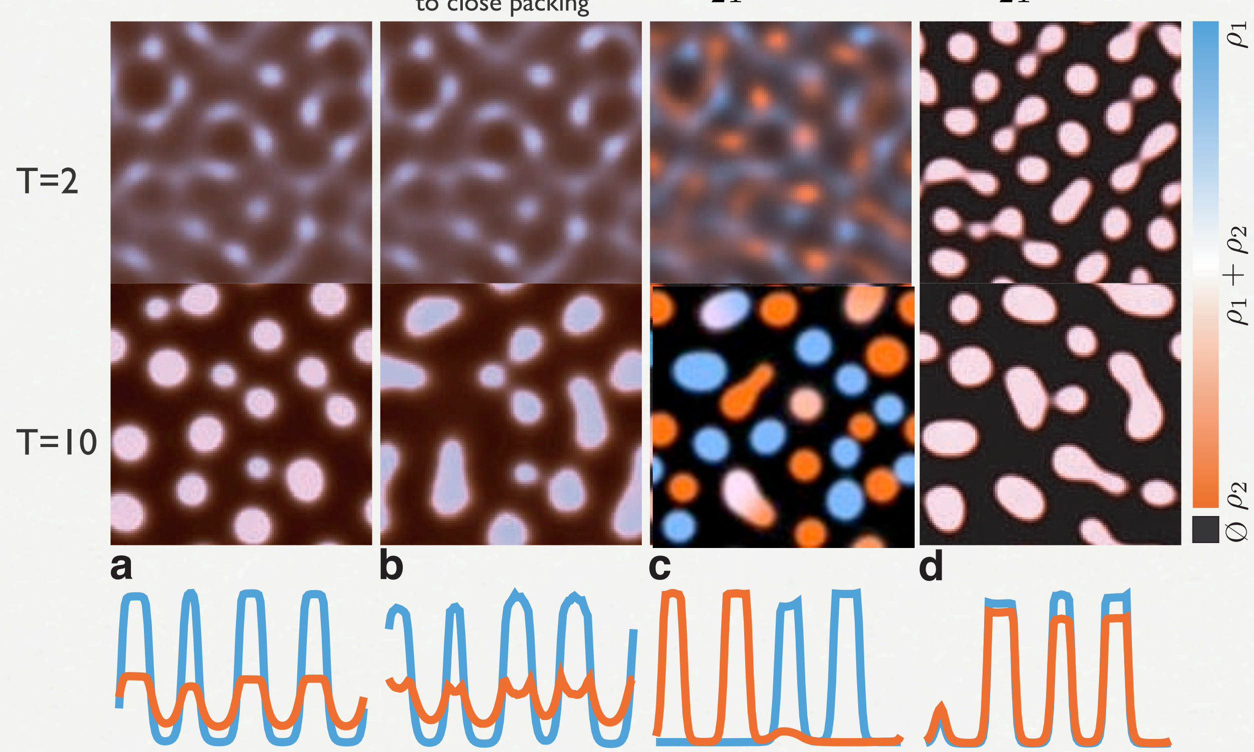

[1] M. S. STEINBERG. DIFFERENTIAL ADHESION IN MORPHOGENESIS: A MODERN VIEW. *CURR. OPIN. GENET. DEV.*, 17(4):281–286, 2007.

Extracellular Matrix : Structure

- Material occupying the space between cells
- Fibers of structural glycoproteins
  (collagen, laminin and fibrillin are distributed throughout the ECM, occupying ~30% of the ECM)
- Collagens (the main component of the ECM cross-link with neighbouring collagens to form bundles)

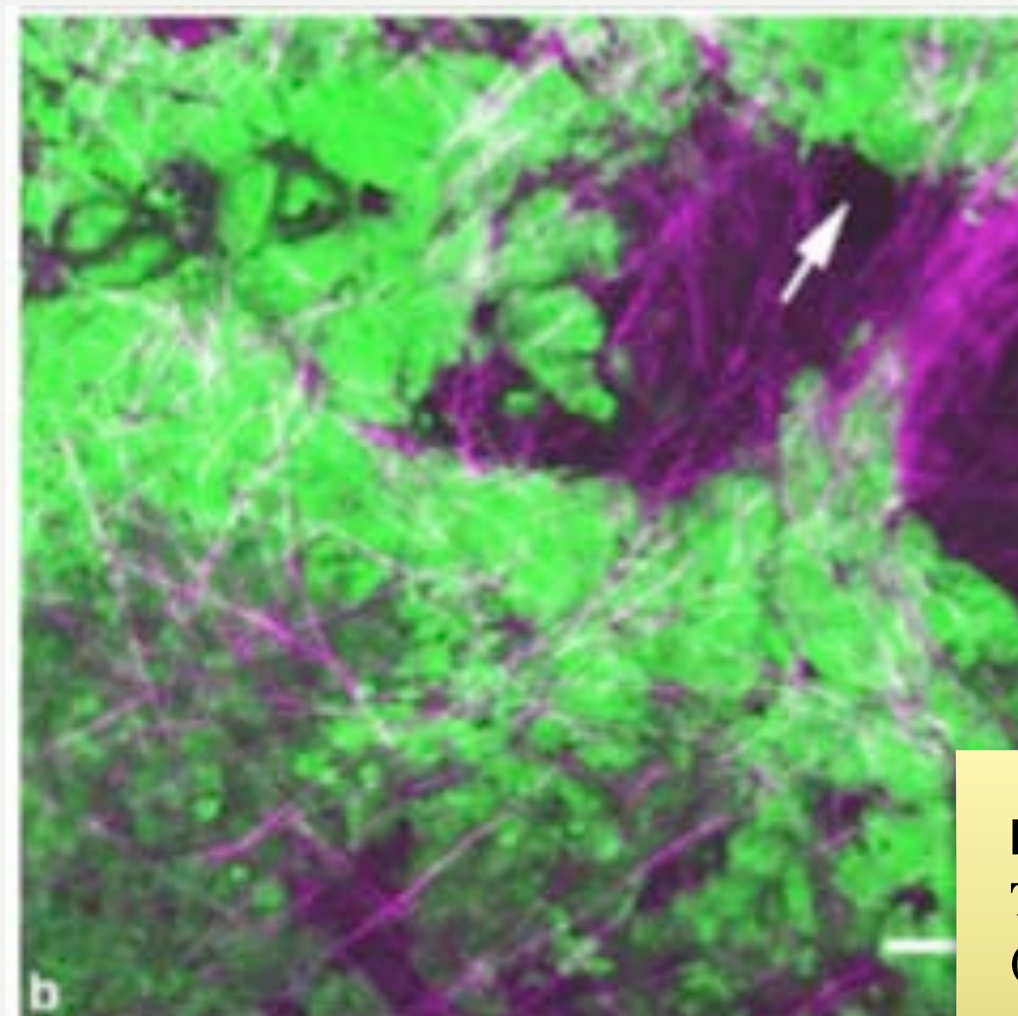

IN M
TUM
(GRI
ASSO
WIT
FIBE

[3] M. SIDANI, J. WYCKOFF, C. XUE, J. E. SEALL, AND J. CONDEELIS. PROBING THE MICROENVIRONMENT OF MAMMARY TUMORS USING MULTIPHOTON MICROSCOPY. *J. MAMMARY GLAND BIOL. NEOPLASIA, V11(2):151-163, 2006*

Extracellular Matrix (ECM)

- Fibrous structures in ECM provide a guiding structure for migrating endothelial cells
- ECM fibers are subject of remodeling by migrating EC's
- The ECM expresses binding sites for various growth factors and integrins

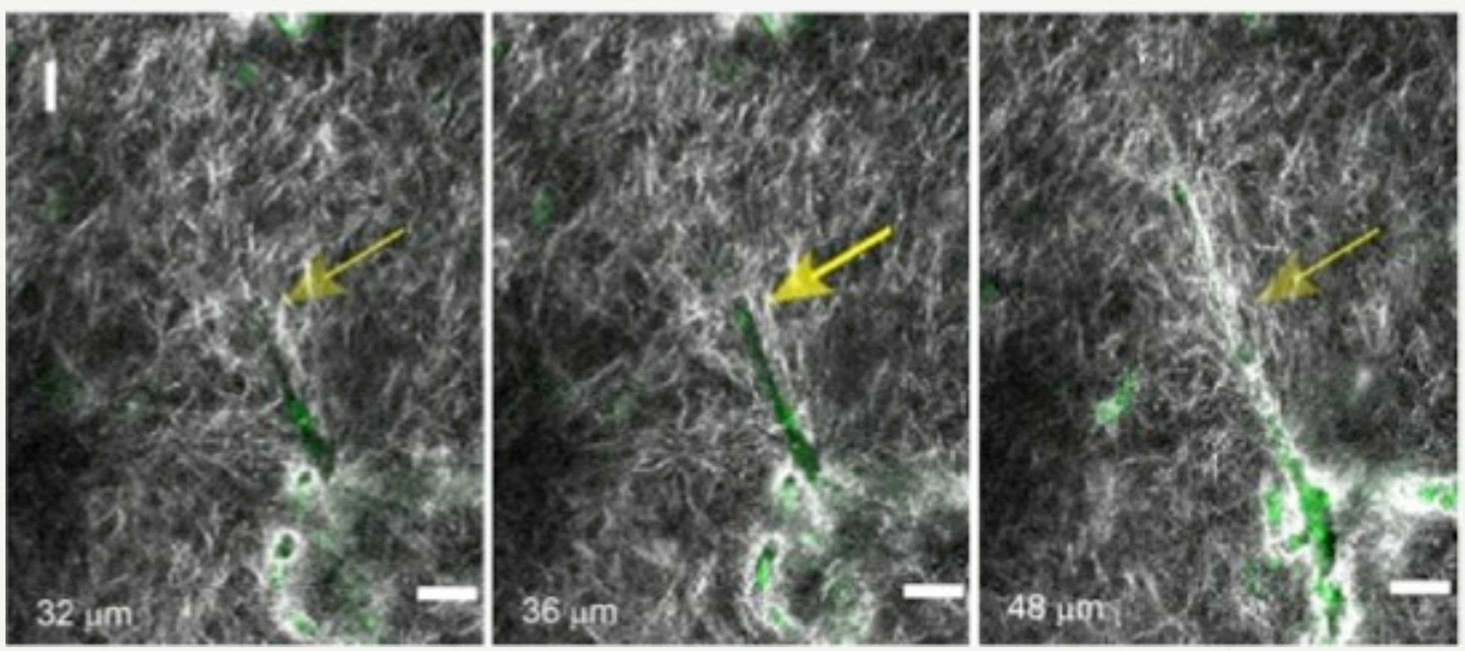

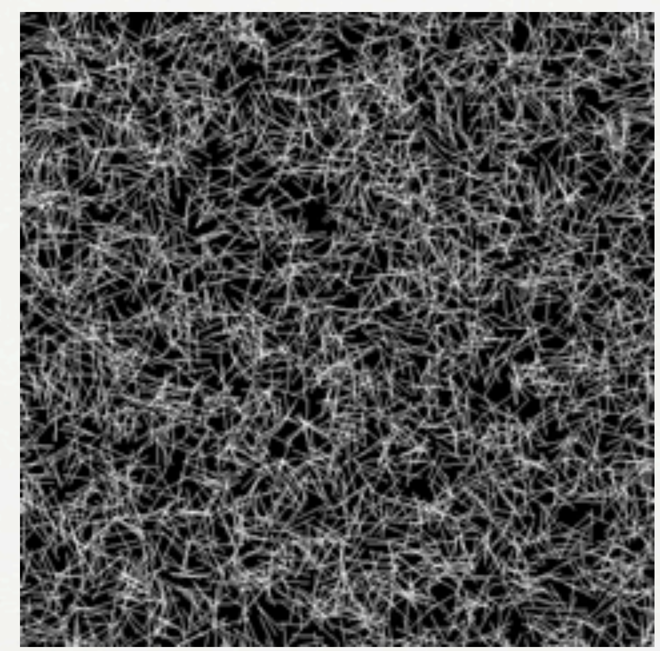

[4] N. D. KIRKPATRICK, S. ANDREOU, J. B. HOYING, AND U. UTZINGER. LIVE IMAGING OF COLLAGEN REMODELING DURING ANGIOGENESIS. *AJP HEART.*. PAGES 0124.2006-,2007

Modeling the Matrix:

Model matrix explicitly:

- structure: collection of fiber bundles
- function: cell-matrix adhesion sites

Fibers:

- straight
- random direction
- distribution of lengths

$$l = l_0 \, 2^{m\,z}$$
$$\alpha \in \mathcal{U}([0,\pi])$$
$$z \in \mathcal{N}(0,1)$$

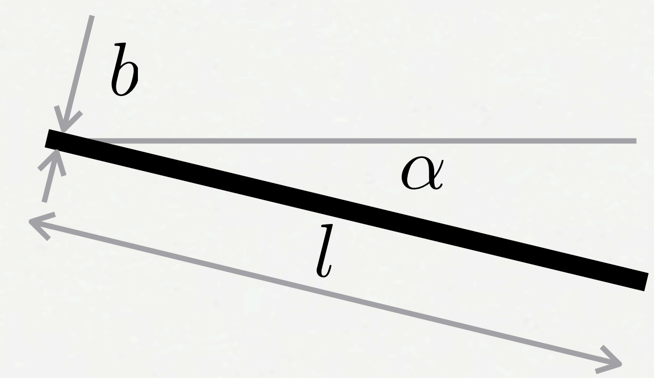

Indicator field :e

- unity where fibers present
- smoothed (implicit filopodia)

Endothelial Cell-ECM Interaction

- ECM fibers provide a guiding structure ($\underline{\mathbf{T}}$) for migrating ECs
- The ECM density E_ρ influences migration speed
- ECM expresses binding sites for matrix-bound VEGF and fibronectin

ECM density: $\alpha\left(E_\rho\right) = \left(0 + E_\rho\right)\left(1 - E_\rho\right)$

ECM direction: $\{\underline{\mathbf{T}}\}_{ij} = \left(1 - E_X\right)\{1\}_{ij} + E_X K_i K_j$

Migration Speed: $\mathbf{a} = \overbrace{\alpha\left(E_\rho\right)\underline{\mathbf{T}}}^{\text{ECM}}\left(\overbrace{w_V \nabla\Psi}^{\text{Chemotaxis}} + \overbrace{w_F \nabla\Phi_b}^{\text{Haptotaxis}}\right)$

Chemotaxis & cell-matrix adhesion

Opportunistic: get to growth factor (GF) source

Existing models: $\boldsymbol{a}_\phi = \nabla\phi$

PM4: $\boldsymbol{a}_{\mathrm{ecm},\phi} =$

$$\left[\left(1 - \left|\frac{\nabla e}{|\nabla e|}\cdot\frac{\nabla\phi}{|\nabla\phi|}\right|\right)\nabla e + \nabla\phi\right](e + e_o)(\rho_{\mathrm{cpd}} - e)$$

γ CLING TO FIBER AN ADVANTAGE?

WHERE IS THE FIBER?

WHERE IS THE GF SOURCE?

FIBERS FACILITATE MIGRATION

TOO MANY FIBERS BLOCK MIG. PATH

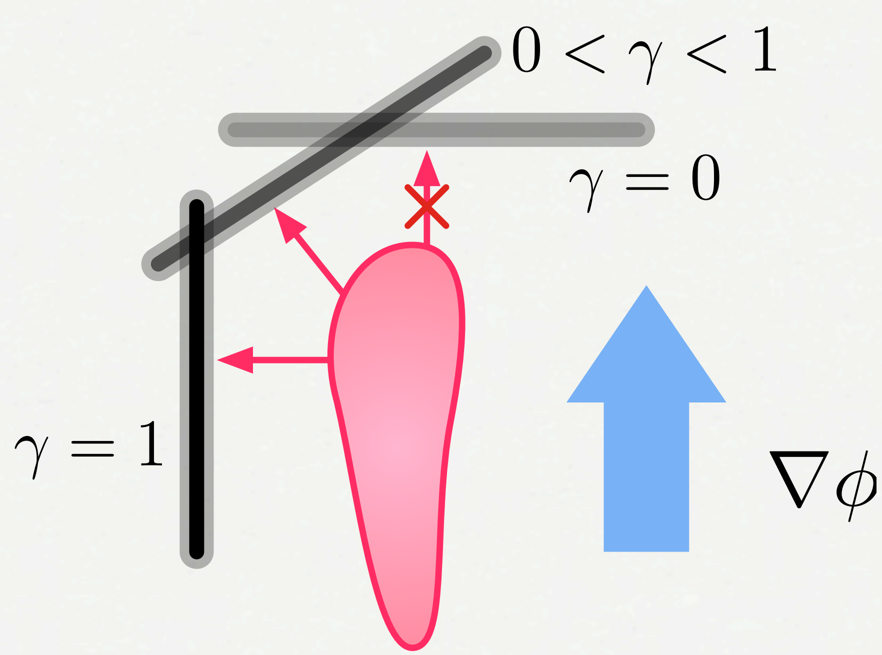

Endothelial Cell representation

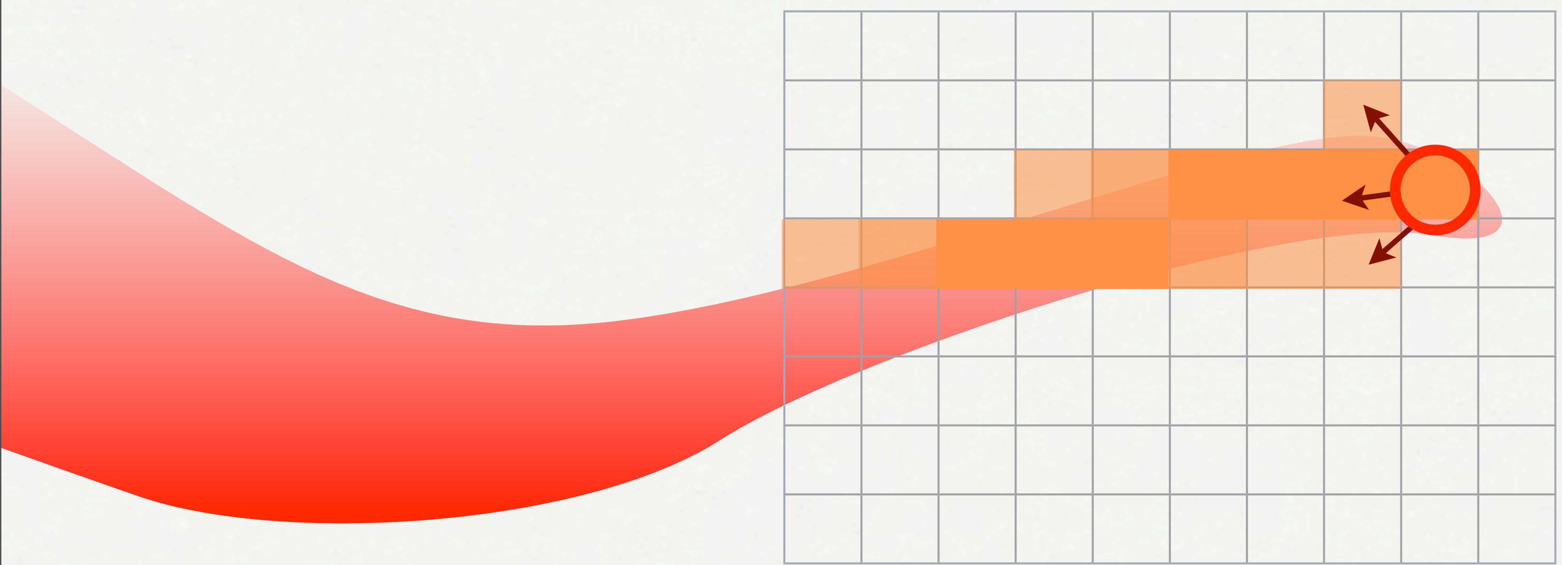

Tip Cell “deposes” endothelial cells

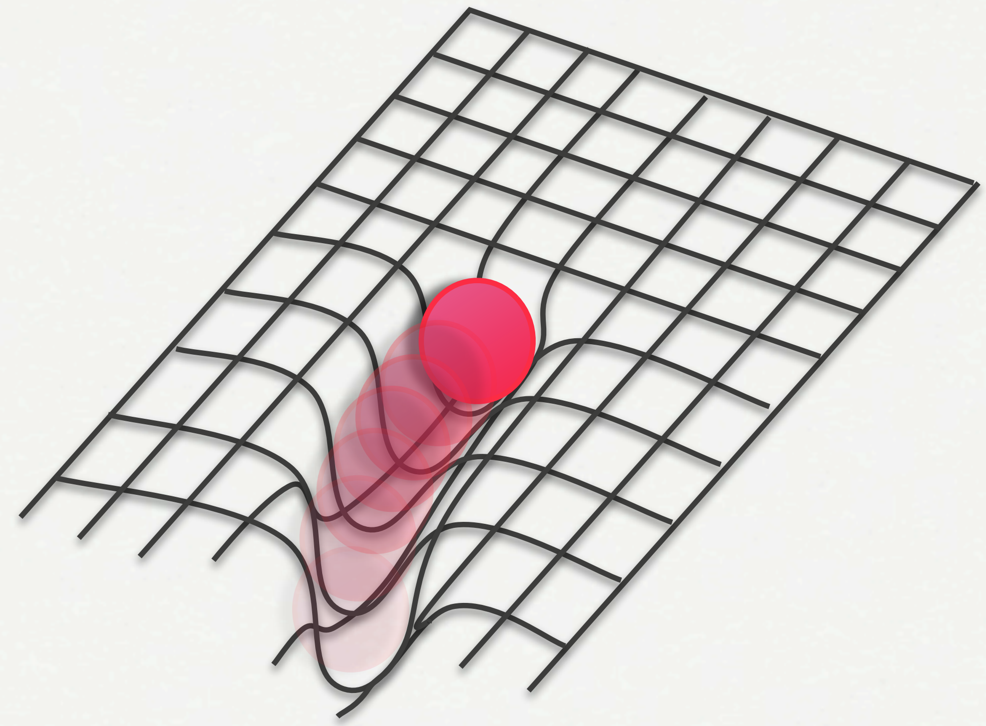

Hybrid representation of ECs:

Tip cell particles Q_p:

- Discrete particle representation
- Particle location: $\boldsymbol{x}_p$
- Migration acceleration: $\boldsymbol{u}_p$
- Drag coefficient: λ

$$\frac{\boldsymbol{x}_p}{\partial t} = \boldsymbol{u}_p, \quad \frac{\boldsymbol{u}_p}{\partial t} = \boldsymbol{a}_p - \lambda \boldsymbol{u}_p$$

Stalk cell density ρ:

- Continuum vessel representation
- Tip and stalk communicate through Particle-Mesh, Mesh-Particle interpolations

$$\rho_{\boldsymbol{i}}^{n+1} = max\left(\rho_{\boldsymbol{i}}^{n}, \sum_p B(\boldsymbol{i}\,h - \boldsymbol{x}_p)\,Q_p\right)$$

$$Q_p = \sum_{\boldsymbol{i}} h^3 q_{\boldsymbol{i}} M_4' \left(\boldsymbol{x}_p - \boldsymbol{i}h\right)$$

Tip Cell Migration

The elements of migration

cells are guided by extracellular matrix

transmembrane CAMs: integrins,...)
facilitates migration

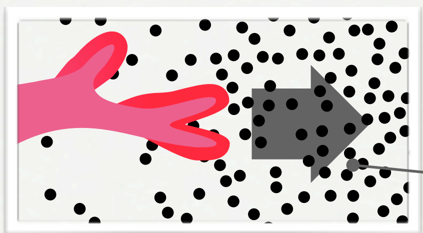

cells sense chemical gradients

gradients of "chemoattractant" serve as migratory cues

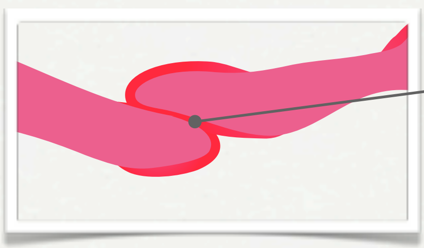

cells stick to cells

gradient of "haptotactic" molecules serve as migration cues

Migration Speed

$$\mathbf{a} = \alpha\left(E_\rho\right) \underline{\mathbf{T}} \left(w_V \nabla \Psi + w_F \nabla \Phi_b\right)$$

Growth Factors: Assumptions

- We model only one representative growth factor (VEGF)
- VEGF exists in a soluble and a matrix bound isoform
- Soluble VEGF is released from a tumor source
- Unbound VEGF diffuses through the ECM
- VEGF is subject to uptake by endothelial cells
- decays naturally

Soluble VEGF (sVEGF) - Assumptions

- Model : One VEGF isoform in soluble and bound state
- sVEGF establishes global chemotactic gradient

  - Tumor source modeled by boundary conditions
  - sVEGF diffuses through ECM
  - Uptake of sVEGF by endothelial cells ρ
  - Subject of natural decay

$$\frac{\partial[\text{sVEGF}]}{\partial t} = k_V \nabla^2 [\text{sVEGF}] - U\left([\text{sVEGF}], \rho\right) - \delta_V [\text{sVEGF}]$$

$$U\left([\text{sVEGF}], \rho\right) = min\left([\text{sVEGF}], \upsilon_V \rho\right)$$

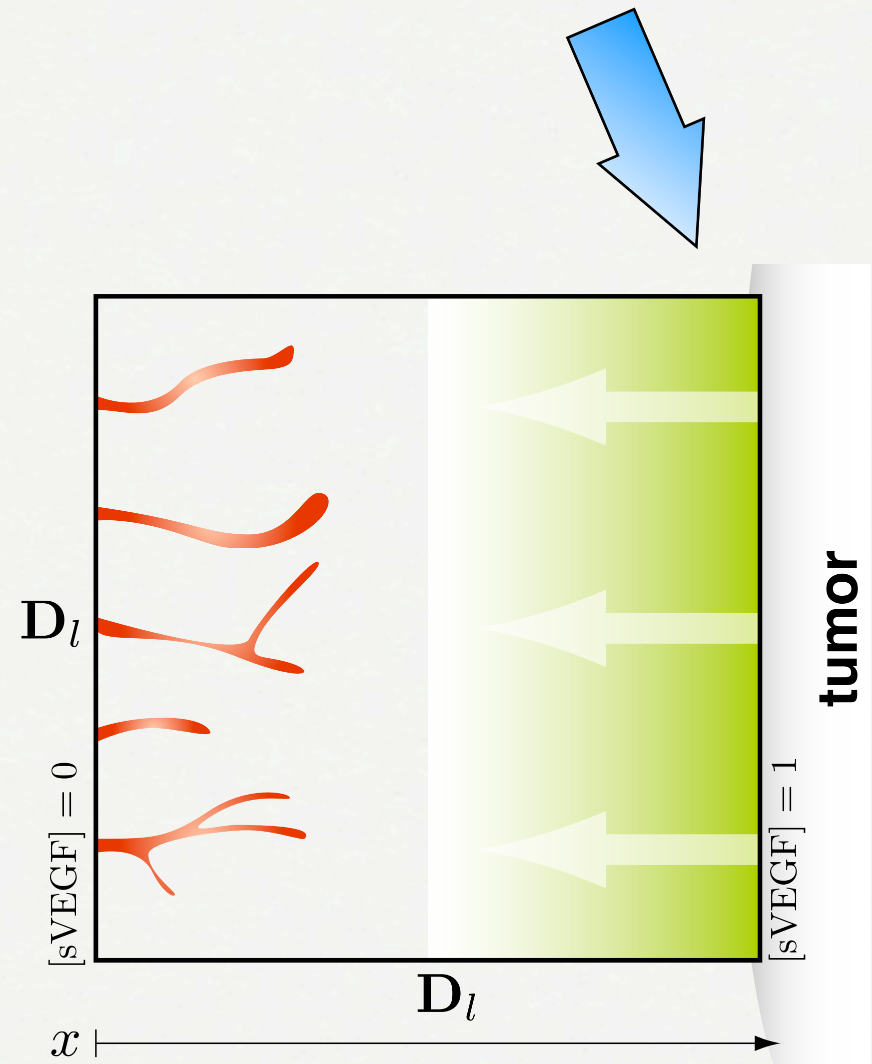

Matrix-bound VEGF (bVEGF)

- Some VEGF isoforms express heparin-binding sites binding to domains in the ECM
- Local gradients of matrix bound VEGF influence sprout morphology
- Matrix bound VEGF is cleaved by MMPs released at endothelial sprout tips

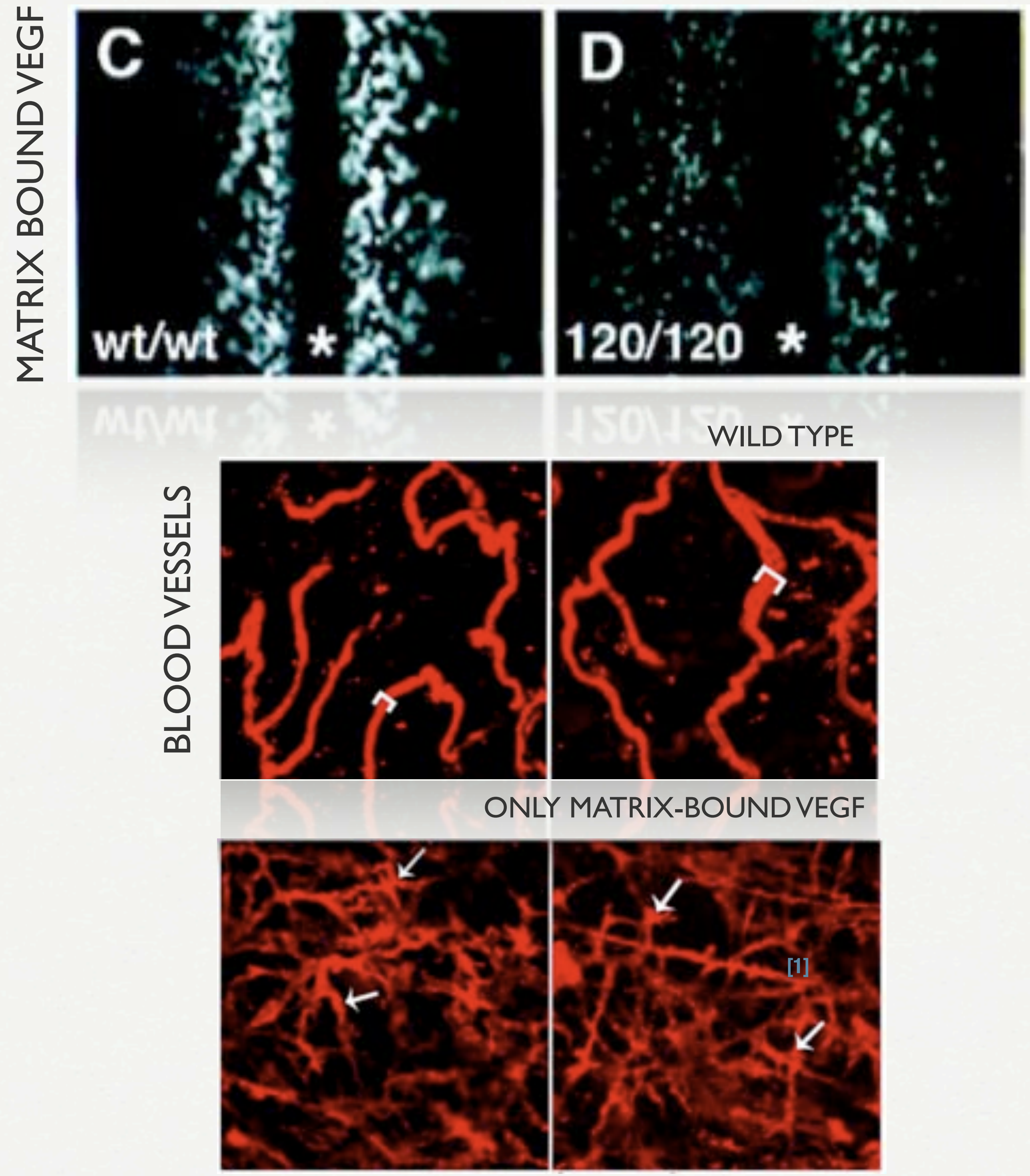

[1] C. RUHRBERG, H. GERHARDT, M. GOLDING, R. WATSON, S. IOANNIDOU, H. FUJISAWA, C. BETSHOLTZ AND D. T. SHIMA. SPATIALLY RESTRICTED PATTERNING CUES PROVIDED BY HEPARIN-BINDING VEGF-A CONTROL BLOOD VESSEL BRANCHING MORPHOGENESIS. *GENES DEV.*, 16(20):2684-2698, 2002.
[2] S. LEE, S. M. JILAI, G. V. NIKOLOVA, D. CARPIZO, AND M. L. IRUELA-ARISPE. PROCESSING OF VEGF-A BY MATRIX METALLOPROTEINASES REGULATES BIOAVAILABILITY AND VASCULAR PATTERNING IN TUMORS. *J. CELL BIOL.*, V42(3):195-238, 2001

Matrix-bound VEGF - Assumptions

- Initially distributed in pockets
- establishes local chemotactic gradient
- cleaved VEGF (cVEGF) becomes soluble

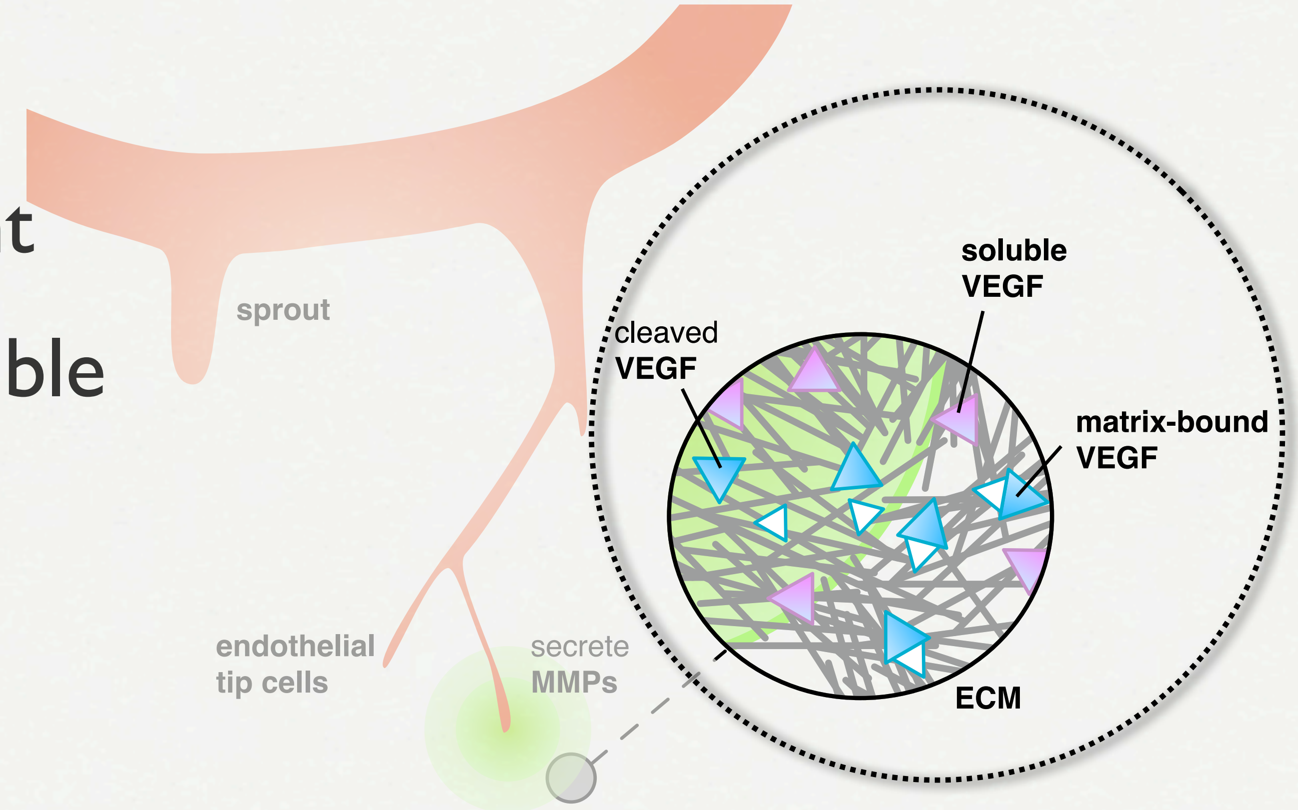

  - bVEGF is cleaved by MMPs
  - Uptake of cVEGF by ECs ρ
  - cVEGF diffuses through ECM
  - cVEGF is subject to natural decay

$$\frac{\partial[\text{bVEGF}]}{\partial t} = -C\left([\text{bVEGF}],[\text{MMP}]\right) - U\left([\text{bVEGF}],\rho\right)$$

$$C\left([\text{bVEGF}],[\text{MMP}]\right) = min\left([\text{bVEGF}], \upsilon_{bV}[\text{MMP}][\text{bVEGF}]\right)$$

$$\frac{\partial[\text{cVEGF}]}{\partial t} = k_V \nabla^2[\text{cVEGF}] + C\left([\text{bVEGF}],[\text{MMP}]\right) - U\left([\text{cVEGF}],\rho\right) - \delta_V[\text{cVEGF}]$$

Angiogenesis: Post-dicting Experiments

Matrix-bound VEGF leads to increased branching.
vessel branching ↔ capillary function

BLOOD VESSEL FORMATION IN A MOUSE MODEL

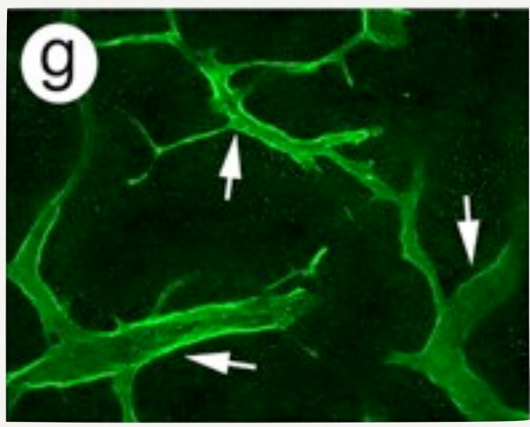

ONLY SOLUBLE VEGF
> THICKER VESSELS

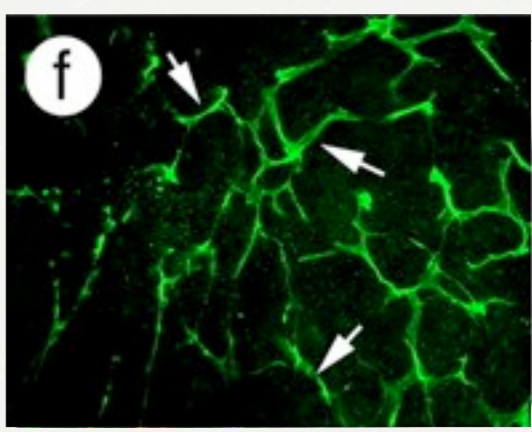

SOLUBLE + MATRIX-BOUND VEGF
> INCREASED BRANCHING

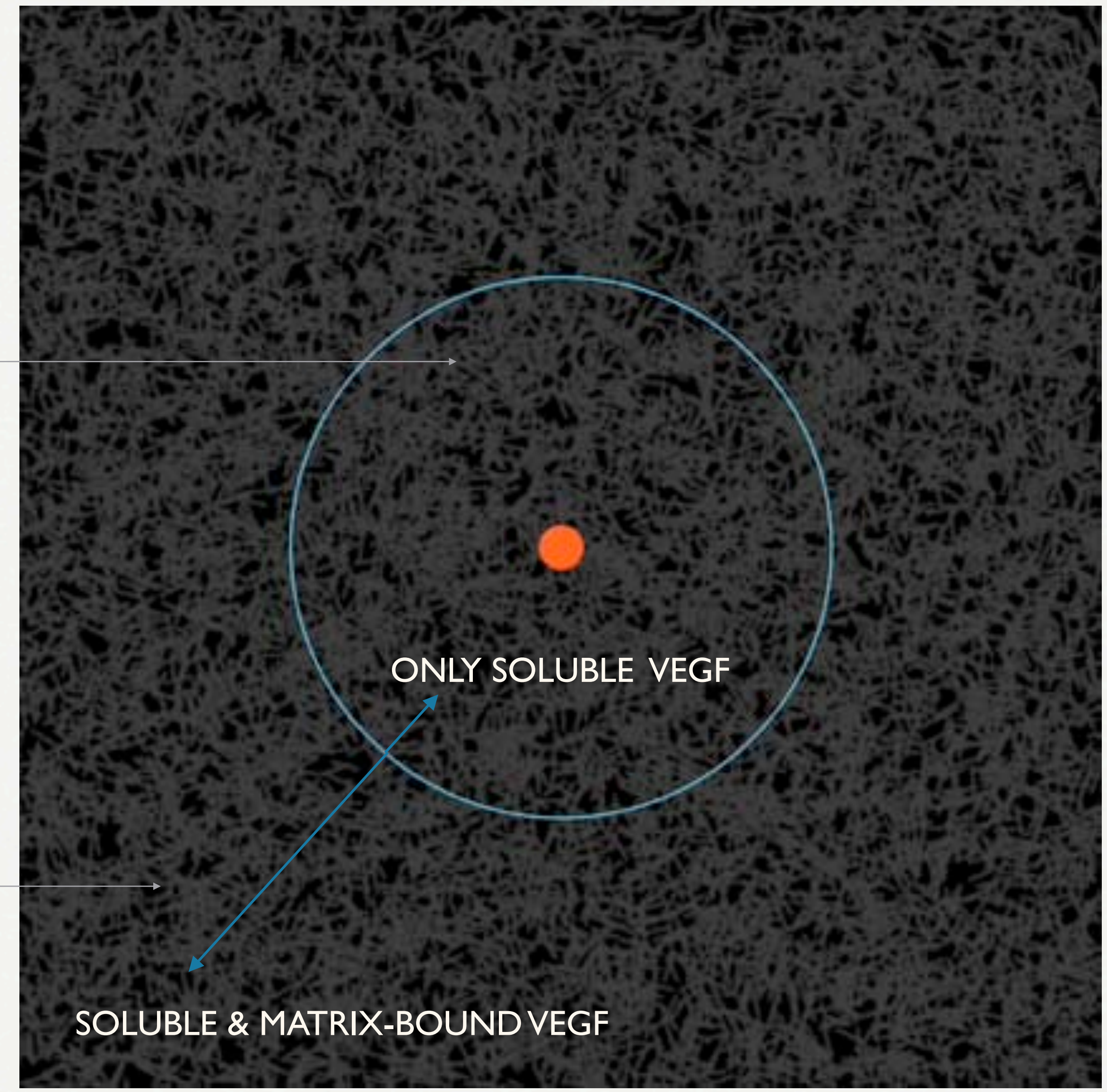

RADIAL SOLUBLE VEGF GRADIENT AND
LOCALIZED MATRIX-BOUND VEGF

new: branching is an output of the simulation

[1] S. LEE, S. M. JILANI, G. V. NIKOLOVA, D. CARPIZO, AND M. L. IRUELA-ARISPE. PROCESSING OF VEGF-A BY MATRIX METALLOPROTEINASES REGULATES BIOAVAILABILITY AND VASCULAR PATTERNING IN TUMORS. *J. CELL BIOL.*, 169(4):681–691, 2005.

MATRIX METALLOPROTEINASES

- decreases local chemotactic gradients

- RELEASED BY MIGRATING TIP-CELLS $[\mathrm{EC}]$
- RELEASE BOUND BY THRESHOLD LEVEL M_{th}
- DIFFUSE THROUGH ECM
- SUBJECT TO NATURAL DECAY

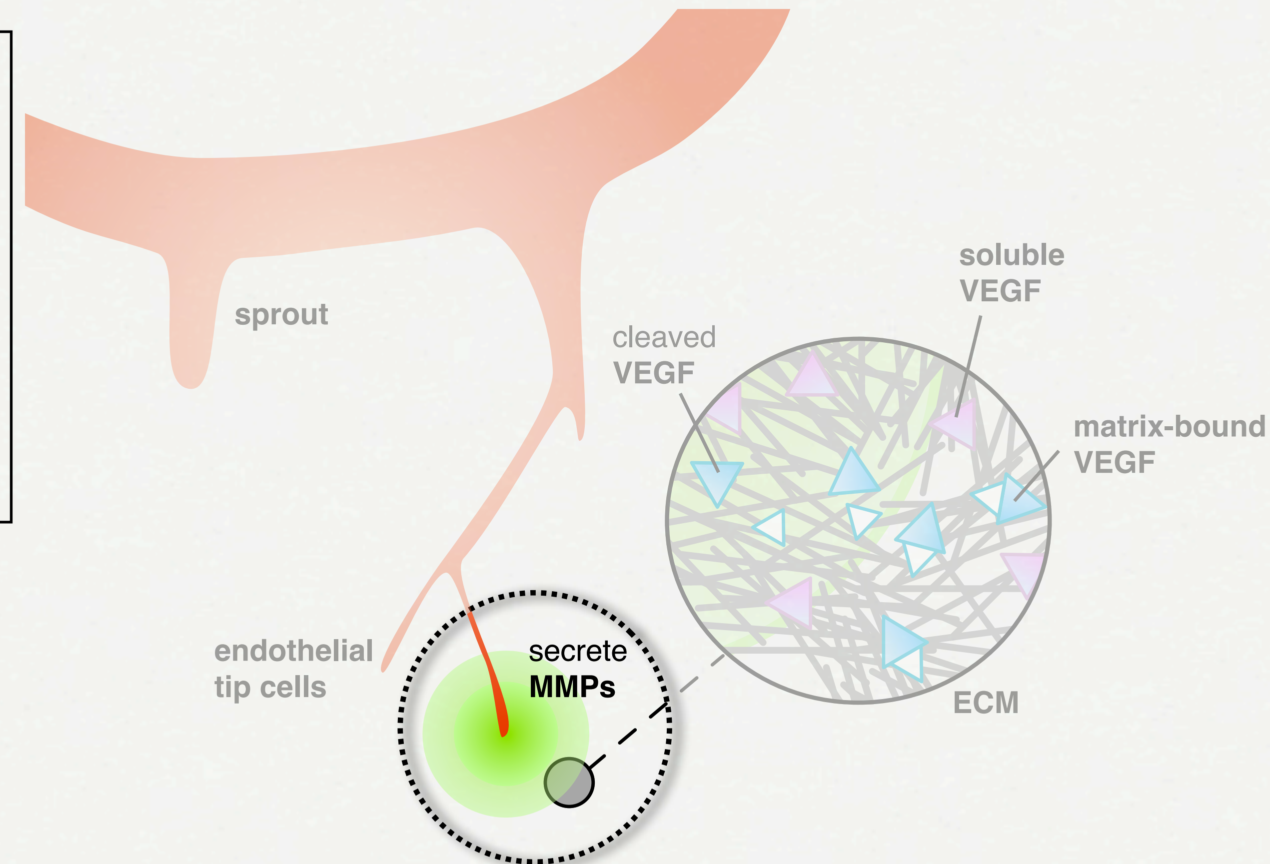

$$\frac{\partial[\mathrm{MMP}]}{\partial t} = k_M \nabla^2 [\mathrm{MMP}] + \gamma_M G\left(M_{th}, [\mathrm{MMP}]\right)[\mathrm{EC}] - \delta_M [\mathrm{MMP}]$$

$$G\left(M_{th}, [\mathrm{MMP}]\right) = \frac{M_{th} - [\mathrm{MMP}]}{M_{th}}$$

Milde F., Bergdorf M., Koumoutsakos P., A hybrid model of sprouting angiogenesis, **Biophysical J.. 2008**

Effect of Matrix structure on branching - Mesenchymal cells

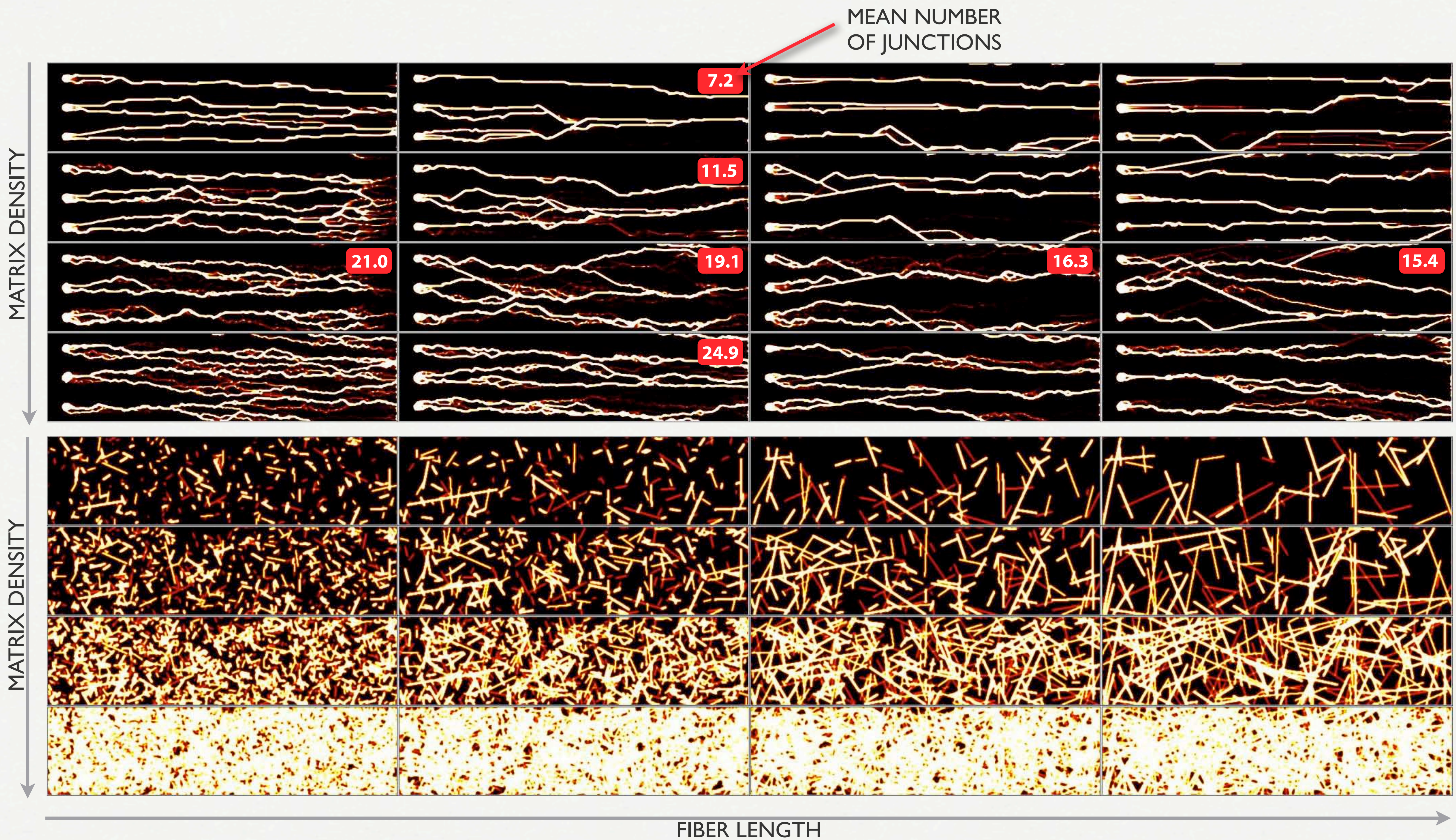

statistics over n = 50 different matrices
junctions identified with AngioQuant

What Next ?

Multiscaling

Open Source Software

Mathematicians in Labs

Computer Science

PhD students: Basil BAYATI, Alvaro FOLETTI, Mattia GAZZOLA, Babak HEJAZIALHOSSEINI, Florian MILDE, Angelos KOTSALIS, Manfred QUACK, Wim van REES, Diego ROSSINELLI, Gerardo TAURIELLO

Post-docs : Michael BERGDORF, Philippe CHATELAIN, Jens WALTHER, Ding YI

Administration: Sonja SCHLAEPFER

and : Ari Helenius, Michael Detmar (ETHZ), Urs Greber (Uni ZH), Donald McDonald (UCSF)